

Thermodynamic Properties of Propane. III. A Reference Equation of State for Temperatures from the Melting Line to 650 K and Pressures up to 1000 MPa

Eric W. Lemmon* and Mark O. McLinden

Thermophysical Properties Division, National Institute of Standards and Technology, 325 Broadway, Boulder, Colorado 80305

Wolfgang Wagner

Lehrstuhl für Thermodynamik, Ruhr-Universität Bochum, D-44780 Bochum, Germany

An equation of state is presented for the thermodynamic properties of propane that is valid for temperatures from the triple point temperature (85.525 K) to 650 K and for pressures up to 1000 MPa. The formulation can be used for the calculation of all thermodynamic properties, including density, heat capacity, speed of sound, energy, and saturation properties. Comparisons to available experimental data are given that establish the accuracy of calculated properties. The approximate uncertainties of properties calculated with the new equation are 0.01 % to 0.03 % in density below 350 K, 0.5 % in heat capacities, 0.03 % in the speed of sound between (260 and 420) K, and 0.02 % in vapor pressure above 180 K. Deviations in the critical region are higher for all properties except vapor pressure.

Introduction

Characteristics of Propane. Propane (C_3H_8 , R-290) is the third alkane in the saturated hydrocarbon (paraffin) series starting with methane. Propane is a gas at atmospheric conditions and can be compressed into a liquid for transportation. As a commodity in this state, it is often termed liquefied petroleum gas (LPG) and contains small amounts of propylene, butane, and butylene. Because it can be stored as a liquid at atmospheric temperatures, propane has a huge advantage over natural gas, which must be highly compressed to store the same amount of energy in a similar sized tank.

Propane is extracted from natural gas processing or from the removal of light hydrocarbons in oil recovery. Propane is nontoxic but is considered an asphyxiate in large doses. It is used in many applications, primarily as a fuel, but also as a propellant or chemical feedstock in the production of other chemicals, including propyl alcohol. It is the third most common vehicle fuel after gasoline and diesel and has a lower greenhouse gas emission than that typical of motor fuels.

Propane is becoming popular as a refrigerant as traditional refrigerants are being replaced due to their ozone depletion potential or global warming potential. Propane is one of the so-called “natural refrigerants”, a group that also includes water, carbon dioxide, and ammonia. It can be used in its pure form or mixed with isobutane. Some applications mix propane with other refrigerants to improve the oil solubility.

With so many industrial and scientific uses, propane has been widely measured to characterize its chemical, thermal, caloric, and combustion properties. Numerous experimental studies have been carried out over the full temperature and pressure range of nearly all applications. In the thermodynamics arena, experimental data are available for density, vapor pressure, speed of sound, virial coefficients, heat capacities, enthalpies, and enthalpies of vaporization as given in refs 1 to 186. These data

have been used over the last century to develop many equations of state to describe the gas phase, the liquid phase, or the full surface of state of propane. The work presented here represents the latest development on equations of state for propane and is part of an international collaboration between the Ruhr-University in Bochum, the Helmut-Schmidt University of the Federal Armed Forces in Hamburg, and the National Institute of Standards and Technology in Boulder to characterize the properties of ethane (Bücker and Wagner¹⁸⁷), propane (this work), and the butanes (Bücker and Wagner¹⁸⁸). This work relies heavily on new measurements from these three laboratories. Pressure–density–temperature and vapor pressure measurements were made by Glos et al.⁴⁸ in Bochum and by McLinden¹²⁰ in Boulder; heat capacities and derived vapor pressures were made by Perkins et al.¹³⁹ in Boulder; and speed of sound measurements were made by Meier¹²¹ in Hamburg. These data together with other selected literature data form the basis of the new equation of state. The physical characteristics and properties of propane are given in Table 1.

Equations of State. Equations of state are used to calculate the thermodynamic properties of pure fluids and mixtures and are often expressed as a function of the pressure with independent variables of temperature and density or as a function of the Helmholtz energy with independent variables of temperature and density. Equations expressed in terms of the Helmholtz energy have the advantage that all thermodynamic properties are simple derivatives of the equation of state, and thus only one equation is required to obtain any thermodynamic property, including those that cannot be measured, such as entropy. The location of the saturation boundaries requires an iterative solution of the physical constraints on saturation (the so-called Maxwell criteria, i.e., equal pressures and Gibbs energies at constant temperature for phases in equilibrium). Equations expressed in terms of pressure require integration to calculate caloric properties such as heat capacities and sound speeds.

* Corresponding author. E-mail: eric.lemmon@nist.gov.

Table 1. Physical Constants and Characteristic Properties of Propane

symbol	quantity	value
R	molar gas constant	$8.314\,472\text{ J}\cdot\text{mol}^{-1}\cdot\text{K}^{-1}$
M	molar mass	$44.09562\text{ g}\cdot\text{mol}^{-1}$
T_c	critical temperature	369.89 K
p_c	critical pressure	4.2512 MPa
ρ_c	critical density	$5.00\text{ mol}\cdot\text{dm}^{-3}$
T_{tp}	triple point temperature	85.525 K
p_{tp}	triple point pressure	0.00017 Pa
ρ_{tpv}	vapor density at the triple point	$2.4\cdot 10^{-10}\text{ mol}\cdot\text{dm}^{-3}$
ρ_{tpl}	liquid density at the triple point	$16.626\text{ mol}\cdot\text{dm}^{-3}$
T_{nbp}	normal boiling point temperature	231.036 K
ρ_{nbpv}	vapor density at the normal boiling point	$0.0548\text{ mol}\cdot\text{dm}^{-3}$
ρ_{nbpl}	liquid density at the normal boiling point	$13.173\text{ mol}\cdot\text{dm}^{-3}$
T_0	reference temperature for ideal gas properties	273.15 K
p_0	reference pressure for ideal gas properties	0.001 MPa
h_0^0	reference ideal gas enthalpy at T_0	$26148.48\text{ J}\cdot\text{mol}^{-1}$
s_0^0	reference ideal gas entropy at T_0 and p_0	$157.9105\text{ J}\cdot\text{mol}^{-1}\cdot\text{K}^{-1}$

Equations of state are generally composed of an ideal gas contribution and a real gas contribution. The ideal gas portion is composed of the ideal gas law, $p = \rho RT$ (where p is pressure, ρ is molar density, T is temperature, and R is the gas constant), and an equation to describe the isobaric heat capacity at zero pressure. The real gas is generally composed of an analytical equation with multiple terms, with typical equations comprising 10 to 50 terms. High accuracy equations have often required more terms than those of low accuracy; however, the most recent equation by Lemmon and Jacobsen¹⁸⁹ for the properties of pentafluoroethane (R-125) introduced a modified functional form that allowed the magnitude of the exponents on temperature to be reduced dramatically. This allowed fitting the experimental data with fewer terms but with high accuracy. The work on R-125 was the forerunner for the development of the propane equation presented here.

Most equations of state that are explicit in the Helmholtz energy are made up of a combination of up to four different types of terms. The two most common are simple polynomial terms, $\rho^d T^t$ (where d and t are exponents in the polynomial terms), polynomial terms with the addition of an exponential part, $\rho^d T^t \exp(-\rho^j)$, Gaussian bell-shaped terms (which will be explained later), and nonanalytical terms that are present in only a few high accuracy equations and will not be discussed in this work. Further information is given by Span and Wagner.¹⁹⁰ Equations have almost always required high values of the exponent t to accurately calculate the properties of the fluid. These high values have led to some extremely unphysical behavior of the equation within the two-phase portion of the fluid. Although this area is not encountered in typical usage, it can cause problems with poorly written root solving routines and introduces false roots for two-phase states that appear to have a lower energy state and thus a more favorable state as compared with the true properties of the fluid. Various mixture models use states in the two-phase region of at least one of the pure fluid components in the calculation of the mixture properties, and in such applications, it is important that the two-phase region be well behaved. The modification of the functional form in the R-125 work expanded the exponential terms to include a temperature dependency, $\rho^d T^t \exp(-\rho^j) \exp(-T^m)$. This final piece allowed much lower values on the exponent t , which resulted in a more physically correct functional form and removed the possibility of false two-phase state points.

The work on propane continued the research into a functional form that can more correctly represent the true physical properties. The new term introduced in the R-125 equation was not used in this work, but rather emphasis was placed on redefining the usage of the Gaussian bell-shaped terms so that they would describe the change in the critical region, allowing the polynomial terms to model only the vapor and liquid states away from the critical region. This produced a similar effect in that the magnitude of the exponent t was greatly reduced.

Although pure compounds generally exist as an identifiable fluid only between the triple point temperature at the low extreme and the dissociation limit at the other extreme, every effort has been made to shape the functional form of the equation of state so that it extrapolates well to extreme values of temperature, pressure, and density. For example, at low temperatures, virial coefficients should approach negative infinity, and at extremely high temperatures and densities, isotherms should not cross one another and pressures should not be negative. Although such conditions exceed the physical limits of a normal fluid, there are applications that may extend into such regions, and the equation of state should be capable of describing these situations. Calculated properties shown here at extreme conditions that are not defined by experiment are intended only for qualitative examination of the behavior of the equation of state, and reliable uncertainty estimates cannot be established in the absence of experimental data.

Propane has a very low reduced triple point temperature (T_{tp}/T_c) of 0.23 that makes it a prime candidate for corresponding states applications. There are only a handful of other fluids, such as 1-butene, that have slightly lower values. In addition, a substantial quantity of high accuracy measurements is available for propane, allowing a reference equation of state to be developed. This reference equation of state can then be used in corresponding states models (described below) to predict properties of a host of other fluids. Since nearly all other fluids have reduced triple point temperatures higher than propane, all calculations for other fluids will be at states where experimental data were used to develop the propane surface.

Phase Equilibria of Propane

The single most important state of any fluid in the development of equations of state is the critical point. This point becomes the reducing parameter for the equation and defines liquid and vapor states, as well as supercritical states that behave like gases (when the density is less than the critical density) and like liquids (when the density exceeds the critical density). Nearly all fluids show similar behavior when their properties are scaled by the critical parameters. The law of corresponding states uses this aspect to predict properties for any fluid by mapping the surface of an unknown substance onto that for a well-known substance. The prediction can be improved as additional experimental data become available.

The triple point of a fluid defines the lowest temperature at which most substances can remain in the liquid state. Below this temperature only solid and gas states are possible in most applications, and the boundary between these states is known as the sublimation line. The melting (or freezing) line describes the boundary between the liquid and solid states for temperatures above the triple point. Equations of state such as that described here can calculate the properties at the melting point in the liquid phase but cannot calculate properties of the solid phase.

Critical and Triple Points. Critical parameters for propane have been reported by numerous authors and are listed in Table 2 (temperatures are given on ITS-90). The difficulties in the

Table 2. Summary of Critical Point Parameters

author	year	T_c	p_c	ρ_c
		K	MPa	mol·dm ⁻³
Abdulagatov et al. ²	1996	369.96		5.044
Abdulagatov et al. ³	1995	369.948		4.995
Ambrose and Tsonopoulos ⁵	1995	369.83	4.248	4.989
Barber ⁸	1964	369.693	4.261	5.13
Barber et al. ⁹	1982	369.995	4.26	5.063
Beattie et al. ¹²	1935	369.934	4.2567	5.13
Brunner ¹⁵	1985	369.955	4.243	
Brunner ¹⁶	1988	369.885	4.26	
Chun et al. ²⁵	1981	369.695	4.261	5.128
Clegg and Rowlinson ²⁸	1955	369.784	4.2486	4.92
Deschner and Brown ³⁶	1940	369.974	4.2658	5.08
Glowka ⁴⁹	1972	369.725	4.3529	5.025
Gomez-Nieto and Thodos ⁵¹	1977	369.945	4.2567	
Hainlen ⁵⁷	1894	375.124	4.9143	
Higashi ⁶⁴	2004	369.818	4.2465	5.148
Holcomb et al. ⁷⁰	1995	369.77	4.244	4.996
Honda et al. ⁷²	2008	370.01	4.26	5.035
Horstmann et al. ⁷³	2001	369.7	4.25	
Jou et al. ⁸⁰	1995	369.75	4.27	
Kay ⁸⁵	1964	369.924	4.2557	
Kay and Ramesek ⁸⁶	1953	369.79	4.2492	5.122
Kratzke ⁹⁸	1980	369.775	4.239	
Kratzke ⁹⁷	1983	369.825	4.246	4.955
Kreglewski and Kay ¹⁰⁰	1969	369.994	4.2603	5.125
Kuenen ¹⁰²	1903	370.124	4.3468	
Lebeau ¹⁰⁶	1905	370.624	4.5596	
Maass and Wright ¹¹⁴	1921	368.723		
Matschke and Thodos ¹¹⁶	1962	369.862	4.2568	
Matteson ¹¹⁷	1950	369.935	4.2568	4.976
Mousa ¹²⁷	1977	369.715	4.2537	4.853
Mousa et al. ¹²⁸	1972	369.715	4.2537	4.853
Olzewski ¹³²	1895	370.124	4.4583	
Opfell et al. ¹³³	1956	369.946	4.2548	4.987
Reamer et al. ¹⁴⁴	1949	369.957	4.2568	5.003
Roof ¹⁴⁸	1970	369.797	4.2492	
Sage and Lacey ¹⁵⁰	1940	369.679	4.2885	5.272
Sage et al. ¹⁵¹	1934	373.235	4.4354	5.268
Scheeline and Gilliland ¹⁵⁴	1939	372.013	4.3851	
Sliwinski ¹⁶¹	1969	369.816		
Thomas and Harrison ¹⁶⁸	1982	369.825	4.2471	4.955
Tomlinson ¹⁷⁰	1971	369.797		4.914
Yasumoto et al. ¹⁷⁸	2005	369.84	4.247	4.898
Yesavage et al. ¹⁸⁰	1969	369.957	4.2541	
this work	2009	369.89	4.2512	5.00

experimental determination of the critical parameters and impurities in the samples cause considerable differences among the results obtained by the various investigators. The critical density is difficult to determine accurately by experiment because of the infinite compressibility at the critical point and the associated difficulty of reaching thermodynamic equilibrium. Therefore, reported values for the critical density are often calculated by extrapolation of rectilinear diameters with measured saturation densities or by correlating single-phase data close to the critical point.

Figures 1, 2, and 3 show the critical temperature, pressure, and density as a function of the year that they were published. It is interesting to note how the differences between the reported values and the true critical point cannot be described as a function of the year published. With the availability of new high accuracy density data in the critical region, we allowed the reducing parameters (critical point) of the equation of state to be determined simultaneously with the other coefficients and exponents in the equation (as explained later). This is one of the first successful attempts to accurately derive the critical temperature and density solely from fitting experimental data for both the single phase and saturated states of a substance during the fitting process (also see Schmidt and Wagner¹⁹¹). Other such equations used critical parameters taken from a single experimental source. During many months of fitting, the range of the fitted values for the reducing parameters was

monitored closely. For temperature, it ranged from (369.86 to 369.92) K but was most stable around 369.89 K. This latter value was chosen as the critical temperature of propane. The critical density was also monitored closely and stayed remarkably centered around a value of 5.00 mol·dm⁻³, which was taken as the final value for the critical point. The critical pressure was determined from the final equation of state as a calculated point at the critical temperature and density. The resulting values of the critical properties are

$$T_c = (369.89 \pm 0.03) \text{ K} \quad (1)$$

$$\rho_c = (5.00 \pm 0.04) \text{ mol} \cdot \text{dm}^{-3} \quad (2)$$

and

$$p_c = (4.2512 \pm 0.005) \text{ MPa} \quad (3)$$

where all uncertainties are estimated as 2σ combined values. These values should be used for all property calculations with the equation of state.

Figure 4 shows calculations of the saturation properties from the equation of state very close to the critical point. The rectilinear diameter (the average of the saturated liquid and vapor densities) is also shown to be linear on this scale as it approaches the critical density value of 5.00 mol·dm⁻³ (as expected). In recent work on equations of state, including some of the equations in the work of Lemmon and Span,¹⁹² where equations of state were presented for 20 different fluids, the shape of the rectilinear diameter was checked to ensure that it was linear in the critical region. Cases where this line curved to the left or right indicated incorrect representation of the critical region properties, and either the critical density was modified or the values of the saturation states were changed until the rectilinear diameter was linear. This was especially important for fluids with limited or low accuracy data in the critical region because the high flexibility in the equation resulted in properties that were often incorrect. Adjusting the saturation lines and critical density so that the rectilinear diameter was linear resulted in much better representation of the critical properties, as is shown in this work.

The triple point temperature of propane was measured by Perkins et al.¹³⁹ by slowly applying a constant heat flux to a frozen sample contained within the cell of an adiabatic calorimeter and noting the sharp break in the temperature rise, resulting in

$$T_{tp} = 85.525 \text{ K} \quad (4)$$

Pavese and Besley¹⁹³ also measured the triple point temperature and reported a value of 85.528 K. The triple point pressure is extremely low and very difficult to measure directly, and thus it was calculated from the equation of state with a value of $p_{tp} = 0.00017 \text{ Pa}$.

Vapor Pressures. The boundaries between liquid and vapor are defined by saturation states, and ancillary equations can be used to give good estimates. These ancillary equations are not required when a full equation of state is available since application of the Maxwell criteria to the equation of state can yield the saturation states. This criteria for a pure fluid requires finding a state in the liquid and a state in the vapor that have the same temperature, pressure, and Gibbs energy. The ancillary equations can be used to give close estimates for the pressure and densities required in the iterative procedure to find the saturation states.

Table 3 summarizes the available experimental data for propane, including vapor pressures. Data labeled as "TRC" were

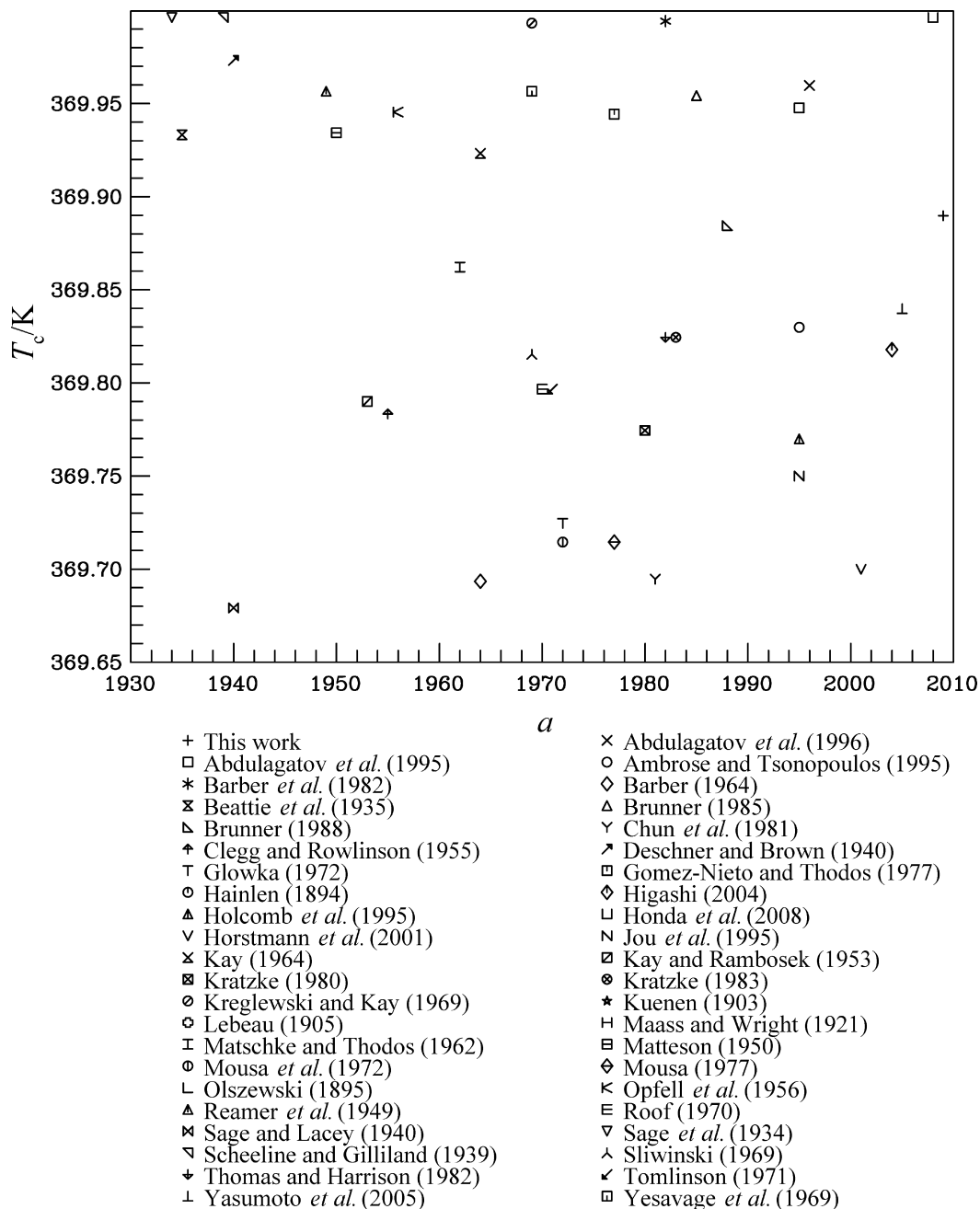


Figure 1. Reported critical temperatures T_c of propane as a function of the year a published.

taken from Frenkel *et al.*¹⁹⁴ and are explained in the data comparison section. The vapor pressure can be represented with the ancillary equation

$$\ln\left(\frac{p_\sigma}{p_c}\right) = \frac{T_c}{T}[N_1\theta + N_2\theta^{1.5} + N_3\theta^{2.2} + N_4\theta^{4.8} + N_5\theta^{6.2}] \quad (5)$$

where $N_1 = -6.7722$, $N_2 = 1.6938$, $N_3 = -1.3341$, $N_4 = -3.1876$, $N_5 = 0.94937$, $\theta = (1 - T/T_c)$, and p_σ is the vapor pressure. This equation is a modification of the equation first proposed by Wagner¹⁹⁵ in 1974. The original form of the equation has been used to model the vapor pressures for a large number of substances. The exponents on the first two terms are fixed by theory as explained by Wagner or by Lemmon and Goodwin.¹⁹⁶ In the modified form, the exponents on the last three terms are substance specific, and when accurate data

are available, the exponents can be fitted nonlinearly to produce an equation with very low uncertainties. In this work, the values of the coefficients and exponents were determined simultaneously with nonlinear fitting techniques. The values of the critical parameters are given above in eqs 1 to 3.

Saturated Densities. Table 3 summarizes the saturated liquid and vapor density data for propane. The saturated liquid density can be represented by the ancillary equation

$$\frac{\rho'}{\rho_c} = 1 + N_1\theta^{0.345} + N_2\theta^{0.74} + N_3\theta^{2.6} + N_4\theta^{7.2} \quad (6)$$

where $N_1 = 1.82205$, $N_2 = 0.65802$, $N_3 = 0.21109$, $N_4 = 0.083973$, $\theta = (1 - T/T_c)$, and ρ' is the saturated liquid density. The saturated vapor density can be represented by the equation

$$\ln\left(\frac{\rho''}{\rho_c}\right) = N_1\theta^{0.3785} + N_2\theta^{1.07} + N_3\theta^{2.7} + N_4\theta^{5.5} + N_5\theta^{10} + N_6\theta^{20} \quad (7)$$

where $N_1 = -2.4887$, $N_2 = -5.1069$, $N_3 = -12.174$, $N_4 = -30.495$, $N_5 = -52.192$, $N_6 = -134.89$, and ρ'' is the saturated vapor density. Values calculated from the equation of state with the Maxwell criteria were used in developing eq 7. The values of the coefficients and exponents for eqs 6 and 7 were determined with nonlinear least-squares fitting techniques.

Functional Form of the Equation of State

Modern equations of state are often formulated with the Helmholtz energy as the fundamental property with independent variables of density and temperature

$$a(\rho, T) = a^0(\rho, T) + a^r(\rho, T) \quad (8)$$

where a is the Helmholtz energy, $a^0(\rho, T)$ is the ideal gas contribution to the Helmholtz energy, and $a^r(\rho, T)$ is the residual Helmholtz energy, which corresponds to the influence of intermolecular forces. Thermodynamic properties can be calculated as derivatives of the Helmholtz energy. For example, the pressure is

$$p = \rho^2 \left(\frac{\partial a}{\partial \rho} \right)_T \quad (9)$$

Additional equations are given in Appendix A.

In modern applications, the functional form is explicit in the dimensionless Helmholtz energy, α , with independent variables of dimensionless density and temperature. The form of this equation is

$$\frac{a(\rho, T)}{RT} = \alpha(\delta, \tau) = \alpha^0(\delta, \tau) + \alpha^r(\delta, \tau) \quad (10)$$

where $\delta = \rho/\rho_c$ and $\tau = T/T_c$.

Properties of the Ideal Gas. The Helmholtz energy of the ideal gas is given by

$$a^0 = h^0 - RT - Ts^0 \quad (11)$$

The ideal gas enthalpy is given by

$$h^0 = h_0^0 + \int_{T_0}^T c_p^0 dT \quad (12)$$

where c_p^0 is the ideal gas heat capacity. The ideal gas entropy is given by

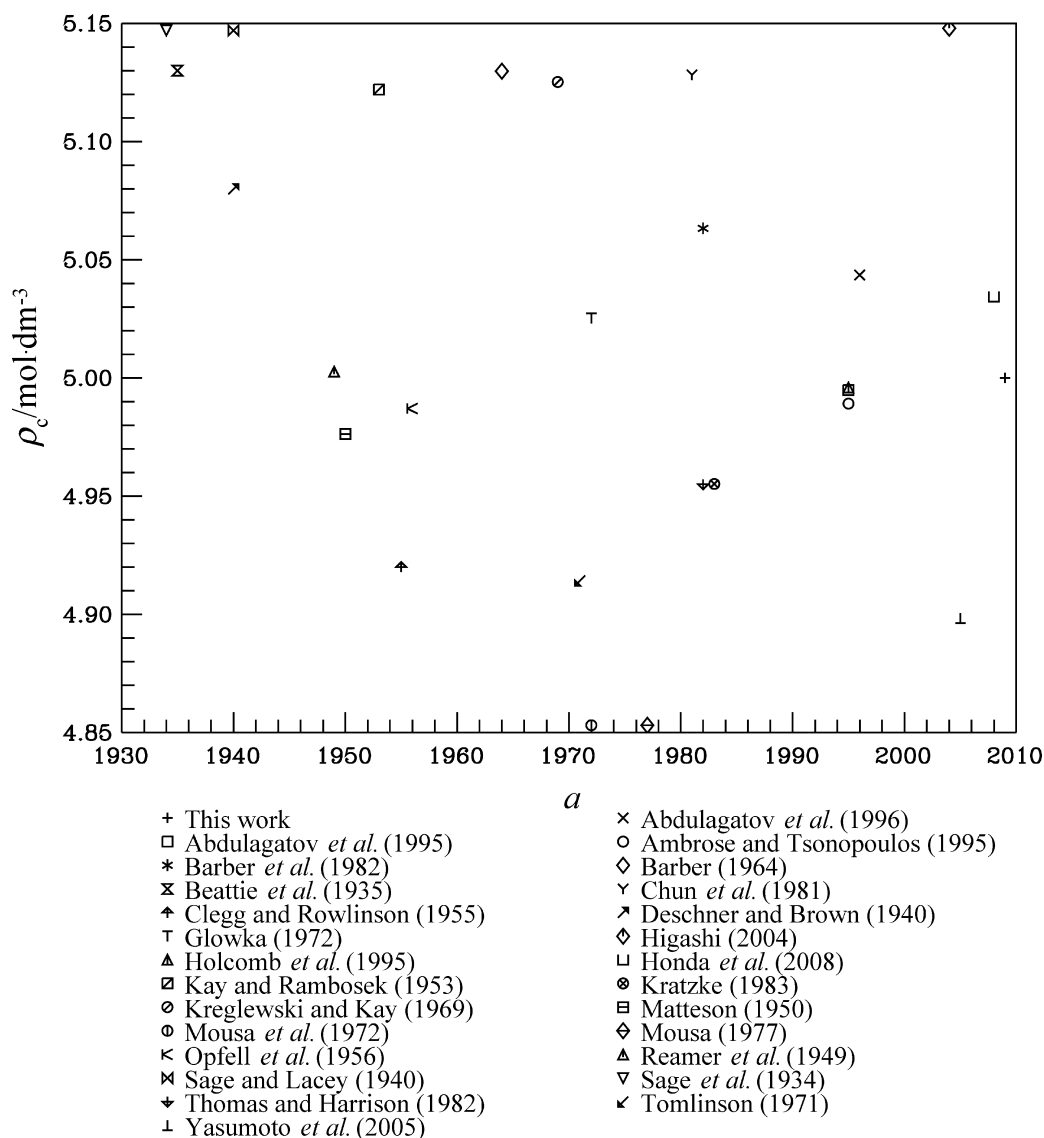


Figure 2. Reported critical densities ρ_c of propane as a function of the year a published.

$$s^0 = s_0^0 + \int_{T_0}^T \frac{c_p^0}{T} dT - R \ln \left(\frac{\rho T}{\rho_0 T_0} \right) \quad (13)$$

where ρ_0 is the ideal gas density at T_0 and p_0 [$\rho_0 = p_0/(T_0 R)$], and T_0 and p_0 are arbitrary reference states. Combining these equations results in the following equation for the Helmholtz energy of the ideal gas

$$a^0 = h_0^0 + \int_{T_0}^T c_p^0 dT - RT - T \left[s_0^0 + \int_{T_0}^T \frac{c_p^0}{T} dT - R \ln \left(\frac{\rho T}{\rho_0 T_0} \right) \right] \quad (14)$$

The ideal gas Helmholtz energy is given in dimensionless form by

$$\alpha^0 = \frac{h_0^0 \tau}{RT_c} - \frac{s_0^0}{R} - 1 + \ln \frac{\delta \tau_0}{\delta_0 \tau} - \frac{\tau}{R} \int_{\tau_0}^{\tau} \frac{c_p^0}{\tau^2} d\tau + \frac{1}{R} \int_{\tau_0}^{\tau} \frac{c_p^0}{\tau} d\tau \quad (15)$$

where $\delta_0 = \rho_0/\rho_c$ and $\tau_0 = T_0/T_0$. The ideal gas Helmholtz energy is often reported in a simplified form for use in equations of state as

$$\alpha^0 = \ln \delta - a_1 \ln \tau + \sum a_k \tau^{i_k} + \sum a_k \ln[1 - \exp(-b_k \tau)] \quad (16)$$

where standard models to describe the ideal gas heat capacity have been assumed.

Properties of the Real Fluid. Unlike the ideal gas, the real fluid behavior is often described with empirical models that are only loosely supported by theoretical considerations. Although it is possible to extract values such as second and

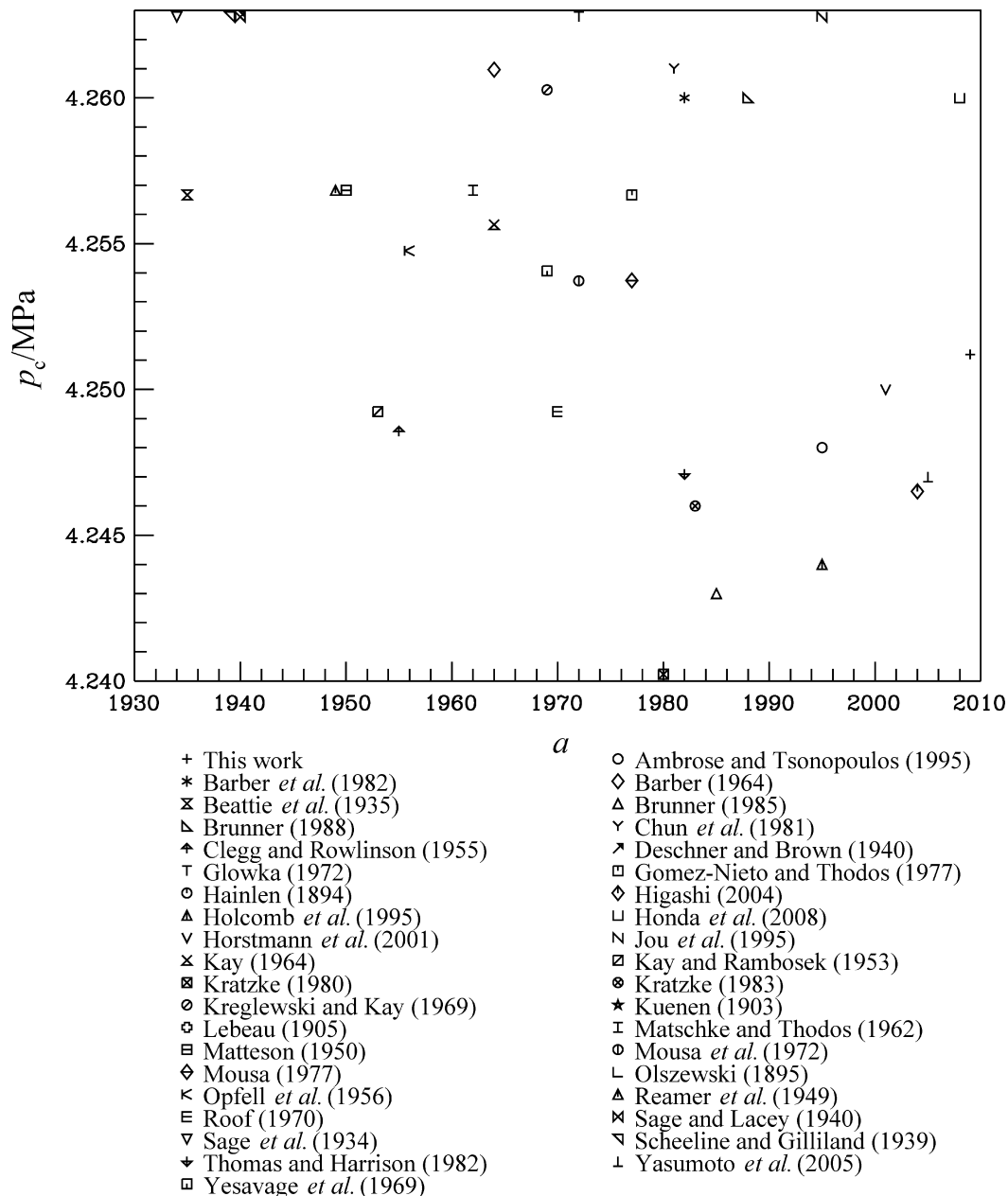


Figure 3. Reported critical pressures p_c of propane as a function of the year a published.

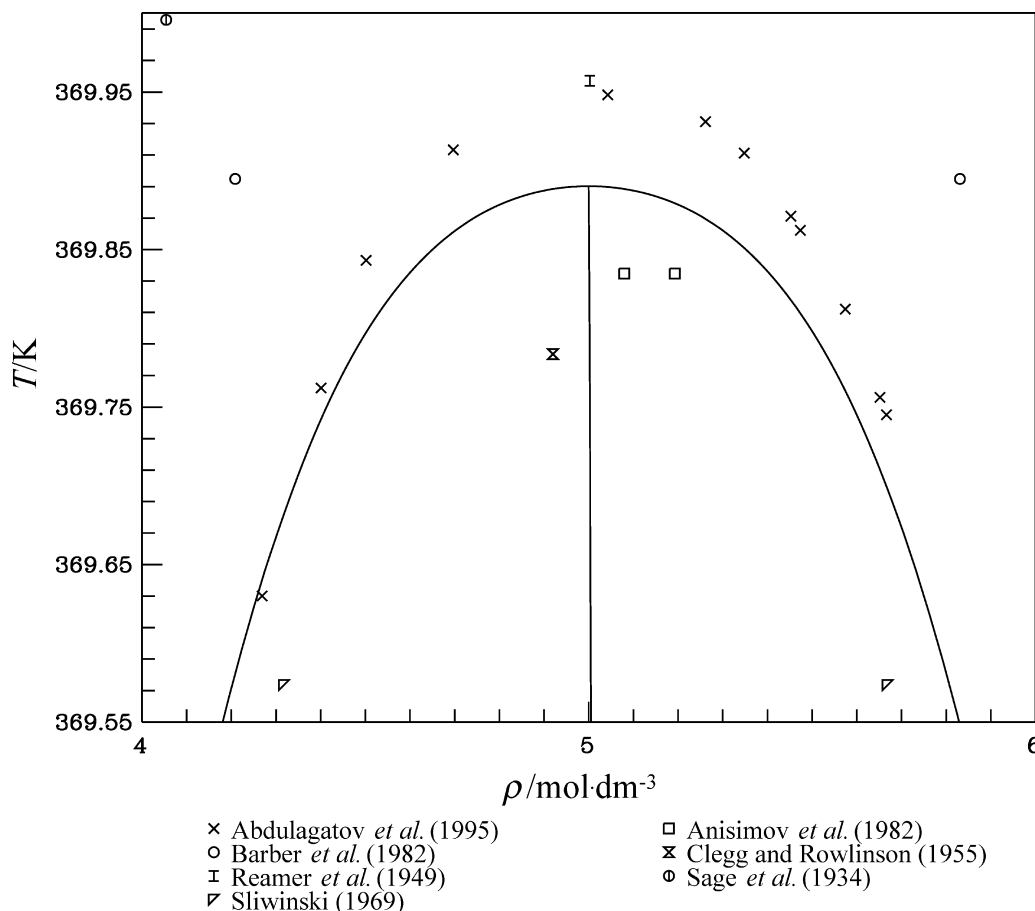


Figure 4. Saturation data in the critical region, the phase boundaries calculated from the Maxwell criteria, and the rectilinear diameter (average of the saturation values) as a function of density ρ and temperature T .

third virial coefficients from the fundamental equation, the terms in the equation are empirical, and any functional connection to theory is not entirely justified. The coefficients of the equation depend on the experimental data for the fluid and are constrained by various criteria explained elsewhere in this manuscript and in the works of Span and Wagner¹⁹⁷ and Lemmon and Jacobsen.¹⁸⁹

The common functional form for Helmholtz energy equations of state is

$$\alpha^r(\delta, \tau) = \sum N_k \delta^{d_k} \tau^{t_k} + \sum N_k \delta^{d_k} \tau^{t_k} \exp(-\delta^{l_k}) \quad (17)$$

where each summation typically contains 4 to 20 terms and where the index k points to each individual term. The values of t_k should be greater than zero, and d_k and l_k should be integers greater than zero. The functional form used in this work contains additional Gaussian bell-shaped terms

$$\alpha^r(\delta, \tau) = \sum N_k \delta^{d_k} \tau^{t_k} + \sum N_k \delta^{d_k} \tau^{t_k} \exp(-\delta^{l_k}) + \sum N_k \delta^{d_k} \tau^{t_k} \exp(-\eta_k(\delta - \varepsilon_k)^2 - \beta_k(\tau - \gamma_k)^2) \quad (18)$$

These terms were first successfully used by Setzmann and Wagner¹⁹⁸ for the methane equation of state. In that work, these terms are significant only near the critical point and rapidly go to zero away from the critical point. As such, they are extremely sensitive but powerful in modeling the properties of fluids in the critical region, especially for densities; their ability to model caloric properties (e.g., the steep increase of c_v near the critical point) is limited. As explained by Wagner and Pruss,¹⁹⁹ the

strong sensitivity of these terms made it difficult to determine the values automatically in the optimization and nonlinear fitting process. Thus, they determined these parameters based on comprehensive precalculations, and only two of them were fitted at a time in their nonlinear regression.

In this work, because linear optimization was not used, the coefficients and exponents of the Gaussian bell-shaped terms were fitted simultaneously with all of the other parameters in the equation of state. The terms had to be monitored closely to ensure that irregular behavior did not creep into the equation, as was evident by plots of heat capacities or speeds of sound. Initially, the values of η and β were forced to be in the same range as values in other equations reported by Wagner's group. However, the fitting algorithm tended toward much smaller values, indicating that these terms would be numerically significant over a broader range of temperature and density. The final values of these two coefficients in this work are significantly different from those of other equations, except for the very last term in the equation.

Most multiparameter equations of state have shortcomings that affect the determination of phase boundaries, the calculation of metastable states within the two-phase region, and the shapes of isotherms in the low-temperature vapor phase. These can be traced to the magnitude of t in τ^t in eq 17. As the temperature goes to zero, τ^t goes to infinity for values of $t > 1$, causing the pressure to increase rapidly to infinity. The effect is more pronounced for higher values of t . The primary use of terms with high values of t is for modeling the area around the critical region, where the properties change rapidly. Outside the critical region, the effect is dampened out with the δ^d contribution in

Table 3. Summary of Experimental Data for Propane

author	year	no. of points	temperature range	pressure range	density range	AARD ^a (%)
			(T/K)	(p/MPa)	(ρ/mol·dm ⁻³)	
Ideal Gas Isobaric Heat Capacities						
Beeck ¹³	1936	4	273 to 573			4.36
Chao et al. ²²	1973	19	50 to 1500			0.22
Dailey and Felsing ³¹	1943	8	344 to 693			0.591
Ernst and Büsser ⁴²	1970	4	293 to 353			0.205
Esper et al. ⁴³	1995	26	230 to 350			0.297
Goodwin and Lemmon ⁵²	1995	14	265 to 355			1.02
He et al. ⁶²	2002	4	293 to 323			0.206
Kistiakowsky et al. ⁹²	1940	14	148 to 259			0.523
Kistiakowsky and Rice ⁹³	1940	4	272 to 369			0.361
Scott ¹⁵⁶	1974	8	272 to 369			0.282
Trusler and Zarari ¹⁷²	1996	7	225 to 375			0.028
Yesavage ¹⁷⁹	1968	7	339 to 422			0.646
Vapor Pressures						
TRC (Frenkel et al.) ¹⁹⁴		120	130 to 426	0.00002 to 4.25		1.54
Barber et al. ¹⁰	1982	18	329 to 370	1.94 to 4.23		0.48
Beattie et al. ¹²	1935	17	323 to 348	1.71 to 2.85		0.018
Bobbo et al. ¹⁴	2002	5	248 to 295	0.203 to 0.875		0.095
Burrell and Robertson ¹⁸	1916	16	149 to 229	0.0004 to 0.101		18.3
Calado et al. ¹⁹	1997	13	175 to 211	0.003 to 0.037		0.786
Carruth and Kobayashi ²¹	1973	12	97.6 to 179	10 ⁻⁸ to 0.005		13.9
Chun ²⁴	1964	10	348 to 367	2.85 to 4.09		0.6
Clark ²⁶	1973	10	327 to 370	1.88 to 4.21		0.494
Clegg and Rowlinson ²⁸	1955	9	323 to 370	1.72 to 4.25		0.184
Coquelet et al. ²⁹	2003	17	277 to 353	0.536 to 3.13		0.108
Dana et al. ³²	1926	43	210 to 323	0.037 to 1.71		0.512
Delaplace ³⁵	1937	27	90.2 to 126	10 ⁻⁸ to 0.00001		40.9
Deschner and Brown ³⁶	1940	36	302 to 370	1.05 to 4.26		0.996
Djordjevich and Budenholzer ³⁸	1970	6	128 to 255	0.00001 to 0.259		6.92
Echols and Gelus ⁴⁰	1947	4	134 to 250	0.00003 to 0.215		11.6
Francis and Robbins ⁴⁵	1933	34	301 to 337	1.05 to 2.4		4.72
Giles and Wilson ⁴⁷	2000	4	273 to 333	0.474 to 2.12		0.144
Glos et al. ⁴⁸	2004	5	130 to 170	0.00002 to 0.002		0.741
Glos et al. ⁴⁸	2004	17	180 to 340	0.005 to 2.43		0.002
Hainlen ⁵⁷	1894	13	240 to 375	0.182 to 4.91		6.76
Hanson et al. ⁵⁸	1952	4	270 to 330	0.425 to 2		0.225
Harteck and Edse ⁵⁹	1938	145	163 to 232	0.001 to 0.107		0.846
Higashi et al. ⁶⁵	1994	8	283 to 313	0.644 to 1.38		0.891
Hipkin ⁶⁶	1966	4	267 to 366	0.385 to 3.92		1.25
Hirata et al. ⁶⁷	1969	5	197 to 273	0.016 to 0.476		0.728
Ho et al. ⁶⁹	2006	6	273 to 313	0.474 to 1.37		0.086
Holcomb et al. ⁷⁰	1995	19	240 to 364	0.149 to 3.79		0.198
Holcomb and Outcalt ⁷¹	1998	4	290 to 350	0.769 to 2.95		0.09
Honda et al. ⁷²	2008	4	320 to 369	1.6 to 4.23		0.164
Im et al. ⁷⁷	2006	6	313 to 363	1.37 to 3.77		0.201
Kahre ⁸¹	1973	5	278 to 328	0.548 to 1.88		0.581
Kay ⁸³	1970	10	332 to 368	2.07 to 4.14		0.41
Kay ⁸⁴	1971	9	332 to 390	2.07 to 4.83		0.438
Kayukawa et al. ⁸⁷	2005	13	240 to 360	0.148 to 3.55		0.102
Kemp and Egan ⁸⁹	1938	12	166 to 231	0.002 to 0.103		0.252
Kim and Kim ⁹⁰	2005	8	253 to 323	0.244 to 1.71		0.08
Kim et al. ⁹¹	2003	8	253 to 323	0.244 to 1.72		0.134
Kleiber ⁹⁵	1994	3	255 to 298	0.261 to 0.949		0.034
Kratzke ⁹⁸	1980	14	312 to 368	1.33 to 4.07		0.05
Kratzke and Müller ⁹⁹	1984	5	300 to 357	1.01 to 3.36		0.01
Laurance and Swift ¹⁰⁵	1972	10	311 to 344	1.3 to 2.64		0.068
Lee et al. ¹⁰⁷	2003	7	268 to 318	0.408 to 1.53		0.313
Lim et al. ¹¹⁰	2004	4	273 to 303	0.475 to 1.08		0.103
Lim et al. ¹¹¹	2004	6	268 to 313	0.408 to 1.36		0.362
Lim et al. ¹¹²	2006	13	268 to 323	0.408 to 1.71		0.228
Maass and Wright ¹¹⁴	1921	6	230 to 250	0.114 to 0.269		15.3
Manley and Swift ¹¹⁵	1971	5	244 to 311	0.176 to 1.3		0.177
McLinden ¹²⁰	2009	38	270 to 369	0.431 to 4.18		0.017
Miksovsky and Wichterle ¹²²	1975	6	303 to 369	1.08 to 4.19		0.269
Miranda et al. ¹²³	1976	5	266 to 355	0.385 to 3.28		0.66
Miyamoto and Uematsu ¹²⁵	2006	8	280 to 369	0.583 to 4.18		0.082
Mousa ¹²⁷	1977	11	335 to 370	2.2 to 4.25		0.496
Niesen and Rainwater ¹³⁰	1990	4	311 to 361	1.3 to 3.63		0.08
Noda et al. ¹³¹	1993	4	273 to 293	0.473 to 0.836		0.182
Outcalt and Lee ¹³⁵	2004	12	260 to 360	0.311 to 3.55		0.064
Park and Jung ¹³⁶	2002	5	273 to 313	0.475 to 1.37		0.049
Park et al. ¹³⁷	2007	5	273 to 313	0.472 to 1.37		0.298
Perkins et al. ¹³⁹	2009	53	85.5 to 241	10 ⁻⁸ to 0.154		0.162
Prasad ¹⁴¹	1982	14	298 to 368	0.941 to 4.07		1.76

Table 3. Continued

author	year	no. of points	temperature range	pressure range	density range	AARD ^a (%)
			(T/K)	(p/MPa)	($\rho/\text{mol}\cdot\text{dm}^{-3}$)	
Ramjugernath et al. ¹⁴²	2009	6	263 to 323	0.344 to 1.72		0.194
Reamer et al. ¹⁴⁴	1949	10	313 to 370	1.38 to 4.26		0.316
Reamer et al. ¹⁴⁵	1951	6	278 to 361	0.545 to 3.62		0.183
Sage et al. ¹⁵¹	1934	21	294 to 371	0.862 to 4.31		0.511
Scheeline and Gilliland ¹⁵⁴	1939	5	315 to 372	1.41 to 4.39		1.1
Schindler et al. ¹⁵⁵	1966	8	173 to 348	0.007 to 2.9		10.5
Seong et al. ¹⁵⁹	2008	6	273 to 323	0.476 to 1.71		0.302
Skripka et al. ¹⁶⁰	1970	10	123 to 273	0.000005 to 0.472		4.34
Teichmann ¹⁶⁶	1978	15	325 to 363	1.77 to 3.78		0.047
Thomas and Harrison ¹⁶⁸	1982	25	258 to 370	0.292 to 4.25		0.022
Tickner and Lossing ¹⁶⁹	1951	13	105 to 165	10 ⁻⁷ to 0.001		6.13
Uchytíl and Wichterle ¹⁷³	1983	32	296 to 368	0.893 to 4.12		0.156
Wichterle and Kobayashi ¹⁷⁷	1972	9	130 to 214	0.00002 to 0.044		2.47
Young ¹⁸²	1928	12	161 to 312	0.001 to 1.33		11.7
Yucelen and Kidnay ¹⁸⁴	1999	5	240 to 344	0.151 to 2.64		0.582
Zanolini ¹⁸⁵	1964	13	273 to 347	0.475 to 2.79		0.412
Zhang et al. ¹⁸⁶	2007	13	241 to 247	0.155 to 0.199		0.645
Saturated Liquid Densities						
TRC (Frenkel et al.) ¹⁹⁴		15	85.5 to 363		7.7 to 16.6	0.836
Abdulagatov et al. ³	1995	26	305 to 370		5.04 to 10.9	0.596
Anisimov et al. ⁶	1982	5	271 to 370		5.08 to 12	2.41
Barber et al. ¹⁰	1982	9	329 to 370		5.83 to 9.83	1.66
Carney ²⁰	1942	34	228 to 333		9.78 to 13.3	0.162
Clark ²⁶	1973	5	327 to 370		6.37 to 9.9	2.59
Clegg and Rowlinson ²⁸	1955	9	323 to 370		4.92 to 10.2	2.92
Dana et al. ³²	1926	12	273 to 329		9.96 to 12	0.557
Deschner and Brown ³⁶	1940	14	303 to 368		6.64 to 11	0.979
Ely and Kobayashi ⁴¹	1978	18	166 to 288		11.5 to 14.8	0.061
Glos et al. ⁴⁸	2004	27	90 to 340		9.34 to 16.5	0.003
Haynes and Hiza ⁶¹	1977	16	100 to 289		11.5 to 16.3	0.088
Helgeson and Sage ⁶³	1967	16	278 to 361		7.76 to 11.9	0.251
Holcomb et al. ⁷⁰	1995	14	313 to 364		7.42 to 10.6	0.071
Holcomb and Outcalt ⁷¹	1998	4	290 to 350		8.66 to 11.5	0.268
Jensen and Kurata ⁷⁸	1969	5	93.2 to 133		15.5 to 16.4	0.043
Kahre ⁸¹	1973	10	278 to 328		9.94 to 11.9	0.104
Kaminishi et al. ⁸²	1988	6	273 to 323		10.2 to 12	0.034
Kayukawa et al. ⁸⁷	2005	13	240 to 360		7.89 to 12.9	0.078
Klosek and McKinley ⁹⁶	1968	4	94.8 to 130		15.6 to 16.4	0.036
Kratzke and Müller ⁹⁹	1984	5	245 to 325		10.1 to 12.8	0.043
Legatski et al. ¹⁰⁸	1942	20	228 to 333		9.78 to 13.3	0.21
Luo and Miller ¹¹³	1981	6	220 to 289		11.5 to 13.5	0.055
Maass and Wright ¹¹⁴	1921	13	195 to 249		12.7 to 14.1	0.31
McClune ¹¹⁸	1976	17	93.2 to 173		14.6 to 16.4	0.037
Miyamoto and Uematsu ¹²⁶	2007	6	280 to 365		7.2 to 11.8	0.144
Niesen and Rainwater ¹³⁰	1990	4	311 to 361		7.71 to 10.7	0.038
Orrit and Laupretre ¹³⁴	1978	31	86.7 to 244		12.8 to 16.6	0.026
Reamer et al. ¹⁴⁴	1949	10	313 to 370		5 to 10.6	0.54
Rodosevich and Miller ¹⁴⁷	1973	4	91 to 115		15.9 to 16.5	0.049
Sage et al. ¹⁵¹	1934	21	294 to 371		6.51 to 11.4	2.42
Seeman and Urban ¹⁵⁷	1963	27	278 to 299		11.1 to 11.9	0.056
Sliwinski ¹⁶²	1969	14	283 to 372		5.67 to 11.7	0.342
Thomas and Harrison ¹⁶⁸	1982	22	258 to 369		6.08 to 12.4	0.12
Tomlinson ¹⁷⁰	1971	11	278 to 323		10.2 to 11.8	0.047
van der Vet ¹⁷⁴	1937	9	283 to 323		10.2 to 11.7	0.079
Saturated Vapor Densities						
Abdulagatov et al. ³	1995	11	342 to 370		1.4 to 4.7	1.65
Anisimov et al. ⁶	1982	1	368		3.61	0.833
Barber et al. ¹⁰	1982	9	329 to 370		1.02 to 4.21	0.886
Clark ²⁶	1973	5	327 to 370		0.981 to 3.67	3.9
Clegg and Rowlinson ²⁸	1955	9	323 to 370		0.859 to 4.92	1.55
Dana et al. ³²	1926	5	290 to 323		0.381 to 0.859	0.967
Deschner and Brown ³⁶	1940	14	303 to 368		0.454 to 3.58	3.69
Glos et al. ⁴⁸	2004	24	110 to 340		0 to 1.34	2.11
Helgeson and Sage ⁶³	1967	16	278 to 361		0.267 to 2.4	0.597
Holcomb and Outcalt ⁷¹	1998	4	290 to 350		0.374 to 1.72	1.1
Holcomb et al. ⁷⁰	1995	14	313 to 364		0.689 to 2.69	0.958
Niesen and Rainwater ¹³⁰	1990	4	311 to 361		0.646 to 2.42	1.36
Reamer et al. ¹⁴⁴	1949	10	313 to 370		0.695 to 5	1.89
Sage et al. ¹⁵¹	1934	21	294 to 371		0.433 to 4.05	2.42
Sliwinski ¹⁶²	1969	15	283 to 370		0.314 to 4.32	0.557
Thomas and Harrison ¹⁶⁸	1982	11	323 to 369		0.876 to 3.92	0.115

Table 3. Continued

author	year	no. of points	temperature range (T/K)	pressure range (p/MPa)	density range ($\rho/\text{mol}\cdot\text{dm}^{-3}$)	AARD ^a (%)
Enthalpies of Vaporization						
Dana et al. ³²	1926	14	234 to 293			1.12
Guigo et al. ⁵⁴	1978	12	186 to 363			0.49
Helgeson and Sage ⁶³	1967	14	311 to 330			0.931
Kemp and Egan ⁸⁹	1938	1	231			0.046
Sage et al. ¹⁴⁹	1939	16	313 to 348			2.21
Densities						
Aalto and Liukkonen ¹	1996	55	343 to 373	3.99 to 6.99	5.58 to 9.97	0.988
Babb and Robertson ⁷	1970	63	308 to 473	63.8 to 1070	13 to 18.5	0.368
Beattie et al. ¹²	1935	82	370	4.25 to 4.29	4.2 to 5.92	9.12
Burgoyne ¹⁷	1940	41	243 to 294	0.507 to 6.08	11.4 to 13.2	1.26
Cherney et al. ²³	1949	25	323 to 398	1.08 to 4.98	0.383 to 2.58	0.1
Claus et al. ²⁷	2002	130	340 to 520	1.99 to 30.2	0.543 to 11.5	0.015
Dawson and McKetta ³³	1960	18	243 to 348	0.049 to 0.184	0.021 to 0.071	0.034
Defibaugh and Moldover ³⁴	1997	945	245 to 372	1.2 to 6.51	6.23 to 13	0.094
Deschner and Brown ³⁶	1940	275	303 to 609	0.101 to 14.8	0.023 to 11.7	0.667
Dittmar et al. ³⁷	1962	335	273 to 413	0.981 to 103	7.26 to 13.4	0.218
Ely and Kobayashi ⁴¹	1978	222	166 to 324	0.096 to 42.8	11.5 to 14.8	0.09
Galicía-Luna et al. ⁴⁶	1994	60	323 to 398	2.5 to 39.5	6.34 to 12.1	0.075
Glos et al. ⁴⁸	2004	72	95 to 340	0.201 to 12.1	0.078 to 16.5	0.003
Golovskoi et al. ⁵⁰	1991	155	88.2 to 272	1.54 to 61	13.5 to 16.7	0.204
Haynes ⁶⁰	1983	196	90 to 300	0.614 to 37.5	11.2 to 16.8	0.123
Huang et al. ⁷⁴	1966	36	173 to 273	0 to 34.5	12 to 15.2	0.386
Jepson et al. ⁷⁹	1957	8	457 to 529	0.993 to 3.29	0.273 to 0.815	0.521
Kayukawa et al. ⁸⁷	2005	192	240 to 380	0.148 to 7.07	0.27 to 13.1	0.104
Kayukawa and Watanabe ⁸⁸	2001	26	305 to 380	0.583 to 3.81	0.253 to 1.93	0.169
Kitajima et al. ⁹⁴	2005	38	270 to 425	3.66 to 28.7	6.81 to 12.2	0.171
Kratzke and Müller ⁹⁹	1984	60	247 to 491	2.24 to 60.9	10 to 12.8	0.035
Manley and Swift ¹¹⁵	1971	19	244 to 333	2.07 to 11	10 to 13.1	0.111
McLinden ¹²⁰ (excluding critical region)	2009	261	265 to 500	0.262 to 35.9	0.101 to 13.2	0.021
McLinden ¹²⁰ (critical region)	2009	33	369 to 372	4.24 to 4.42	4.0 to 5.56	0.750
Miyamoto and Uematsu ¹²⁵	2006	63	340 to 400	3 to 200	7.59 to 14.3	0.099
Miyamoto and Uematsu ¹²⁶	2007	59	280 to 365	0.581 to 4.03	7.21 to 11.8	0.153
Miyamoto et al. ¹²⁴	2007	147	280 to 440	1 to 200	7.59 to 15	0.094
Perkins et al. ¹³⁹	2009	253	99.7 to 346	1.61 to 34.7	10.4 to 16.3	0.012
Prasad ¹⁴¹	1982	111	373 to 423	0.177 to 4.66	0.052 to 2.5	0.634
Reamer et al. ¹⁴⁴	1949	306	311 to 511	0.101 to 68.9	0.024 to 13.1	0.145
Richter et al. ¹⁴⁶	2009	1	273	0.101	0.046	0.009
Rodosevich and Miller ¹⁴⁷	1973	4	91 to 115	0.013 to 0.05	15.9 to 16.5	0.048
Sage et al. ¹⁵¹	1934	154	294 to 378	0.172 to 20.7	0.056 to 12.3	1.15
Seeman and Urban ¹⁵⁷	1963	28	203 to 230	0.101	13.2 to 13.9	0.038
Seibt ¹⁵⁸	2008	108	373	0.07 to 29.8	0.023 to 10.7	0.568
Starling et al. ¹⁶³	1984	25	273 to 323	0.05 to 1.4	0.021 to 0.657	0.027
Straty and Palavra ¹⁶⁴	1984	144	363 to 598	0.221 to 34.6	0.051 to 7.88	0.179
Teichmann ¹⁶⁶	1978	148	323 to 573	2.77 to 60.9	2.44 to 10.5	0.075
Thomas and Harrison ¹⁶⁸	1982	834	258 to 623	0.511 to 40	0.8 to 12.5	2.73
Tomlinson ¹⁷⁰	1971	40	278 to 328	1.06 to 13.8	10.3 to 12	0.123
Warowny et al. ¹⁷⁶	1978	51	373 to 423	0.319 to 6.31	0.105 to 3.85	0.332
Second Virial Coefficients ^a						
TRC (Frenkel et al.) ¹⁹⁴		27	244 to 523			5.11
Barber et al. ¹⁰	1982	8	329 to 398			4.55
Barkan ¹¹	1983	18	220 to 560			1.36
Chun ²⁴	1964	7	370 to 493			20.1
Dawson and McKetta ³³	1960	6	243 to 348			11
Esper et al. ⁴³	1995	13	230 to 350			10
Eubank et al. ⁴⁴	1973	13	260 to 550			15.4
Glos et al. ⁴⁸	2004	5	260 to 340			0.852
Gunn ⁵⁵	1958	11	311 to 511			6.69
Hahn et al. ⁵⁶	1974	10	211 to 493			2.49
Hirschfelder et al. ⁶⁸	1942	17	303 to 570			6.83
Huff et al. ⁷⁵	1963	5	311 to 511			4.99
Kretschmer and Wiebe ¹⁰¹	1951	3	273 to 323			16.2
Lichtenthaler and Schäfer ¹⁰⁹	1969	5	288 to 323			8.18
McGlashan and Potter ¹¹⁹	1962	12	295 to 413			4.2
Patel et al. ¹³⁸	1988	4	373 to 423			2.39
Pompe and Spurling ¹⁴⁰	1974	34	294 to 609			8.49
Prasad ¹⁴¹	1982	6	373 to 423			2.15
Schäfer et al. ¹⁵³	1974	5	353 to 512			9.2
Strein et al. ¹⁶⁵	1971	11	296 to 493			1.15
Thomas and Harrison ¹⁶⁸	1982	23	323 to 623			0.71
Trusler et al. ¹⁷¹	1996	7	225 to 375			0.695
Warowny et al. ¹⁷⁶	1978	6	373 to 423			2.02

Table 3. Continued

author	year	no. of points	temperature range (T/K)	pressure range (p/MPa)	density range ($\rho/\text{mol}\cdot\text{dm}^{-3}$)	AARD ^a (%)
Second Acoustic Virial Coefficients ^a						
Esper et al. ⁴³	1995	26	230 to 350			11.4
Goodwin and Lemmon ⁵²	1995	14	265 to 355			7.03
He et al. ⁶²	2002	4	293 to 323			12.4
Trusler and Zarari ¹⁷²	1996	7	225 to 375			4.85
Third Virial Coefficients ^a						
Chun ²⁴	1964	7	370 to 493			21.5
Glos et al. ⁴⁸	2004	5	260 to 340			3.71
Patel et al. ¹³⁸	1988	4	373 to 423			4.89
Pompe and Spurling ¹⁴⁰	1974	37	294 to 609			10.2
Thomas and Harrison ¹⁶⁸	1982	19	343 to 623			1.31
Trusler et al. ¹⁷¹	1996	7	225 to 375			16.2
Warowny et al. ¹⁷⁶	1978	6	373 to 423			1.66
Third Acoustic Virial Coefficients ^a						
Trusler and Zarari ¹⁷²	1996	7	225 to 375			31.3
Enthalpies						
Van Kasteren and Zeldenrust ¹⁷⁵	1979	17	110 to 270	5.07		0.091
Speeds of Sound						
Goodwin and Lemmon ⁵²	1995	80	265 to 355	0.008 to 1.76		0.077
He et al. ⁶²	2002	24	293 to 323	0.203 to 0.669		0.086
Hurly et al. ⁷⁶	2003	11	298	0.099 to 0.831		0.006
Lacam ¹⁰³	1956	200	298 to 498	1.01 to 101		1.48
Meier ¹²¹	2009	298	240 to 420	1.3 to 100		0.012
Niepmann ¹²⁹	1984	227	200 to 340	0.02 to 60.6		0.323
Rao ¹⁴³	1971	10	143 to 228	<0.9		16.4
Terres et al. ¹⁶⁷	1957	95	293 to 448	<11.8		1.99
Trusler and Zarari ¹⁷²	1996	68	225 to 375	0.01 to 0.851		0.004
Younglove ¹⁸³	1981	180	90 to 300	<35		0.05
Isobaric Heat Capacities						
Beeck ¹³	1936	4	273 to 573	0.101		4.35
Dobratz ³⁹	1941	4	294 to 444	0.101		5.22
Ernst and Büsser ⁴²	1970	36	293 to 353	0.049 to 1.37		0.141
Kistiakowsky and Rice ⁹³	1940	5	294 to 361	0.101		0.405
Lammers et al. ¹⁰⁴	1978	16	120 to 260	2.53 to 5.07		1.21
Sage et al. ¹⁵²	1937	10	294 to 444	0.101		4.84
Van Kasteren and Zeldenrust ¹⁷⁵	1979	24	110 to 270	2.53 to 5.07		1.68
Yesavage et al. ¹⁸¹	1969	199	116 to 422	1.72 to 13.8		2.38
Saturation Heat Capacities						
Cutler and Morrison ³⁰	1965	7	91.1 to 105			0.768
Dana et al. ³²	1926	12	242 to 292			3.15
Goodwin ⁵³	1978	78	81.1 to 289			0.277
Guigo et al. ⁵⁴	1978	22	163 to 363			0.354
Kemp and Egan ⁸⁹	1938	22	89.7 to 230			0.349
Perkins et al. ¹³⁹	2009	223	88.9 to 344			0.321
Isochoric Heat Capacities						
Abdulagatov et al. ²	1996	88	370 to 472		5.04	7.3
Abdulagatov et al. ³	1995	37	305 to 370		1.4 to 10.9	12.2
Anisimov et al. ⁶	1982	52	271 to 374		3.61 to 12	10.3
Goodwin ⁵³	1978	128	85.6 to 337		11.2 to 16.3	1.23
Kitajima et al. ⁹⁴	2005	38	270 to 425		6.81 to 12.2	6.05
Perkins et al. ¹³⁹	2009	231	101 to 345		10.4 to 16.3	0.843
Two-Phase Isochoric Heat Capacities						
Abdulagatov et al. ²	1996	70	292 to 370		5.04	1.4
Abdulagatov et al. ⁴	1997	1582	288 to 370		1.4 to 10.9	1.88
Anisimov et al. ⁶	1982	95	85.7 to 370		3.61 to 12	1.7
Guigo et al. ⁵⁴	1978	22	163 to 363		7.32	0.348
Perkins et al. ¹³⁹	2009	223	88.9 to 344		9.08 to 16.5	1.0

^a Values are given as average absolute differences in $\text{cm}^3\cdot\text{mol}^{-1}$ for the second virial coefficients and in $\text{cm}^6\cdot\text{mol}^{-2}$ for the third virial coefficients.

the vapor phase and the $\exp(-\delta^l)$ part in the liquid phase. Thus, at temperatures approaching the triple point temperature in the vapor phase, where the density is very small, higher values of d in the δ^d part of each term result in a smaller influence of the exponential increase in temperature. Likewise, in the liquid region at similar temperatures, a higher value of l dampens out the effect of the τ^l part in the term. At densities near the critical density, δ^d

$\exp(-\delta^l)$ approaches a constant of around 0.4, and the shape of the τ^l contribution can greatly affect the critical region behavior of the model. Additional graphs and descriptions of these effects from different terms are explained below and in the work of Tillner-Roth.²⁰⁰ Equations of state should use the smallest possible value for t in the polynomial terms; in the new equation for propane developed here, the highest value of t is 4.62.

Fitting Procedures. The development of an equation of state is a process of correlating selected experimental data by least-squares fitting methods with a model that is generally empirical in nature but is designed to exhibit proper limiting behavior in the ideal gas and low density regions and to extrapolate to temperatures and pressures higher than those defined by experiment. In all cases, experimental data are considered paramount, and the validity of any equation of state is established by its ability to represent the thermodynamic properties of the fluid within the uncertainty of the experimental values. The selected data are usually a subset of the available database determined by the correlator to be representative of the most accurate values measured. The type of fitting procedure (e.g., nonlinear versus linear fitting of the parameters) determines how the experimental data will be used. In this work, a small subset of data was used in nonlinear fitting due to the extensive calculations required to develop the equation. The resulting equation was then compared to all experimental data to verify that the data selection was sufficient to accurately represent the available data.

One of the biggest advantages in nonlinear fitting is the ability to fit experimental data using all of the properties that were measured. For example, in linear fitting of the speed of sound, a preliminary equation of state is required to transform measured values of pressure and temperature to the independent variables of density and temperature required by the equation of state. Additionally, the ratio c_p/c_v is required (also from a preliminary equation) to fit sound speed with linear methods. Nonlinear fitting can use pressure, temperature, and sound speed directly without any transformation of the input variables. Shock wave measurements of the Hugoniot curve are another example where nonlinear fitting can directly use pressure–density–enthalpy measurements even when the temperature for any given point is unknown. Another advantage in nonlinear fitting is the ability to use “greater than” or “less than” operators for controlling the extrapolation behavior of properties such as heat capacities or pressures at low or high temperatures. In linear fitting, only equalities can be used; thus curves are often extrapolated by hand, and data points are manually taken from the curves at various temperatures to give the fit the proper shape. With successive fitting, the curves are updated until the correlator is satisfied with the final qualitative behavior. In nonlinear fitting, curves can be controlled by ensuring that a calculated value along a constant property path is always greater (or less) than a previous value; thus, only the shape is specified, not the magnitude. The nonlinear fitter then determines the best value for the properties based on other information in a specific region.

Equations have been developed with linear regression techniques for several decades by fitting comprehensive wide-ranging sets of $p\rho T$ data, isochoric heat capacity data, linearized sound speed data (as a function of density and temperature), second virial coefficients, and vapor pressures calculated from an ancillary equation. This process typically results in final equations with 25 to 40 terms. A cyclic process is sometimes used consisting of linear optimization, nonlinear fitting, and repeated linearization. Ideally this process is repeated until differences between the linear and nonlinear solutions are negligible. In certain cases, this convergence could not be reached—this led to the development of the “quasi-nonlinear” optimization algorithm. However, since this algorithm still involves linear steps, it could not be used in combination with “less than” or “greater than” relations. Details about the quasi-nonlinear regression algorithm can be found elsewhere (Wagner,¹⁹⁵ Wagner and Pruss¹⁹⁹).

In the case of propane, only nonlinear methods were used here to arrive at the final equation. A good preliminary equation is required as a starting point in the nonlinear fitting process; in this work, the equation of Bückner and Wagner¹⁸⁷ for ethane was employed. Nonlinear fitting techniques were used to shorten and improve upon this equation. The exponents for density and temperature, given in eq 18 as t_k , d_k , and l_k , along with the coefficients and exponents in the Gaussian bell-shaped terms, were determined simultaneously with the coefficients of the equation. In addition, the terms in the ideal gas heat capacity equation and the reducing parameters (critical point) of the equation of state were fitted. Thus, with an 18 term equation, there were at times up to 90 values being fitted simultaneously to derive the equation presented here. The end result has very little similarity to the functional form for ethane with which it began.

The nonlinear algorithm adjusted the parameters of the equation of state to minimize the overall sum of squares of the deviations of calculated properties from the input data, where the residual sum of squares was represented as

$$S = \sum W_p F_p^2 + \sum W_\rho F_\rho^2 + \sum W_{c_v} F_{c_v}^2 + \dots \quad (19)$$

where W is the weight assigned to each data point and F is the function used to minimize the deviations. The equation of state was fitted to $p\rho T$ data with either deviations in pressure, $F_p = (p_{\text{data}} - p_{\text{calc}})/p_{\text{data}}$, for vapor phase and critical region data, or deviations in density, $F_\rho = (\rho_{\text{data}} - \rho_{\text{calc}})/\rho_{\text{data}}$, for liquid phase data. Since the calculation of density as a function of temperature and pressure requires an iterative solution that greatly increases calculation time during the fitting process, the nearly equivalent, noniterative form

$$F_\rho = \frac{(p_{\text{data}} - p_{\text{calc}})}{\rho_{\text{data}}} \left(\frac{\partial \rho}{\partial p} \right)_T \quad (20)$$

was used instead, where p_{calc} and the derivative of density with respect to pressure were calculated at the ρ and T of the data point. Other experimental data were fitted in a like manner, e.g., $F_w = (w_{\text{data}} - w_{\text{calc}})/w_{\text{data}}$ for the speed of sound. The weight for each selected data point was individually adjusted according to type, region, and uncertainty. Typical values of W are 1 for $p\rho T$ and vapor pressure values, 0.05 for heat capacities, and 10 to 100 for vapor sound speeds. The equation of state was constrained to the critical parameters by adding the values of the first and second derivatives of pressure with respect to density at the critical point, multiplied by some arbitrary weight, to the sum of squares. In this manner, the calculated values of these derivatives would be zero at the selected critical point given in eqs 1 to 3.

To reduce the number of terms in the equation, terms were eliminated in successive fits by either deleting the term that contributed least to the overall sum of squares in a previous fit or by combining two terms that had similar values of the exponents (resulting in similar contributions to the equation of state). After a term was eliminated, the fit was repeated until the sum of squares for the resulting new equation was of the same order of magnitude as the previous equation. The final functional form for propane included 18 terms, 11 of which were extended polynomials and 7 were Gaussian bell-shaped terms.

The exponents on density in the equation of state must be positive integers so that the derivatives of the Helmholtz energy with respect to density have the correct theoretical expansion around the ideal gas limit. Since noninteger values for the

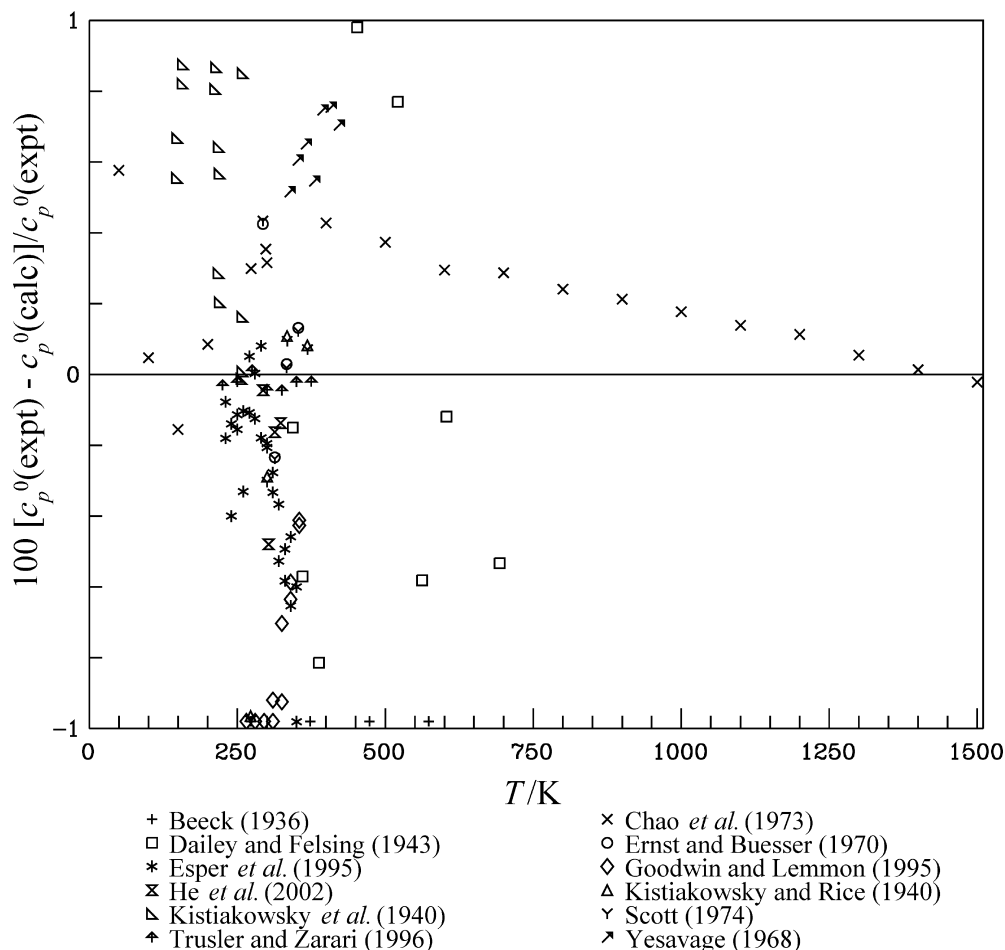


Figure 5. Comparisons of ideal gas heat capacities c_p^0 calculated with the equation of state to experimental and theoretical data as a function of temperature T .

density exponents resulted from the nonlinear fitting methods, a sequential process of rounding each density exponent to the nearest integer, followed by refitting the other parameters to minimize the overall sum of squares, was implemented until all of the density exponents in the final form were positive integers. A similar process was used for the temperature exponents to reduce the number of significant figures to one or two past the decimal point.

In addition to reducing the number of individual terms in the equation compared to that produced by conventional linear least-squares methods, the extrapolation behavior of the shorter equations is generally more accurate, partially because there are fewer degrees of freedom in the final equation. In the longer equations, two or more correlated terms are often needed to match the accuracy of a single term in the nonlinear fit. The values of these correlated terms can be large in magnitude and can lead to unreasonable behavior outside the range of validity. Span and Wagner¹⁹⁷ discuss the effects at high temperatures and pressures from intercorrelated terms.

The new fitting techniques and criteria that were created for the development of the R-125 equation of state (Lemmon and Jacobsen¹⁸⁹) were also used in the development of the propane equation of state. The details, which will not be repeated here, included proper handling of the second and third virial coefficients, elimination of the curvature of low-temperature isotherms in the vapor phase, control of the two-phase loops and the number of false two-phase solutions, convergence of the extremely high temperature isotherms to a single line (resulting

from the term with $t = 1$ and $d = 4$), and proper control of the ideal curves (e.g., the Joule inversion curve). The R-125 paper describes what properties were added to the sum of squares so that the equation of state would behave properly and meet these criteria. As was done with R-125, a minimum number of simple polynomial terms (five) were used: three to represent the second virial coefficients ($d = 1$), one for the third virial coefficients ($d = 2$), and one for the term for the extreme conditions ($d = 4$). This final term is described in detail by Lemmon and Jacobsen.¹⁸⁹

Upon completion of the equation of state for propane, we began fitting an equation for propylene and have since found even better constraints and methods to control the derivatives of the equation of state and to force the extrapolation of the equation to near 0 K without any adverse behavior. This new work was not applied to propane since the equation had been completed and released in version 8 of the REFPROP software (Lemmon et al.²⁰¹). These new techniques will be described in the forthcoming publication of Lemmon et al.²⁰²

Equation of State of Propane

Previous Equations of State. Researchers worldwide have developed many equations of state for propane. Although a preliminary equation of state was presented in the work on the butanes by Bucker and Wagner¹⁸⁸ in 2006, it was intended only as an interim equation of state until the one presented here was finished, and it will not be referred to hereafter. A short equation

Table 4. Parameters and Coefficients of the Equation of State

k	N_k	t_k	d_k	l_k	η_k	β_k	γ_k	ε_k
1	0.042910051	1.00	4	-				
2	1.7313671	0.33	1	-				
3	-2.4516524	0.80	1	-				
4	0.34157466	0.43	2	-				
5	-0.46047898	0.90	2	-				
6	-0.66847295	2.46	1	1				
7	0.20889705	2.09	3	1				
8	0.19421381	0.88	6	1				
9	-0.22917851	1.09	6	1				
10	-0.60405866	3.25	2	2				
11	0.066680654	4.62	3	2				
12	0.017534618	0.76	1	-	0.963	2.33	0.684	1.283
13	0.33874242	2.50	1	-	1.977	3.47	0.829	0.6936
14	0.22228777	2.75	1	-	1.917	3.15	1.419	0.788
15	-0.23219062	3.05	2	-	2.307	3.19	0.817	0.473
16	-0.092206940	2.55	2	-	2.546	0.92	1.500	0.8577
17	-0.47575718	8.40	4	-	3.28	18.8	1.426	0.271
18	-0.017486824	6.75	1	-	14.6	547.8	1.093	0.948

of state was presented for propane in the work of Span and Wagner²⁰³ in 2003 to demonstrate the applicability of one functional form with fixed exponents to represent the properties of a broad range of nonpolar fluids. This form was not aimed at reaching the highest accuracy possible but to establish a new class of equations with a stable functional form that could be applied to fluids for which only limited experimental data were available. Their equations were designed for technical applications and do not compete with high-accuracy equations of state dedicated to a particular fluid. The Span and Wagner equation²⁰³ was used by Kunz et al.²⁰⁴ during the development of the GERG-2004 equation of state for natural gas mixtures. Miyamoto and Watanabe²⁰⁵ presented a 19-term equation in 2000 that is explicit in the Helmholtz energy with only simple and extended polynomial terms of the type described earlier. The 1987 equation of Younglove and Ely²⁰⁶ is a 32-term modified Benedict–Webb–Rubin equation. Sychev et al.²⁰⁷ published an equation of state in 1991 in terms of the compressibility factor with 50 terms with only simple polynomials (without the exponential part).

One of the earlier equations of state that covered the full fluid range was that of Goodwin and Haynes²⁰⁸ from 1982; however, this equation used a unique functional form that cannot be easily implemented in computer algorithms, and it has seen little use since its publication. Their work extensively documents the available measurements prior to 1982. Even earlier equations include those of Böhner et al.²⁰⁹ in 1981 and Teja and Singh²¹⁰ in 1977 that were based on the Bender type of equation, which, although able to compute properties for both liquid and vapor states, lacked the higher accuracies obtained with the more recent equations.

These equations suffer from one or more shortcomings that have been removed in the current equation. These shortcomings include:

(1) State-of-the-art thermodynamic data for propane are not represented to within their experimental uncertainties. These new data were described in the Introduction and were not available when the other equations were developed.

(2) Some of the equations show unacceptable behavior in regions where experimental data were not available at the time of fitting. These regions represent accessible valid states of the fluid surface.

(3) The magnitudes of pressure and other properties within the two-phase region reached enormous values (e.g., some

equations of state can reach up to pressures of $\pm 10^{50}$ MPa) caused by large exponents on the temperature term.

(4) The extrapolation behavior outside the range of validity of the equations is poor or incorrect, especially at high pressures (densities) or at low temperatures.

(5) Data in the extended critical region are not represented within their uncertainty.

(6) The ITS-90 temperature scale was not used.

The new equation presented here is an 18-term fundamental equation explicit in the reduced Helmholtz energy that overcomes all of these shortcomings. New optimization techniques, extrapolation criteria, and experimental data all contribute to make the equation state of the art. The range of validity of the equation of state for propane is from the triple point temperature (85.525 K) to 625 K at pressures to 1000 MPa, but it can be extended in all directions (higher temperatures, pressures, and densities, and lower temperatures) while maintaining physically reasonable behavior. In addition to the equation of state, ancillary functions were developed for the vapor pressure and for the densities of the saturated liquid and saturated vapor. These ancillary equations can be used as initial estimates in computer programs for defining the saturation boundaries but are not required to calculate properties from the equation of state.

The units adopted for this work were in kelvin (ITS-90) for temperature, megapascals for pressure, and moles per cubic decimeter for density. Units of the experimental data were converted as necessary from those of the original publications to these units. Where necessary, temperatures reported on IPTS-48 and IPTS-68 scales were converted to the International Temperature Scale of 1990 (ITS-90) (Preston-Thomas²¹¹). The $p\rho T$ and other data selected for the determination of the coefficients of the equation of state are described later along with comparisons of calculated properties to experimental values to verify the accuracy of the model developed in this research. Data used in fitting the equation of state for propane were selected to avoid redundancy in various regions of the surface.

New Equation of State. The critical temperature and density required in the reducing parameters for the equation of state given in eq 10 are 369.89 K and 5.00 mol·dm⁻³. The ideal gas reference state points are $T_0 = 273.15$ K, $p_0 = 0.001$ MPa, $h_0^0 = 26148.48$ J·mol⁻¹, and $s_0^0 = 157.9105$ J·mol⁻¹·K⁻¹. The values for h_0^0 and s_0^0 were chosen so that the enthalpy and entropy of the saturated liquid state at 0 °C are 200 kJ·kg⁻¹ and 1 kJ·kg⁻¹·K⁻¹, respectively, corresponding to the common convention in the refrigeration industry. Other values for h_0^0 and s_0^0 can be used, depending on the user's interest.

In the calculation of the thermodynamic properties of propane with an equation of state explicit in the Helmholtz energy, an equation for the ideal gas heat capacity, c_p^0 , is needed to calculate the Helmholtz energy for the ideal gas, α^0 . Values of the ideal gas heat capacity derived from low-pressure experimental heat capacity or speed of sound data are given in Table 3 along with theoretical values from statistical mechanics based on spectroscopic data (fundamental frequencies). Differences between the different sets of theoretical values arise from the use of different fundamental frequencies and from the models used to calculate the various couplings between the vibrational modes of the molecule. The equation for the ideal gas heat capacity for propane, used throughout the remainder of this work, was developed in part by fitting values reported by Trusler and Zarari¹⁷² and is given by

$$\frac{c_p^0}{R} = 4 + \sum_{k=3}^6 v_k \frac{u_k^2 \exp(u_k)}{[\exp(u_k) - 1]^2} \quad (21)$$

where $v_3 = 3.043$, $v_4 = 5.874$, $v_5 = 9.337$, $v_6 = 7.922$, $u_3 = 393 \text{ K/T}$, $u_4 = 1237 \text{ K/T}$, $u_5 = 1984 \text{ K/T}$, $u_6 = 4351 \text{ K/T}$, and the gas constant, R , is $8.314472 \text{ J} \cdot \text{mol}^{-1} \cdot \text{K}^{-1}$ (Mohr et al.²¹²). The Einstein functions containing the terms u_3 , u_4 , u_5 , and u_6 were used so that the shape of the ideal gas heat capacity versus temperature would be similar to that derived from statistical mechanical models. However, these are

empirical coefficients and should not be confused with the fundamental frequencies.

Comparisons of values calculated with eq 21 to the ideal gas heat capacity data are given in Figure 5. The sound speeds reported by Goodwin and Lemmon⁵² are greater than those determined by Trusler and Zarari¹⁷² and Hurly et al.⁷⁶ with differences that increase with decreasing temperature. All of the heat capacities derived from sound speed measurements are lower than values obtained from spectroscopic data, for example, as reported by Chao et al.²² A higher sound speed

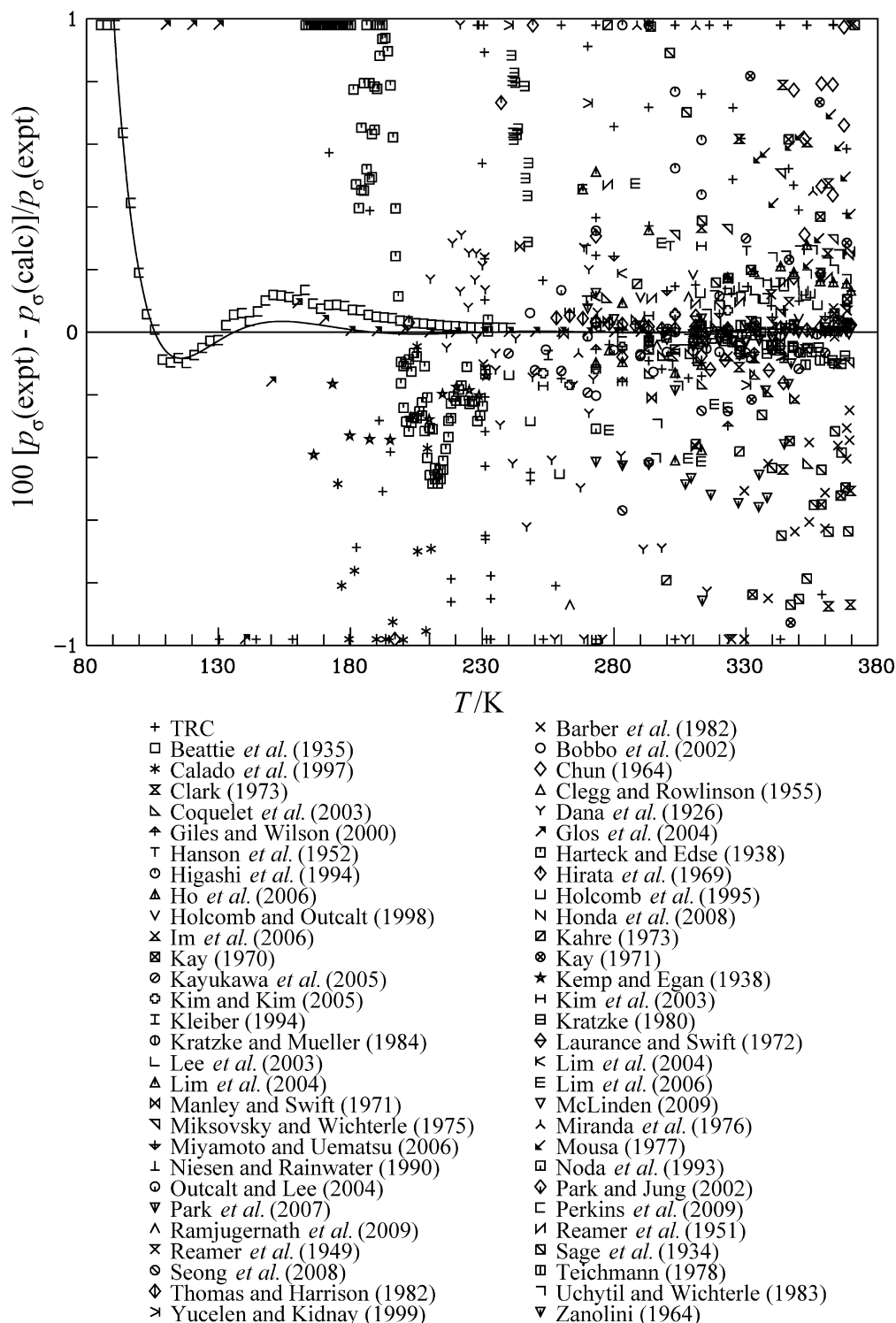


Figure 6. Comparisons of vapor pressures p_σ calculated with the equation of state to experimental data as a function of temperature T . The line corresponds to values calculated from the ancillary equation, eq 5.

implies a lower heat capacity—one plausible source of this difference is an impurity that has a speed of sound greater than propane, which is about $250 \text{ m}\cdot\text{s}^{-1}$. The possible impurities include both air and argon that both have sound speeds of about $300 \text{ m}\cdot\text{s}^{-1}$. It is possible to estimate the quantity of air required to give rise to the differences shown. However, no measurements have been performed to verify this conjecture, and neither Trusler and Zarari¹⁷² nor Esper et al.⁴³ give information about this discrepancy. This observation may be resolved by further experiments that are outside the realm of this work.

The ideal gas Helmholtz energy equation, derived from eqs 15 and 21, is

$$\alpha^0 = \ln \delta + 3 \ln \tau + a_1 + a_2 \tau + \sum_{i=3}^6 v_i \ln[1 - \exp(-b_i \tau)] \quad (22)$$

where $a_1 = -4.970583$, $a_2 = 4.29352$, $b_3 = 1.062478$, $b_4 = 3.344237$, $b_5 = 5.363757$, $b_6 = 11.762957$, and the values of v_k are the same as those used in eq 21. The values of b_k are equal to u_k divided by the critical temperature.

The coefficients N_k and other parameters of the residual part of the equation of state [given in eq 18 and repeated below] are given in Table 4.

$$\alpha^r(\delta, \tau) = \sum_{k=1}^5 N_k \delta^{d_k} \tau^{t_k} + \sum_{k=6}^{11} N_k \delta^{d_k} \tau^{t_k} \exp(-\delta^{l_k}) + \sum_{k=12}^{18} N_k \delta^{d_k} \tau^{t_k} \exp(-\eta_k(\delta - \varepsilon_k)^2 - \beta_k(\tau - \gamma_k)^2) \quad (23)$$

Experimental Data and Comparisons to the Equation of State

Since the identification of propane in 1910 by Dr. Walter O. Snelling at the U.S. Bureau of Mines, many experimental studies of the thermodynamic properties of propane have been reported, e.g., $p\rho T$ properties, saturation properties, critical parameters, heat capacities, speeds of sound, second virial coefficients, and ideal gas heat capacities (see refs 1–186). Goodwin and Haynes²⁰⁸ summarized most of the experimental data published for propane prior to 1982. Selected data were used for the development of the new thermodynamic property formulation reported here. Comparisons were made to all available experi-

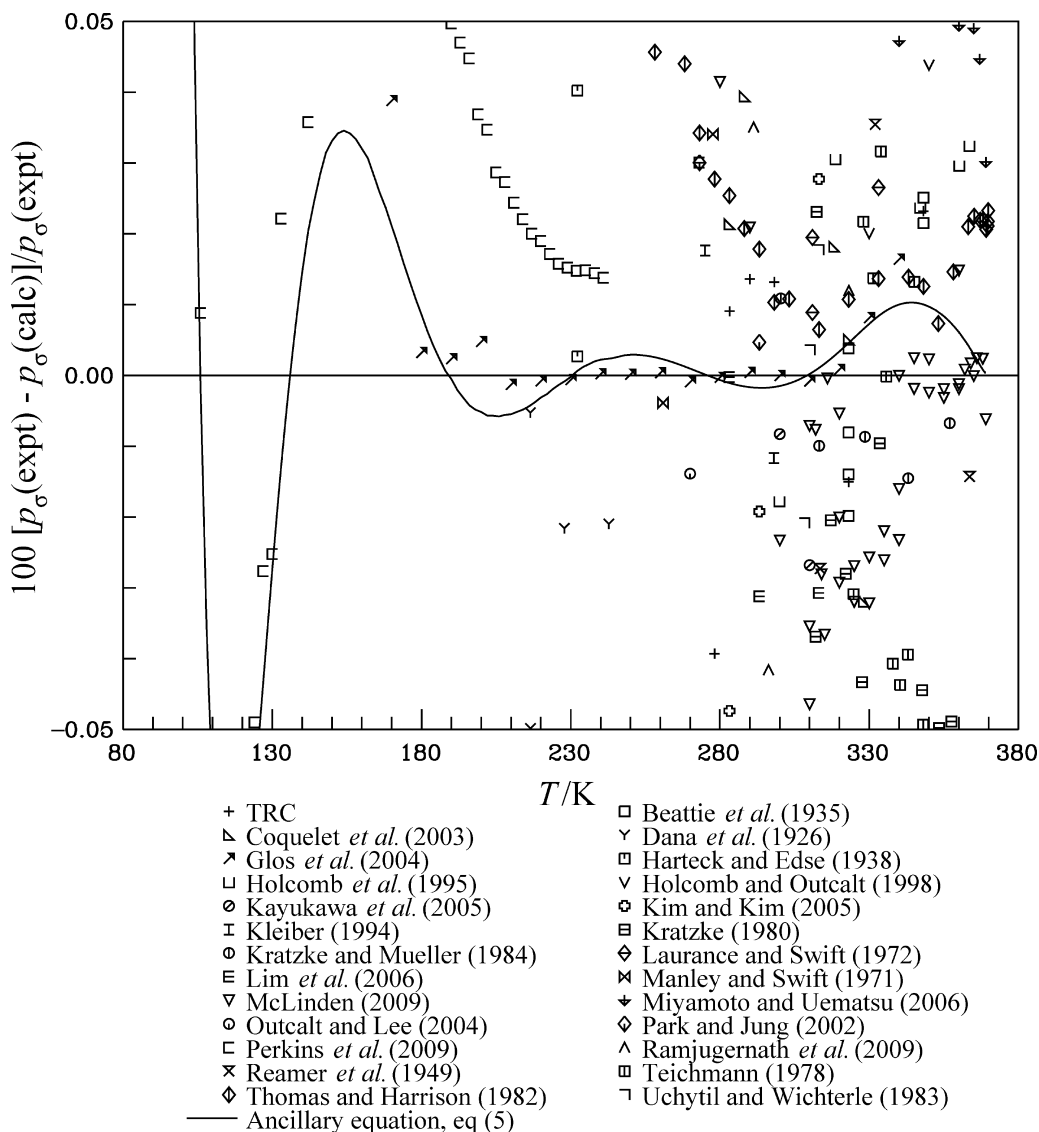


Figure 7. Comparisons of vapor pressures p_{σ} calculated with the equation of state to high-accuracy experimental data as a function of temperature T . The line corresponds to values calculated from the ancillary equation, eq 5.

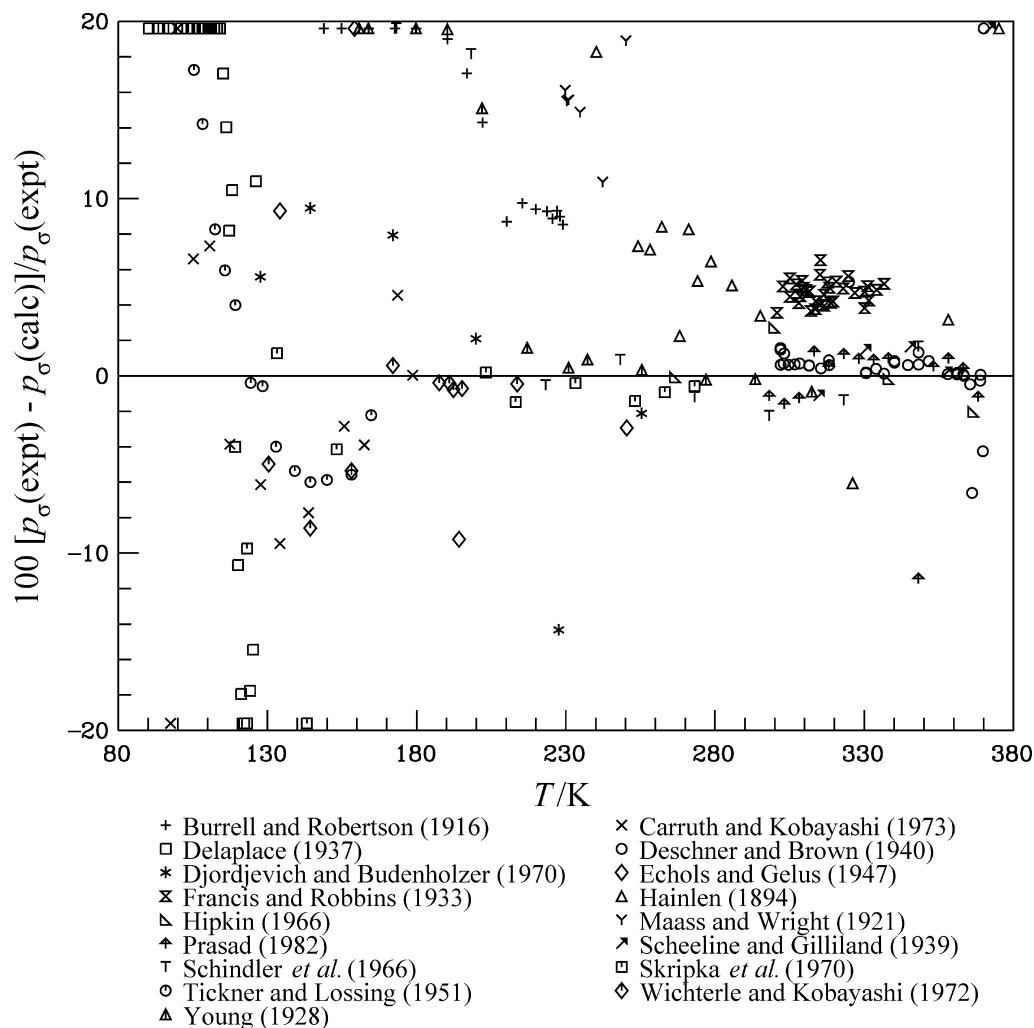


Figure 8. Comparisons of vapor pressures p_o calculated with the equation of state to low-accuracy or low-temperature experimental data as a function of temperature T .

mental data, including those not used in the development of the equation of state. Much of the data reported here was obtained from the Thermodynamic Data Engine (TDE) program (Frenkel *et al.*¹⁹⁴) available from the Thermodynamic Research Center (TRC) of NIST. Data sets with only one to three data points were not included in this work unless the data points were important to the development of the equation of state. Approximately 50 literature sources contained only one to three data points, and they are not identified here. However, these extra measurements are shown in the figures and are labeled as “TRC”.

The accuracy of the equation of state was determined by statistical comparisons of calculated property values to experimental data. These statistics are based on the percent deviation in any property, X , defined as

$$\Delta X = 100 \left(\frac{X_{\text{data}} - X_{\text{calc}}}{X_{\text{data}}} \right) \quad (24)$$

With this definition, the average absolute relative deviation is defined as

$$\text{AARD} = \frac{1}{n} \sum_{i=1}^n |\Delta X_i| \quad (25)$$

where n is the number of data points. The average absolute relative deviations between experimental data and calculated

values from the equation of state are given in Table 3. In this table, measured saturation properties are compared with the equation of state, not with the ancillary equations. The comparisons given in the sections below for the various data sets compare values calculated from the equation of state to the experimental data with the average absolute relative deviations given by eq 25 unless otherwise stated (such as the maximum value). Discussions of maximum errors or of systematic offsets use the absolute values of the deviations. Data points with excessive deviations are shown at the outer limits of the plots to indicate where these outliers were measured.

Comparisons with Saturation Thermal Data. Figures 6 through 8 compare vapor pressures calculated from the equation of state with experimental data. Figure 6 gives an overview of deviations of the equation from most of the data; Figure 7 provides an expanded view of the highest accuracy data (those that were used to test the equation of state); and Figure 8 shows data of low accuracy or at low temperature where the pressures are extremely small (less than 1 Pa) and percentage deviations can be high. The lines in these figures represent the ancillary equation, eq 5. Most of the experimental vapor pressures for propane fall within 1 % of the equation of state above 300 K. Below this, the number of experimental data decreases, and the data that are available fall within 0.5 %. All of these data are scattered evenly around the equation. Of all the data measured

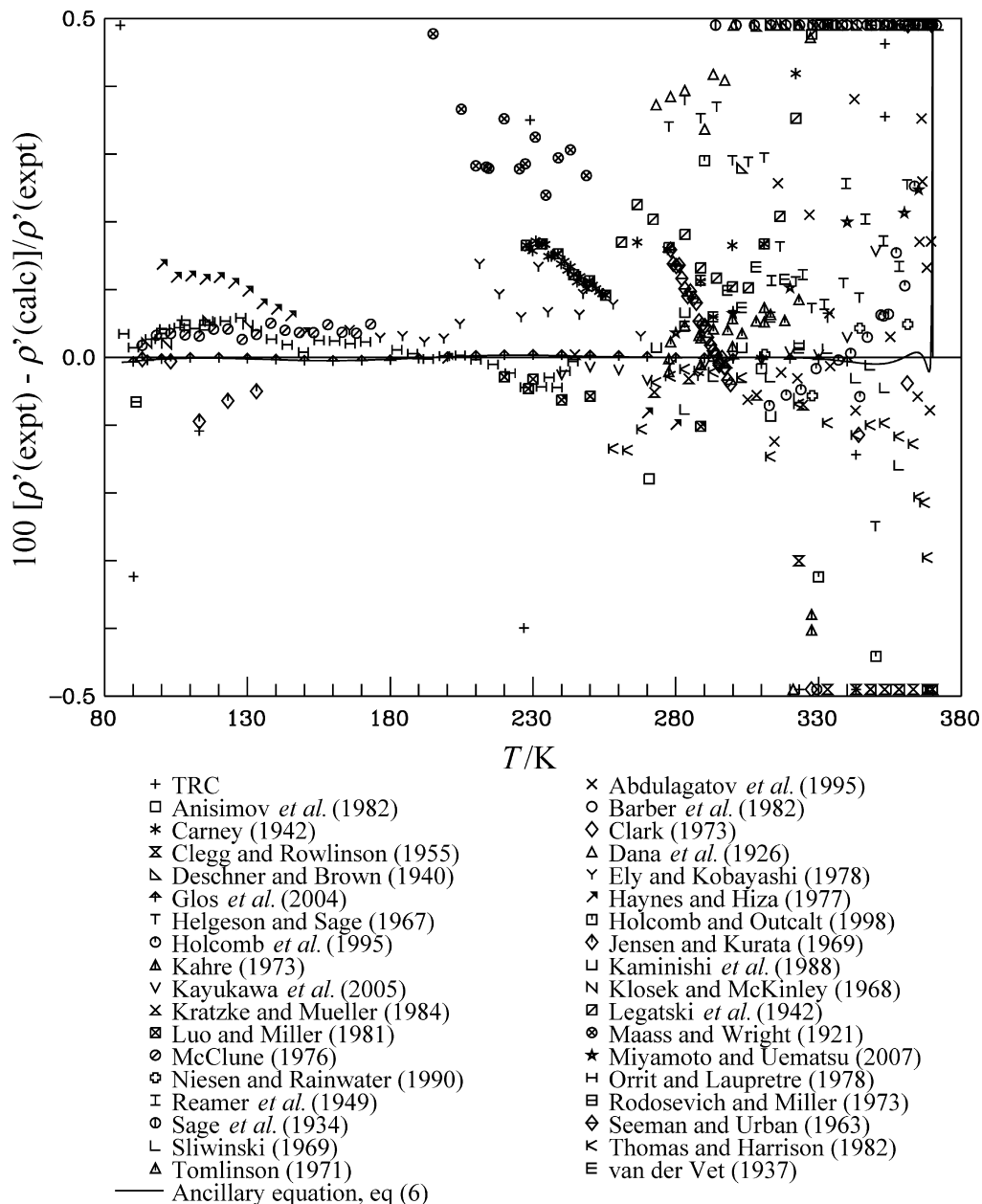


Figure 9. Comparisons of saturated liquid densities ρ' calculated with the equation of state to experimental data as a function of temperature T . The line corresponds to values calculated from the ancillary equation, eq 6.

before 1990, only 5 fall within the 0.1 % range: the data of Beattie *et al.*,¹² Kratzke,⁹⁸ Kratzke and Müller,⁹⁹ Teichmann,¹⁶⁶ and Thomas and Harrison.¹⁶⁸ Of these, only the data of Beattie *et al.* were measured before 1970. Thus, unlike the data for the critical point, experimentalists have been able to greatly reduce the uncertainty in vapor pressure measurements with time. This is especially evident with the data measured after 2000 and which were used in the development of the equation of state. The data of Glos *et al.*⁴⁸ from the Ruhr Universität have an uncertainty in pressure ranging from 0.007 % at the highest temperature to 0.02 % at 230 K, and the equation shows deviations of less than 0.005 % (50 ppm) in the temperature range between (180 and 320) K. Below 150 K, the deviations increase to above 1 %, but the pressure at these low temperatures is extremely low, less than 300 Pa, and it becomes very difficult to make high accuracy measurements, even with very pure samples. The deviations between the data of Glos *et al.* and the equation are all less than the uncertainties in the measurements, even at the lowest temperatures. Above 300 K, there is a slight

difference between the data of Glos *et al.* and the data measured at NIST by McLinden¹²⁰ on the order of 0.03 %. Since the data of Glos *et al.* extend only to 340 K, the equation was fitted to the data of McLinden above this, resulting in a deviation of 0.015 % in the highest temperature measurement of Glos *et al.* Above 340 K, the data of McLinden are fitted within 0.005 %. These data extend to the critical point. The data of Outcalt and Lee,¹³⁵ also measured at NIST with a different apparatus, are fitted to within 0.06 %.

At low temperatures, there is a data set available that used heat capacities in the two-phase region to determine the vapor pressure. These heat capacities are derived from internal energy measurements. This technique is often better than vapor pressure measurements at extremely low pressures, due to the difficulty inherent in experimental techniques. The data of Perkins *et al.*¹³⁹ show deviations of +0.19 % at 100 K and a maximum deviation of +2.2 % at the triple point temperature, where their derived vapor pressure is about 0.17 mPa. The derived values given by Perkins *et al.* were obtained while the equation presented here

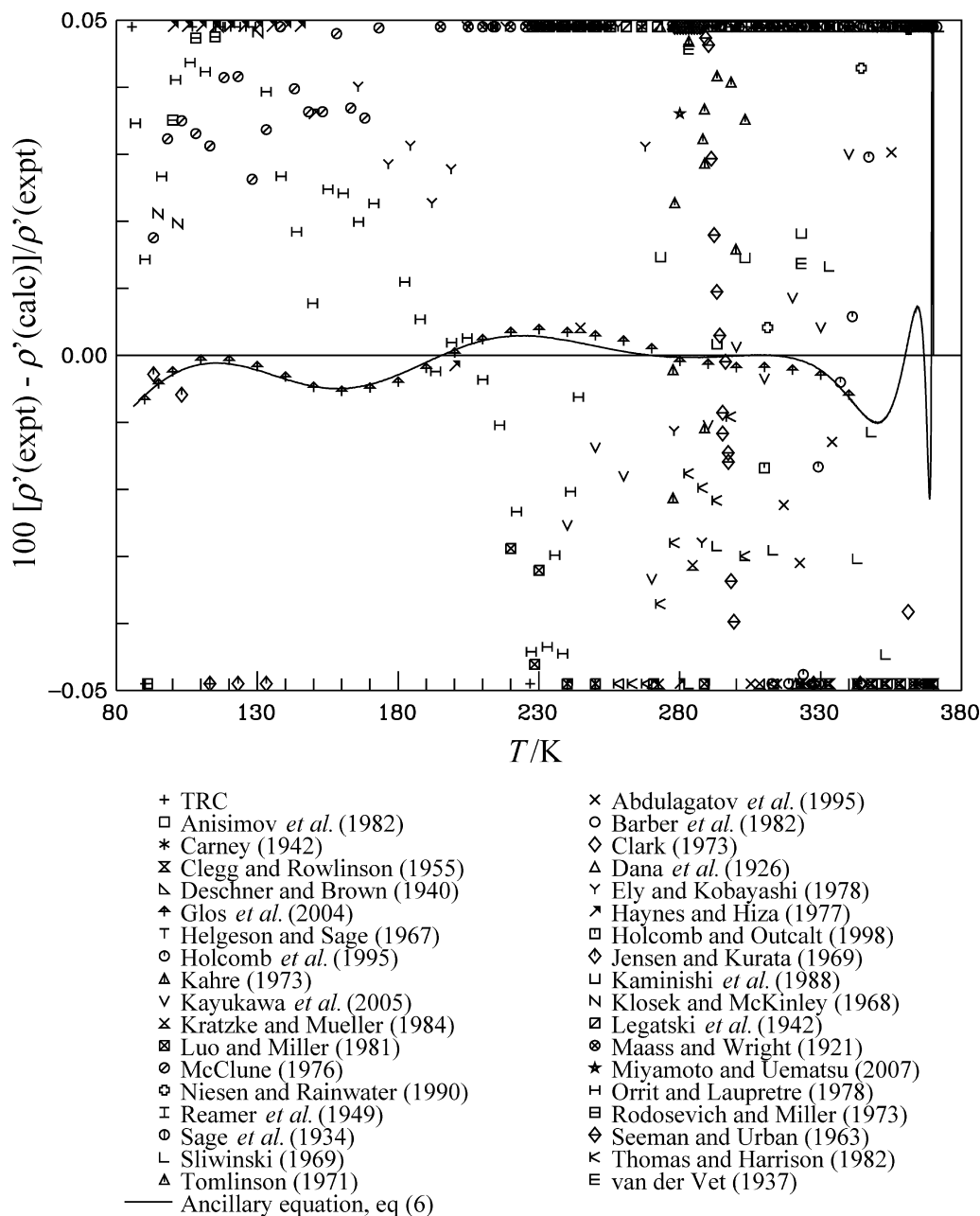


Figure 10. Comparisons of saturated liquid densities ρ' calculated with the equation of state to high-accuracy experimental data as a function of temperature T . The line corresponds to values calculated from the ancillary equation, eq 6.

was being developed, and the measurements and the equation benefitted from an iterative process in which each was influenced by the other's modifications. In the region where the data of Perkins *et al.* and Glos *et al.* overlap, the data of Perkins *et al.* closely follow (generally within 0.01 %) the data of Glos *et al.* Above 105 K, differences between the equation of state and the data of Perkins *et al.* are generally less than 0.1 %.

The consistency between saturated liquid densities below 273 K is quite remarkable; for the most part, the data are all within 0.2 %, as shown in Figures 9 and 10. Figure 9 shows all of the data, and Figure 10 provides an expanded view of the highest-accuracy data. The lines in these figures represent the ancillary equations reported in eq 6. The data sets that fall within 0.05 % include those of Haynes and Hiza,⁶¹ Jensen and Kurata,⁷⁸ Klosek and McKinley,⁹⁶ Luo and Miller,¹¹³ McClune,¹¹⁸ Orrit and Laupretre,¹³⁴ and Rodosevich and Miller.¹⁴⁷ The data of Haynes and Hiza exceed 0.05 % below 150 K. The data measured by Glos *et al.*⁴⁸ have uncertainties of 0.015 % and

are represented by the equation of state to within 0.005 % (50 ppm). Above 273 K, the data of Glos *et al.* are still represented to within 0.005 % up to their maximum temperature of 340 K. Although McLinden¹²⁰ did not measure saturated liquid densities, his $p\rho T$ measurements are concentrated around the critical region and close to the saturation boundaries. Other data above 273 K show higher scatter, especially toward the critical point. Most of the data are within 0.5 %, with many inconsistent data sets showing scatter of up to 0.2 %. Aside from the data of Glos *et al.*, none of the data sets stand out as exceptional.

The scatter in saturated vapor phase measurements is substantially higher, up to 2 % for a number of data sets, as shown in Figure 11. The data sets showing the highest degree of consistency are those of Clark,²⁶ Clegg and Rowlinson,²⁸ Sliwinski,¹⁶² and Thomas and Harrison,¹⁶⁸ although these data are still 0.5 % or more from the equation of state, except for the data of Thomas and Harrison, which are generally within

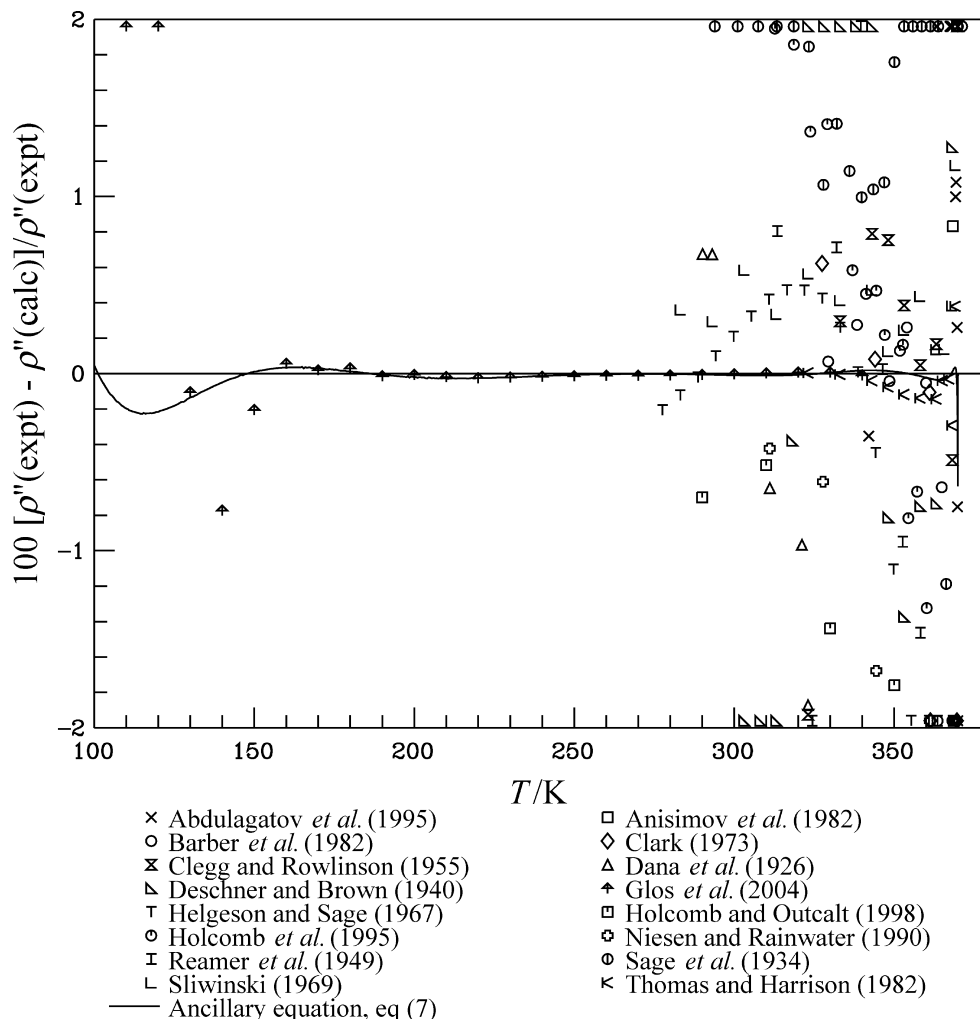


Figure 11. Comparisons of saturated vapor densities ρ'' calculated with the equation of state to experimental data as a function of temperature T . The line corresponds to values calculated from the ancillary equation, eq 7.

0.1 %. The data of Thomas and Harrison have been one of the most accurate sets published for propane before 2000 and have been the foundation for many previous equations of state. The new data of Glos et al.⁴⁸ are a combination of measurements down to 230 K and a truncated virial equation of state at lower temperatures where measurements of density become impossible due to their extremely low values. These data are represented by the equation of state to within 0.02 % for temperatures between (150 and 280) K and within 0.01 % up to their maximum temperature of 340 K.

ppT Data and Virial Coefficients. The experimental ppT data for propane are summarized in Table 3 and shown graphically in Figure 12. For clarity, data in the extended critical region are also shown on temperature–density coordinates in Figure 13. As can be seen in this figure, there is a substantial number of high-quality data in the extended critical region, which is unusual for most fluids. Figure 14 compares densities calculated from the equation of state with experimental data; Figure 15 shows comparisons with only high-accuracy measurements in a similar manner; and Figure 16 compares pressures calculated from the equation of state with the experimental data in the extended critical region of propane. In the figures, the deviations are shown in groups containing data generally within a 10 K interval. The temperature listed at the top of each small plot is the lower bound of the data in the plot.

Three key sets of pressure–density–temperature data are now available to characterize the properties of propane with very

high accuracy. These are the data of Glos et al.,⁴⁸ Claus et al.,²⁷ and McLinden,¹²⁰ and these data are compared in Figure 15 to the equation of state. The first two data sets were available when the fitting of the equation of state began. The third set was measured during the fitting process and was used as both a check on how the equation was progressing and an aid to determine how much more, and in what regions, new data should be measured. Careful attention was given in the critical region so that sufficient data were measured such that the critical parameters could be determined simultaneously with the coefficients and exponents of the equation of state, as described earlier. The apparatuses of McLinden and of Glos et al. are both two-sinker densimeters and use the most accurate measuring technique for density currently available. The high-temperature measurements of Claus et al.,²⁷ which are reported in the work of Glos et al., were performed in a single-sinker apparatus. In the low-temperature region, where only the data of Glos et al. are available (up to 260 K), the equation represents these data with an AARD of 0.002 % (20 ppm). In the liquid region where the data of Glos et al. overlap the data of McLinden [(260 to 340) K], this trend continues, while the equation represents the data of McLinden with an AARD of 0.004 %. Glos et al. measured 13 points in the vapor phase below 340 K and the equation represents these to within 0.005 %. The data of Claus et al. extend the measurements from (340 to 520) K, and the equation shows an AARD of 0.015 % with respect to these data. This data set contains only a few critical region values. The

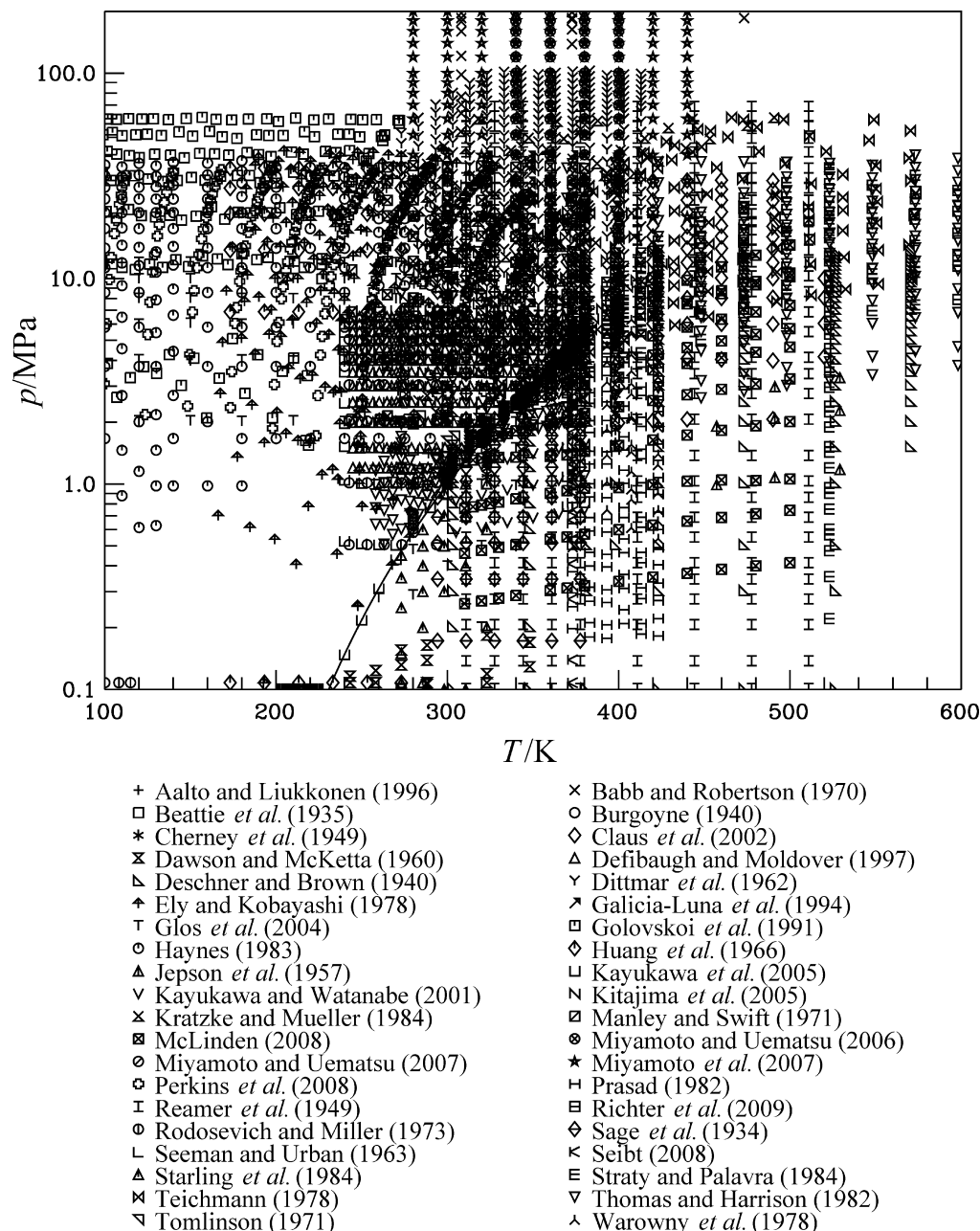


Figure 12. Experimental ppT data as a function of temperature T and pressure p .

work of McLinden also studied the critical region and has to be divided into several areas to give informative statistics that help understand how the equation behaves. Since the slope of pressure with respect to density approaches zero near the critical point, density variations can become large with small changes in temperature or pressure. Thus it is more meaningful instead to report deviations in pressure, which will be done here for the points close to the critical point. The following statistics for the data of McLinden apply to those points above 340 K. At densities greater than $8 \text{ mol} \cdot \text{dm}^{-3}$, the equation represents the data on average to within 0.004 % in density. Between (6 and $8 \text{ mol} \cdot \text{dm}^{-3}$), the average deviations in density are 0.03 %. In the vapor region with densities less than $4 \text{ mol} \cdot \text{dm}^{-3}$, the average deviations in density are 0.02 %. In the critical region between (4 and $6 \text{ mol} \cdot \text{dm}^{-3}$), the average deviations in pressure are 0.009 %. The deviations are much higher for density (0.7 %) but are less meaningful for reasons described above. All of the data of McLinden above 380 K are represented on average to within 0.017 % in density.

Aside from the data of Glos *et al.*,⁴⁸ Claus *et al.*,²⁷ and McLinden,¹²⁰ there are several other data sets for ppT that have low uncertainties and help validate the equation of state. Although the data of Perkins *et al.*¹³⁹ show average deviations of 0.012 %, these data were based on an experimental volume calibrated with the present propane equation and thus cannot be used for validation. The calibration was performed so that measurements with other fluids could be made with lower uncertainties. Richter *et al.*¹⁴⁶ measured one experimental data point with an uncertainty of 0.02 % at 273 K and 1 atm in the vapor phase with a special two-sinker densimeter designed to very accurately measure densities of gases under standard conditions at very low densities. The deviation of the equation from this point is 0.009 %. Other data that are well represented in the vapor phase include those of Starling *et al.*¹⁶³ and Dawson and McKetta,³³ both with average deviations of 0.03 %. In the liquid phase, the data of Kratzke and Müller⁹⁹ span the temperature range from (250 to 490) K and are represented to within 0.035 %. The deviations for the four data points of

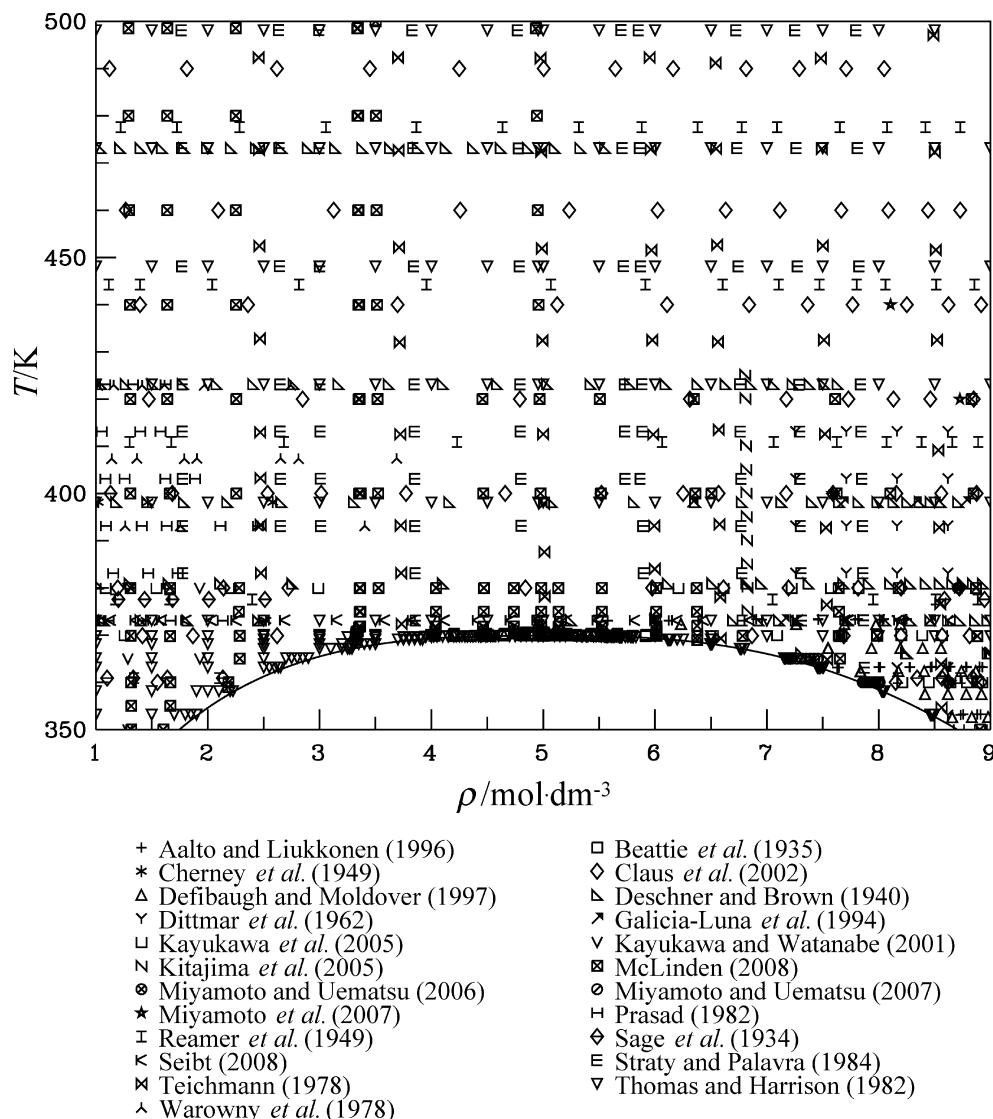


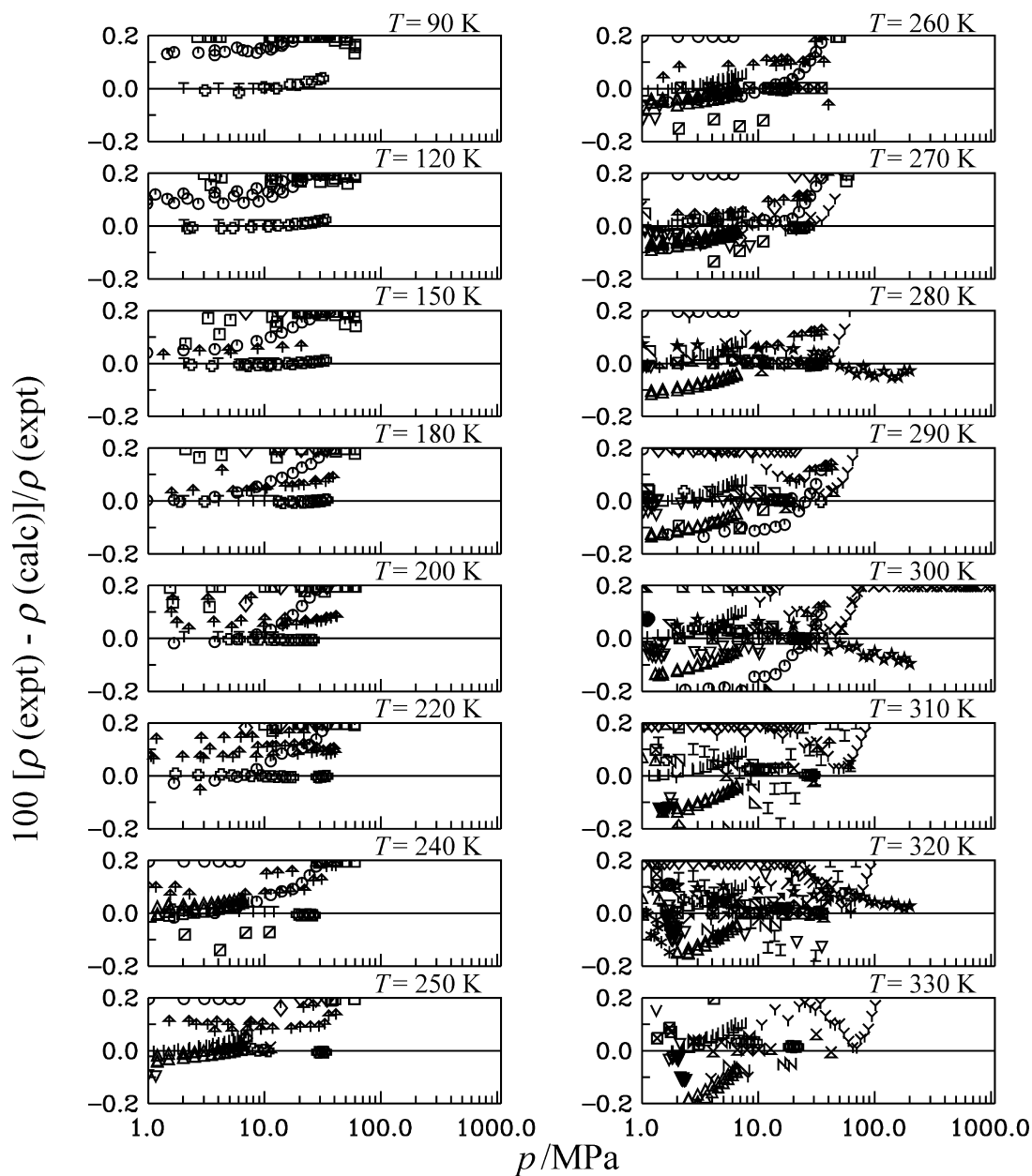
Figure 13. Experimental $p\rho T$ data in the extended critical region as a function of density ρ and temperature T .

Rodosevich and Miller¹⁴⁷ between (90 and 115) K are about 0.04 %. Teichmann¹⁶⁶ measured data at temperatures from (322 to 573) K, and the equation shows average deviations of 0.07 %. Similar deviations are visible with the data of Galicia-Luna *et al.*⁴⁶ Differences of around 0.09 % are seen in the data sets of Defibaugh and Moldover,³⁴ Ely and Kobayashi⁴¹ (which extend down to 166 K), and Miyamoto and Uematsu.¹²⁵ The latter measured densities up to 200 MPa. The equation of state represents the data of Miyamoto and Uematsu best at 200 MPa, where the deviations are about 0.03 %. The only data set that extends to higher pressures is that of Babb and Robertson,⁷ which extends to nearly 1000 MPa. These data show deviations of around 0.4 % and appear to be systematically high when compared to the data of Miyamoto and Uematsu. However, this conclusion is subjective and needs further experimental work to ascertain the true thermodynamic properties of propane at very high pressures. The data of Thomas and Harrison¹⁶⁸ extend up to 623 K, and the deviations range from less than 0.1 % below 18 MPa to generally less than 0.2 % below 40 MPa (the upper pressure limit of the data).

In the critical region, the data of Thomas and Harrison¹⁶⁸ have been used for decades in fitting because they were the most accurate data in the critical region. With the new measurements of McLinden, this situation has now changed,

and the data of Thomas and Harrison appear to be systematically higher by 0.03 % in pressure. Although this is a small amount, such small changes have large impacts on the calculation of density in the critical region. The data still serve a vital purpose in making it possible to extrapolate between the limited measurements made by McLinden. As seen in Figure 16, Thomas and Harrison report about 10 times as many measurements, and these measurements show that the equation is smooth in between the data points where McLinden measured. The data of Beattie *et al.*¹² serve a similar purpose; these data differ in pressure by about 0.05 % from the equation of state.

Table 3 summarizes the sources for the second virial coefficients of propane. Deviations from the equation of state are shown in Figure 17. Many of the data are scattered within $5 \text{ cm}^3\cdot\text{mol}^{-1}$ above 300 K. Additional information about the high uncertainties in the second virial coefficients at low temperatures was reported by Wagner and Pruss.¹⁹⁹ The data of Glos *et al.*⁴⁸ (which extend from (260 to 340) K) are represented to within a maximum of $1.8 \text{ cm}^3\cdot\text{mol}^{-1}$ (0.3 %). Comparisons of third virial coefficients calculated with the equation of state with those presented in the literature are shown in Figure 18. Figure 19 shows a plot of $(Z - 1)/\rho$ vs ρ and demonstrates the behavior of the second and third virial coefficients as well as the shape of the equation of state in the two-phase region. The lines show isotherms calculated from

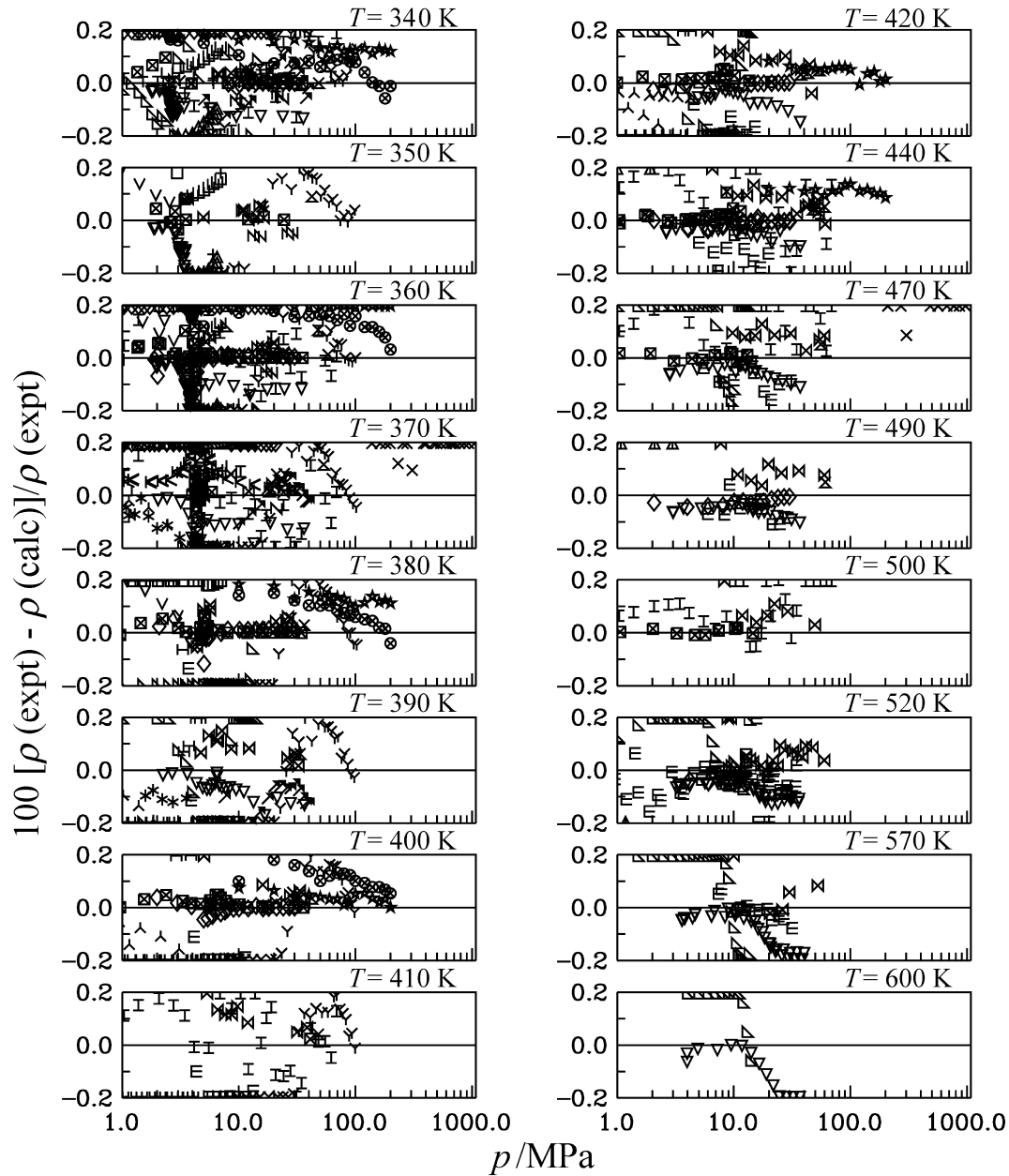


- | | |
|-------------------------------------|--------------------------------|
| + Aalto and Liukkonen (1996) | × Babb and Robertson (1970) |
| □ Beattie <i>et al.</i> (1935) | ○ Burgoyne (1940) |
| * Cherney <i>et al.</i> (1949) | ◇ Claus <i>et al.</i> (2002) |
| △ Defibaugh and Moldover (1997) | ▴ Deschner and Brown (1940) |
| ▽ Dittmar <i>et al.</i> (1962) | ⋈ Ely and Kobayashi (1978) |
| ⋈ Galicia-Luna <i>et al.</i> (1994) | † Glos <i>et al.</i> (2004) |
| □ Golovskoi <i>et al.</i> (1991) | ○ Haynes (1983) |
| ◇ Huang <i>et al.</i> (1966) | △ Jepson <i>et al.</i> (1957) |
| □ Kayukawa <i>et al.</i> (2005) | ▽ Kayukawa and Watanabe (2001) |
| ⋈ Kitajima <i>et al.</i> (2005) | × Kratzke and Mueller (1984) |
| ▣ Manley and Swift (1971) | ▣ McLinden (2009) |
| ⊙ Miyamoto and Uematsu (2006) | ⊙ Miyamoto and Uematsu (2007) |
| ★ Miyamoto <i>et al.</i> (2007) | ⊙ Perkins <i>et al.</i> (2009) |
| ⋈ Prasad (1982) | ⋈ Reamer <i>et al.</i> (1949) |
| ◇ Sage <i>et al.</i> (1934) | ⋈ Seibt (2008) |
| △ Starling <i>et al.</i> (1984) | ⋈ Straty and Palavra (1984) |
| ⋈ Teichmann (1978) | ▽ Thomas and Harrison (1982) |
| ▽ Tomlinson (1971) | ⋈ Warowny <i>et al.</i> (1978) |

Figure 14. Comparisons of densities ρ calculated with the equation of state to experimental data as a function of pressure p .

the equation of state presented here, and the curve represents the saturated vapor density. The y-intercept (zero density) represents the second virial coefficients at a given temperature, and the third

virial coefficients are the slope of each line at zero density. Many equations of state show curvature in the lines at low temperatures caused by high values of the exponent t on temperature. As can



+ Aalto and Liukkonen (1996)
 □ Beattie *et al.* (1935)
 * Cherney *et al.* (1949)
 △ Defibaugh and Moldover (1997)
 ∇ Dittmar *et al.* (1962)
 ⤴ Galicia-Luna *et al.* (1994)
 ◊ Golovskoi *et al.* (1991)
 ◇ Huang *et al.* (1966)
 □ Kayukawa *et al.* (2005)
 ∇ Kitajima *et al.* (2005)
 ▣ Manley and Swift (1971)
 ⊗ Miyamoto and Uematsu (2006)
 ★ Miyamoto *et al.* (2007)
 ⊞ Prasad (1982)
 ◇ Sage *et al.* (1934)
 △ Starling *et al.* (1984)
 ✕ Teichmann (1978)
 ∇ Tomlinson (1971)

× Babb and Robertson (1970)
 ○ Burgoyne (1940)
 ◇ Claus *et al.* (2002)
 ▴ Deschner and Brown (1940)
 ⤴ Ely and Kobayashi (1978)
 † Glos *et al.* (2004)
 ◊ Haynes (1983)
 ▲ Jepson *et al.* (1957)
 ∇ Kayukawa and Watanabe (2001)
 ✕ Kratzke and Mueller (1984)
 ▣ McLinden (2009)
 ⊗ Miyamoto and Uematsu (2007)
 ★ Perkins *et al.* (2009)
 ⊞ Reamer *et al.* (1949)
 ⤴ Seibt (2008)
 ⊞ Straty and Palavra (1984)
 ∇ Thomas and Harrison (1982)
 ⤴ Warowny *et al.* (1978)

Figure 14. Continued.

be seen in this plot, there is no curvature in the lines, and the equation is extremely smooth and linear at low densities, as it

should be. The paper describing the R-125 equation by Lemmon and Jacobsen¹⁸⁹ discusses this point in more detail.

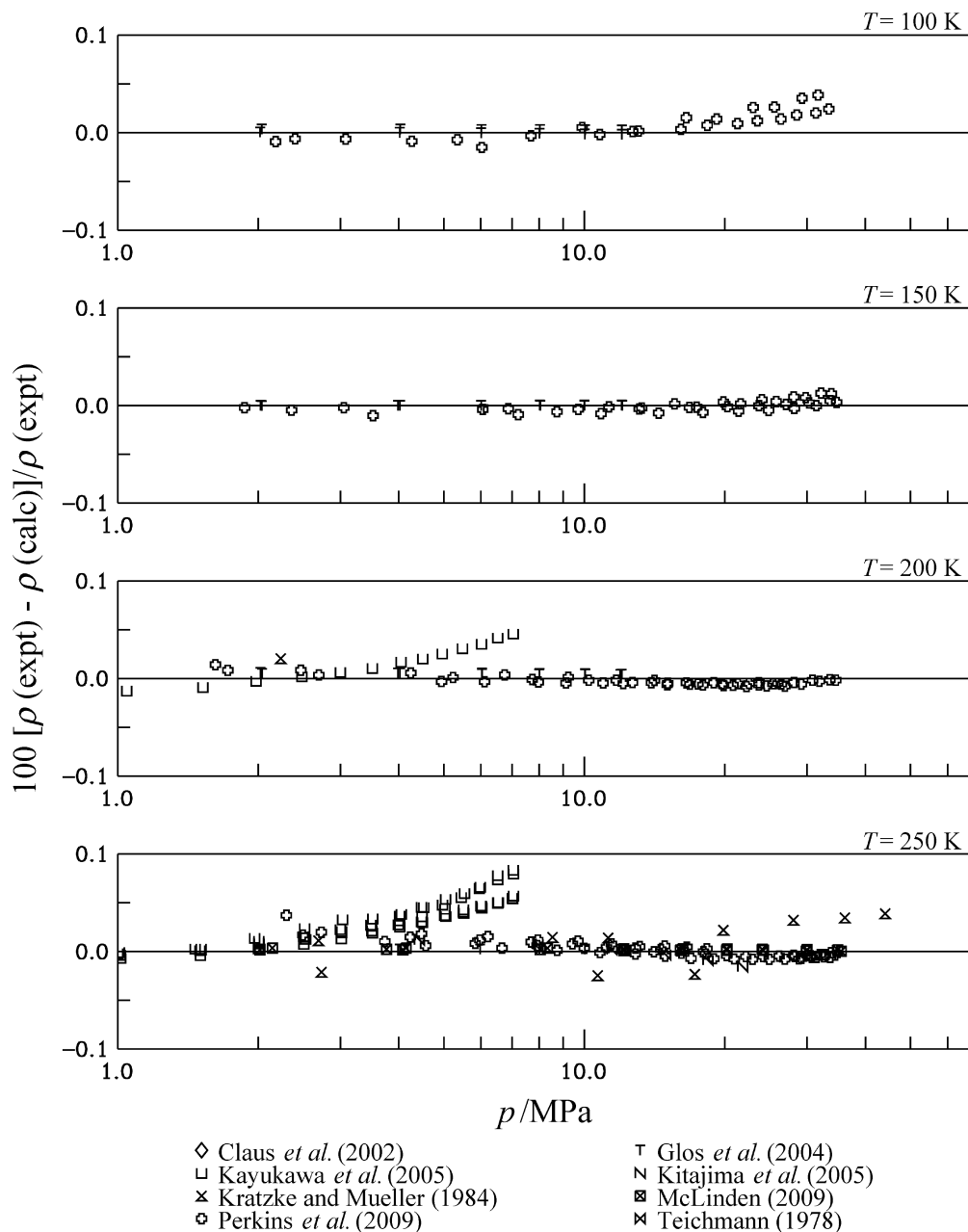


Figure 15. Comparisons of densities ρ calculated with the equation of state to high-accuracy experimental data as a function of pressure p .

Caloric Data. The sources of experimental data for the caloric properties of propane are summarized in Table 3. Comparisons of values calculated from the equation of state for the enthalpy of vaporization are shown in Figure 20. There have been no new measurements on the enthalpy of vaporization of propane over the last 30 years, and many of the data that are available are generally fitted within 1 %. Comparisons of values calculated from the equation of state for the speed of sound are shown in Figure 21 for the liquid phase and in Figure 22 for the vapor phase. As part of the new work on propane, speed of sound measurements were made by Meier.¹²¹ These data have an uncertainty of 0.03 % and are among the most accurate of any liquid phase speed of sound data available. The equation of state represents these data generally to within 0.03 % with an AARD of 0.012 %. The data of Younglove¹⁸³ measured in 1981 at NIST overlap the data of Meier from (240 to 310) K and then extend down to temperatures near the triple point. These data show an offset of about 0.03 % from the data of Meier, and this offset was left as such over all temperatures during the fitting of the equation of state. By so doing,

the scatter in the data of Younglove near the triple point lies between (0 and -0.1 %), but the uncertainty in the equation is most likely 0.05 % at the lowest temperatures. Figure 21 shows how the comparisons would appear if the data of Younglove were modified based on the differences with the new data of Meier (the data are indicated as “adjusted Younglove” in the figure). There is an unexplainable dip in the data of Younglove between (160 and 180) K, and it is unclear why these data are inconsistent with his other data. There are other data sets in the liquid phase that overlap these two data sets, but their uncertainties are much higher (1 % or more) and do not contribute to the development of the equation or in its evaluation.

Several data sets are also available for vapor phase speeds of sound, as shown in Figure 22. The data of He et al.⁶² deviate by 0.2 % from the equation, and the data of Trusler and Zarari¹⁷² and Hurly et al.⁷⁶ are represented to within 0.01 % (and an AARD of 0.006 %). The data of Hurly were measured at 298 K, and the data of Trusler and Zarari were taken over the range from (225 to 375) K. This latter set was of extreme

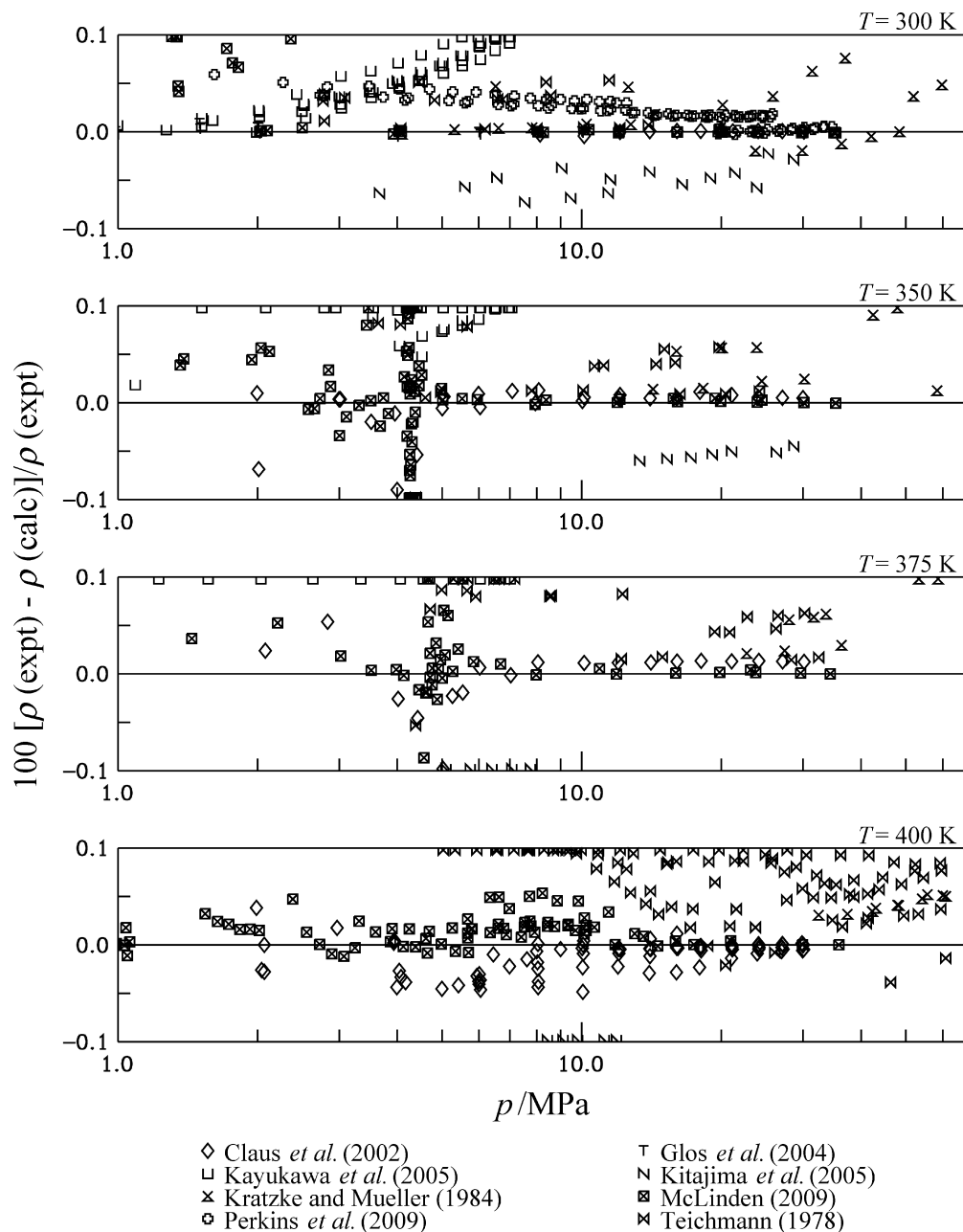


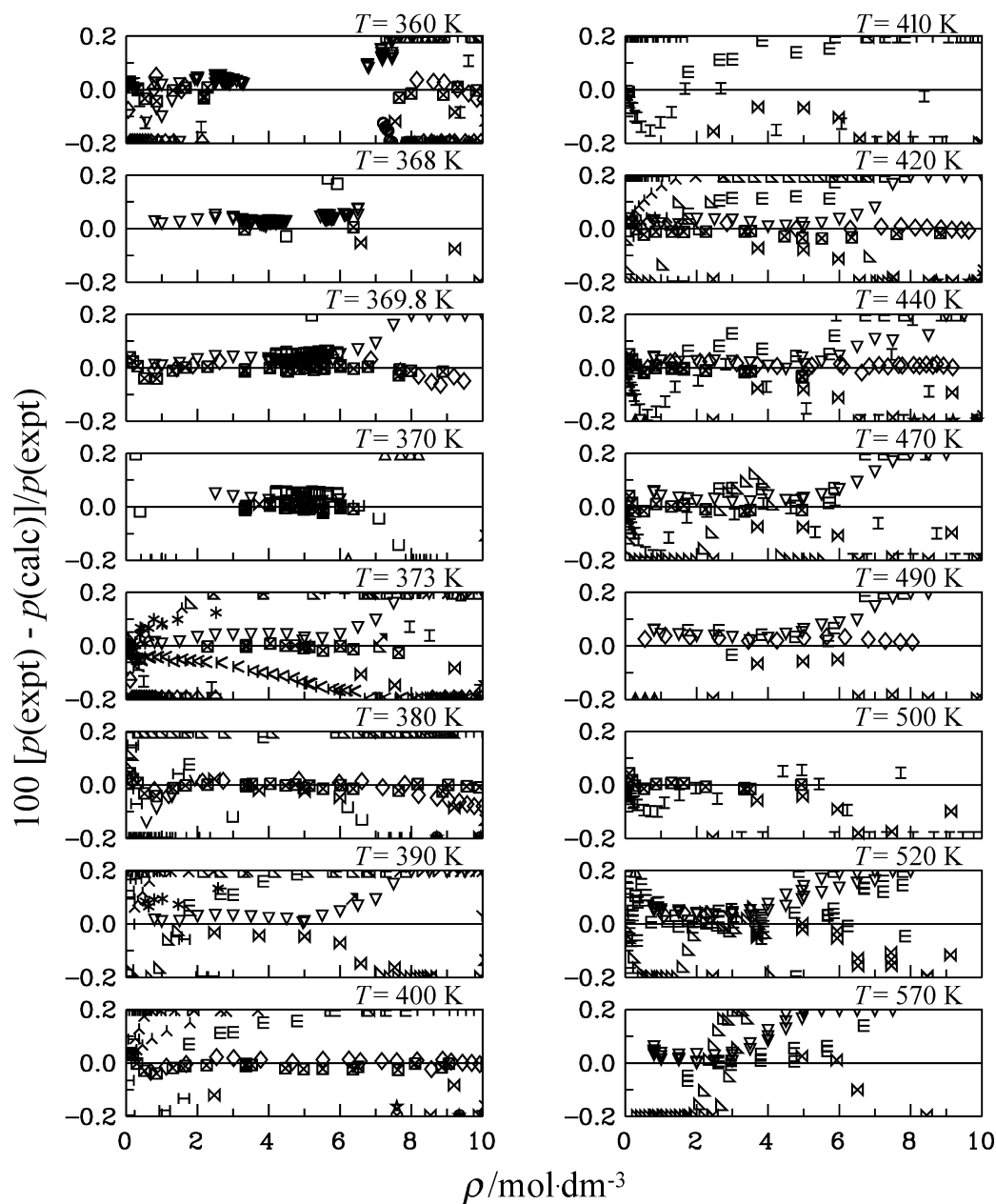
Figure 15. Continued.

importance in the development of the equation because of its low uncertainty and its position on the surface of state of propane, i.e., in the gas phase at very low pressures, where it is difficult to make $p\rho T$ measurements. Additionally, these measurements contributed to the ideal gas heat capacity equation, which was fitted simultaneously with the equation of state.

The reported measurements of the isochoric heat capacity, saturation liquid heat capacity, and isobaric heat capacity for propane are summarized in Table 3. Comparisons of values calculated from the equation of state are shown for the saturation liquid heat capacities in Figure 23, the isobaric heat capacities in Figure 24, and isochoric heat capacities in Figure 25. There are a number of good measurements for the saturation heat capacity of propane (c_p) and for the isobaric heat capacity at saturation (c_p). At low temperatures, these two properties are nearly identical. They start to diverge near 270 K, and by 350 K, they differ by about 15 %. Up to 320 K, the equation of state evenly splits the data sets into two groups: the data of Perkins *et al.*¹³⁹ and of Guigo *et*

al.⁵⁴ show positive deviations, and the data of Cutler and Morrison,³⁰ Dana *et al.*,³² Goodwin,⁵³ and Kemp and Egan⁸⁹ show negative deviations as shown in Figure 23. Between (90 and 220) K, the data are fitted to within 0.5 %, which is the uncertainty of these data sets. There is somewhat higher scatter above 220 K in the data of Perkins *et al.* up to 315 K (the data have higher uncertainties as they approach the critical point). Above this temperature, there is a sharp downward shift as the data approach the critical region. Because of the analytical nature of the equation of state, these data are not as well represented as could be done with a scaling equation developed solely for the critical region.

The data available for the isobaric heat capacity show quite high scatter and were not used in developing the equation of state. In the vapor phase, only the data of Ernst and Büsser⁴² and Kistiakowsky and Rice⁹³ show deviations less than 0.5 %. Generally, speed of sound data are a much better choice for fitting the vapor phase than are isobaric heat capacities, and the latter are rarely used, except for the correlation of the ideal gas heat capacity.



- | | |
|-------------------------------------|---------------------------------|
| + Aalto and Liukkonen (1996) | × Babb and Robertson (1970) |
| □ Beattie <i>et al.</i> (1935) | * Cherney <i>et al.</i> (1949) |
| ◇ Claus <i>et al.</i> (2002) | △ Defibaugh and Moldover (1997) |
| ▴ Deschner and Brown (1940) | ▽ Dittmar <i>et al.</i> (1962) |
| ▴ Galicia-Luna <i>et al.</i> (1994) | △ Jepson <i>et al.</i> (1957) |
| ▢ Kayukawa <i>et al.</i> (2005) | ▽ Kayukawa and Watanabe (2001) |
| ▢ Kitajima <i>et al.</i> (2005) | × Kratzke and Mueller (1984) |
| ▣ McLinden (2009) | ⊗ Miyamoto and Uematsu (2006) |
| ⊗ Miyamoto and Uematsu (2007) | ★ Miyamoto <i>et al.</i> (2007) |
| ⊢ Prasad (1982) | ⊢ Reamer <i>et al.</i> (1949) |
| ◇ Sage <i>et al.</i> (1934) | ◁ Seibt (2008) |
| ⊢ Straty and Palavra (1984) | × Teichmann (1978) |
| ▽ Thomas and Harrison (1982) | ^ Warowny <i>et al.</i> (1978) |

Figure 16. Comparisons of pressures p calculated with the equation of state to experimental data in the extended critical region as a function of density ρ .

The situation in the liquid phase is not much better. The data of Kemp and Egan⁸⁹ show deviations of 0.5 %, and the rest of the available data are scattered by 2 % or more. Fortunately, the extremely accurate speed of sound data of Meier¹²¹ and of Younglove,¹⁸³ along with the saturation heat capacities, are

available, and their use in fitting was sufficient to fully define the liquid phase of propane without the need for heat capacity data at higher pressures. This is possible because an equation of state requires consistency among all of its various properties. For example, fitting very accurate vapor pressures will result in good

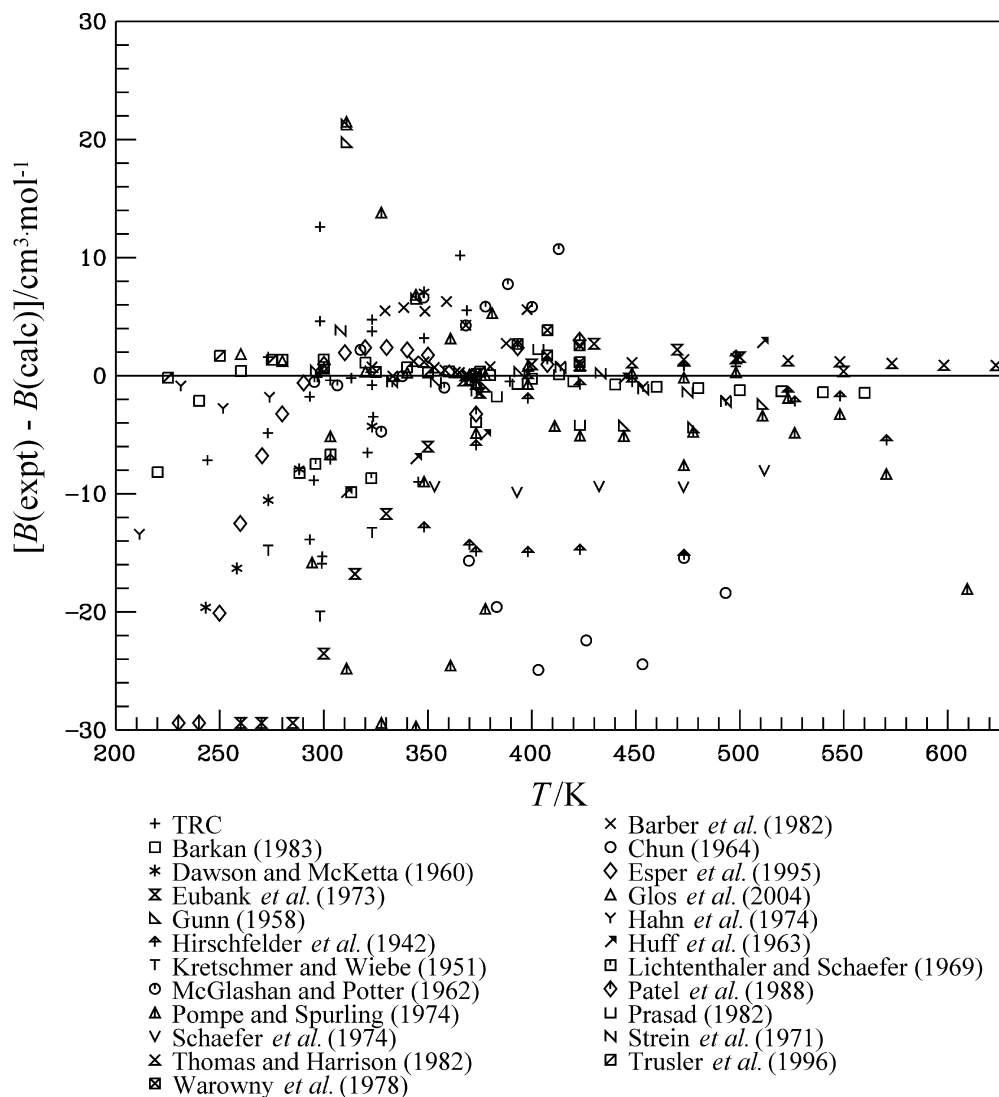


Figure 17. Comparisons of second virial coefficients B calculated with the equation of state to experimental data as a function of temperature T .

values of the enthalpies of vaporization. Likewise, fitting extremely accurate density, speeds of sound, and saturation heat capacity data will result in accurate calculations of the isobaric and isochoric heat capacities. It is not possible to force the equation to fit isobaric heat capacities having deviations of 2 % or more when these other accurate data are available.

There are a number of measurements for the isochoric heat capacity in the liquid phase of propane. These include the data of Perkins *et al.*,¹³⁹ Goodwin,⁵³ Abdulagatov *et al.*,^{2,3} and Anisimov *et al.*⁶ The data of Abdulagatov *et al.* and Anisimov *et al.* were measured in the critical region and at high temperatures. The equation shows substantial deviations from these data sets, and it is unclear whether this is due to deficiencies in the data or in the equation of state. The data of Perkins *et al.* and of Goodwin show deviations of 0.5 % above 290 K and deviations of 1 % below this, except near 100 K for the data of Perkins *et al.*, where the deviations are again around 0.5 %. This is discussed further in the work of Perkins *et al.*¹³⁹

Extrapolation Behavior. Because the equation of state for propane can be used as a reference formulation in corresponding states applications due to its extremely long saturation line and high-quality data, extreme attention was given to the low-temperature regime below the triple point. Although it is possible to cool a liquid below its triple point and maintain its liquid state,

these property measurements are difficult and rare, and thus such data are generally not available. However, it is possible to easily extrapolate the equation to lower temperatures. This extrapolation is important for a number of reasons: (1) if the extrapolation is correct, then state points in normal regions should be more accurate (since bad extrapolations outside the normal range result from incorrect slopes in normal regions, and properties such as heat capacities are highly slope dependent); (2) there are some fluids such as 1-butene that have an even longer saturation line (i.e., a lower reduced triple point temperature); and (3) mixture models can access regions outside the range of validity of the equation of state, depending on what it is mixed with and how nonideal the mixture is.

New fitting techniques developed in the R-125 equation of state (Lemmon and Jacobsen¹⁸⁹) allowed good extrapolation to well below the triple point. One of the best techniques for determining how low an equation can be used is to find the point at which the speed of sound is no longer linear with respect to temperature along the saturated liquid line (ignoring the critical region). For R-125, the speed of sound calculated from the equation started to diverge from a linear trend at about 150 K. This is below its triple point temperature of 172.52 K and represents an approximate reduced temperature of 0.44. For propane, the reduced triple point is 0.23, and thus the functional form for R-125 would have to be modified to allow a proper representation to this lower reduced temperature.

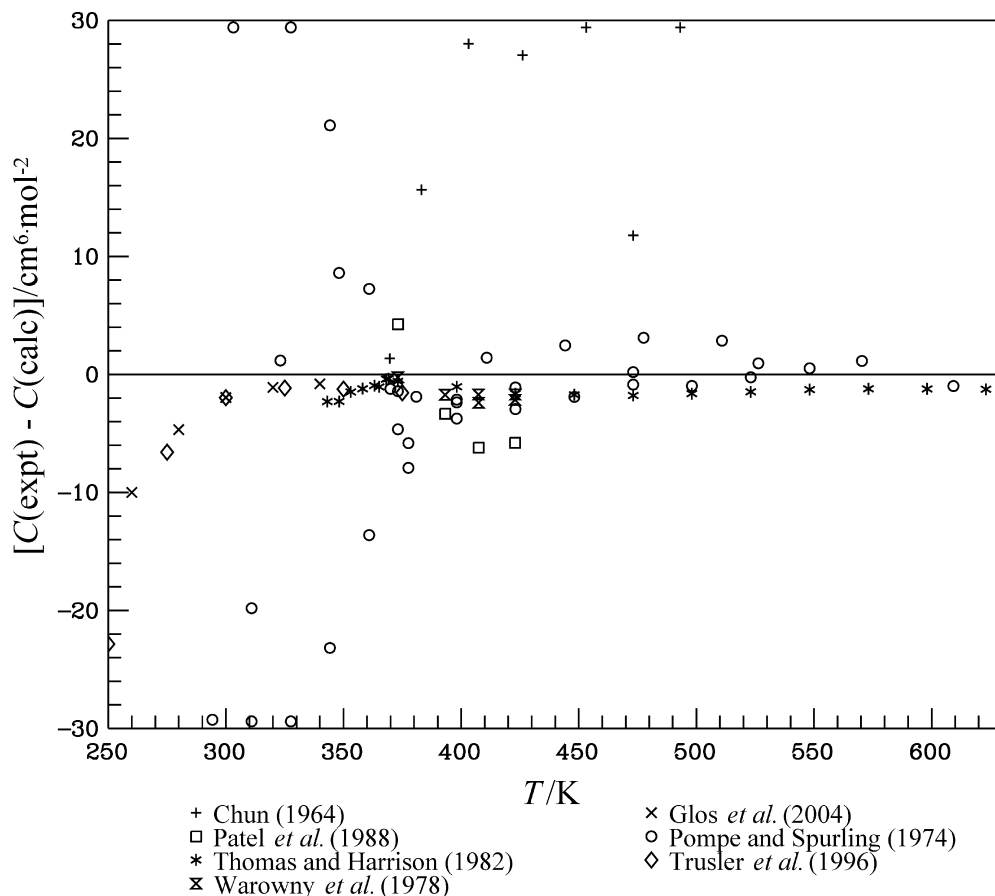


Figure 18. Comparisons of third virial coefficients C calculated with the equation of state to experimental data as a function of temperature T .

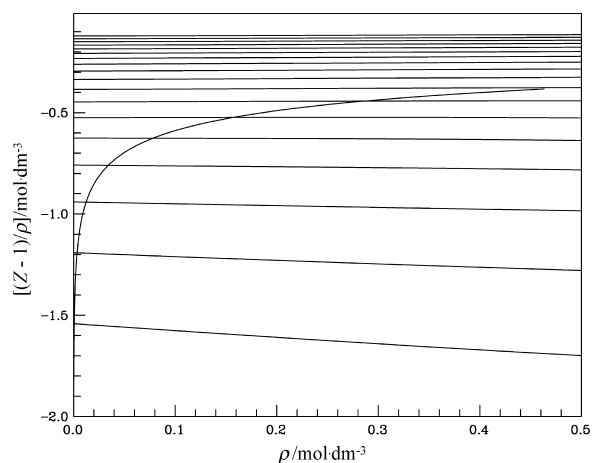


Figure 19. Calculations of $(Z - 1)/\rho$ along isotherms versus density ρ in the vapor phase region and two-phase region. Isotherms are shown from temperatures of (160 to 500) K in steps of 20 K.

The improved fitting techniques developed in this work achieved this goal and further decreased the lowest point at which the speed of sound remained linear. Figure 26 shows the speed of sound versus temperature along the saturation lines and along isobars. The melting line is shown on this plot as the curve that starts at the saturated liquid state at the triple point temperature and then intersects the liquid phase isobars. This figure shows that the saturation line for the liquid remains straight down to about 40 K, a reduced temperature of 0.11. We are currently developing an equation of state for propylene, and the new preliminary equation shows excellent extrapolation down to a reduced temperature of

0.005, which will be very useful in future plans to develop an equation for helium-3.

Additional plots of constant property lines on various thermodynamic coordinates were made to assess other behaviors of the equation of state. Figures 27 and 28 show plots of temperature versus isochoric heat capacity and isobaric heat capacity. These plots indicate that the equation of state exhibits reasonable behavior over all temperatures and pressures within the range of validity and that the extrapolation behavior is reasonable at higher temperatures and pressures. The plot of isochoric heat capacities shows an upward trend in the liquid phase at low temperatures. This is quite common among many fluids and has been validated experimentally for these fluids.

Figure 29 shows a plot of temperature vs density to extremely high conditions that are far beyond the limits of propane as a stable molecule (where dissociation has occurred). The purpose of this plot is to demonstrate that the equation continues to extrapolate extremely well to extremely high pressures, densities, and temperatures and that there are no hidden irregularities beyond normal applications. Most often these regions are overlooked, and most equations of state show adverse behavior at extreme values. Similar to the arguments given above for extrapolation to low temperatures, it is important that the curvature of the equation remains correct in regions of validity. Small changes in these regions have large effects on heat capacities and speeds of sound. One test to determine whether the curvature is correct is to look at extreme values where the curvature becomes apparent. If these regions are bad, then small changes in the curvature are most likely present within the range of validity

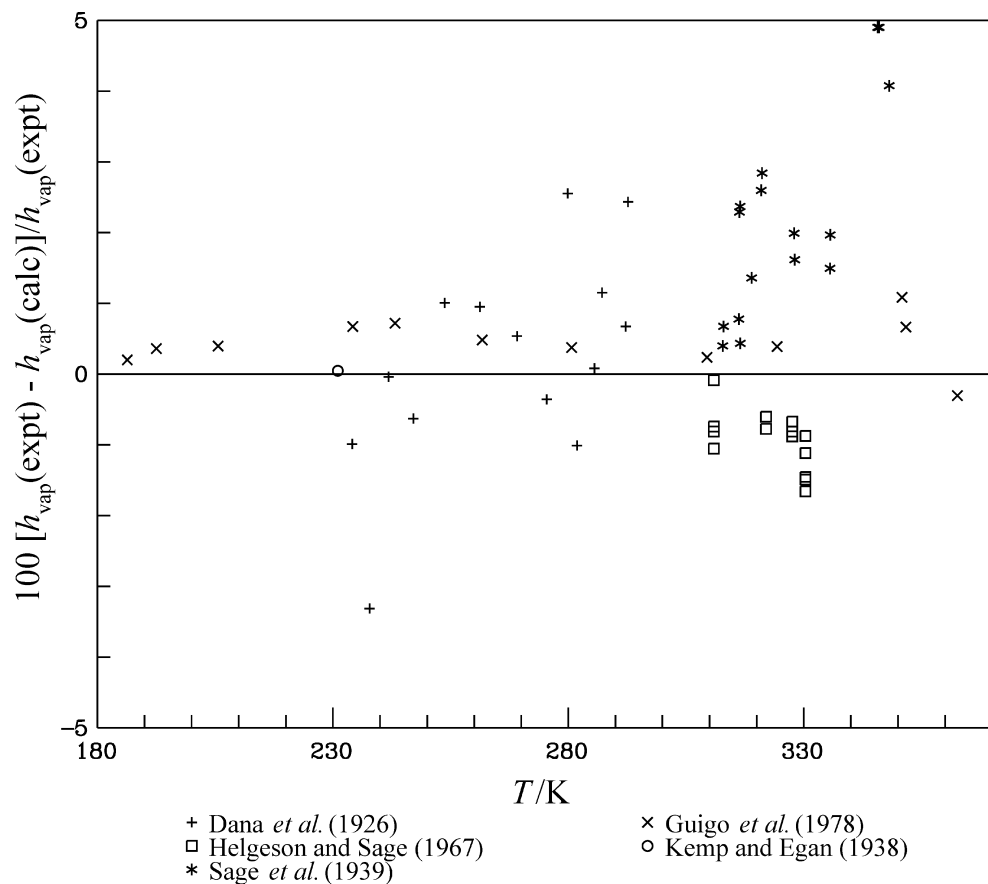


Figure 20. Comparisons of enthalpies of vaporization h_{vap} calculated with the equation of state to experimental data as a function of temperature T .

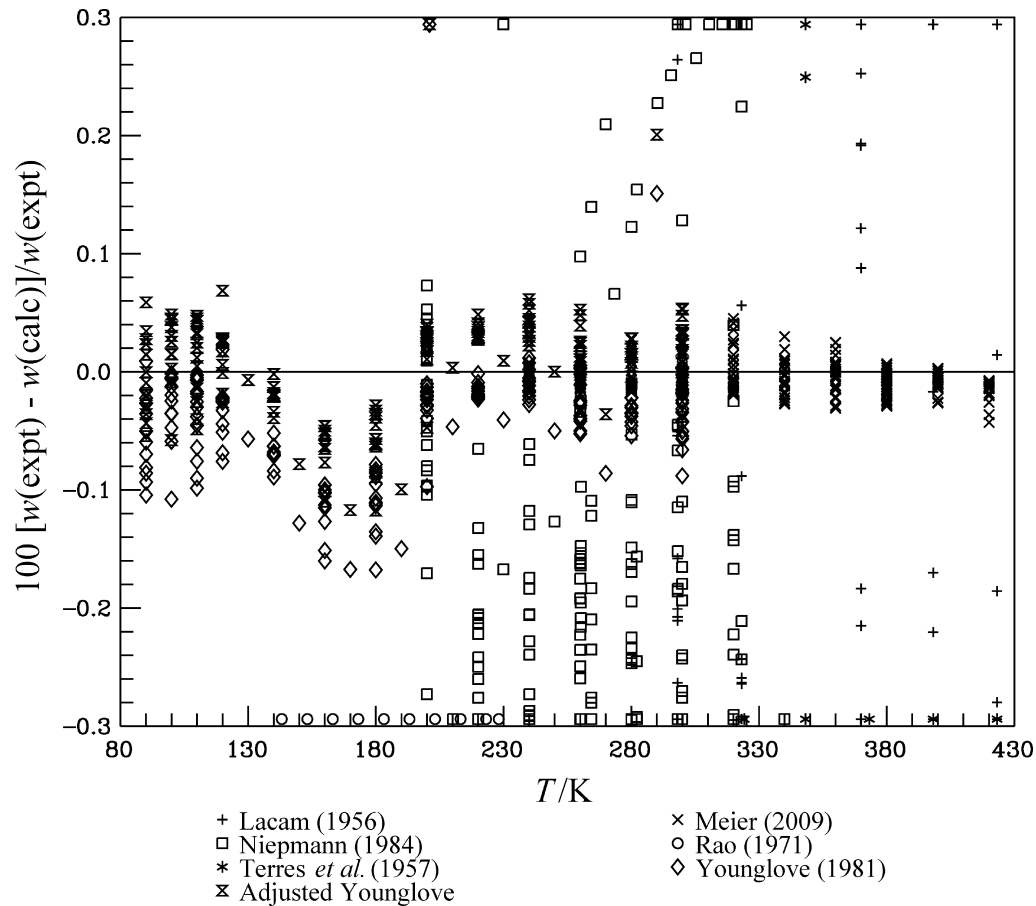


Figure 21. Comparisons of speeds of sound w in the liquid phase calculated with the equation of state to experimental data as a function of temperature T .

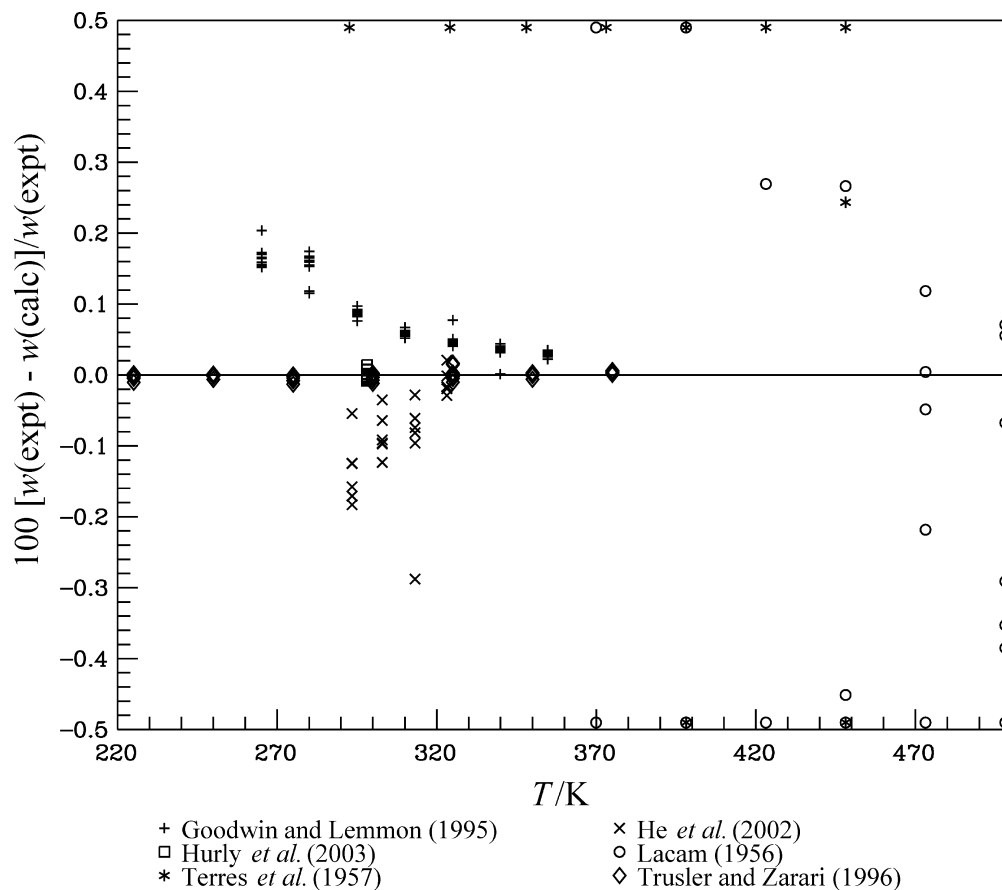


Figure 22. Comparisons of speeds of sound w in the vapor phase calculated with the equation of state to experimental data as a function of temperature T .

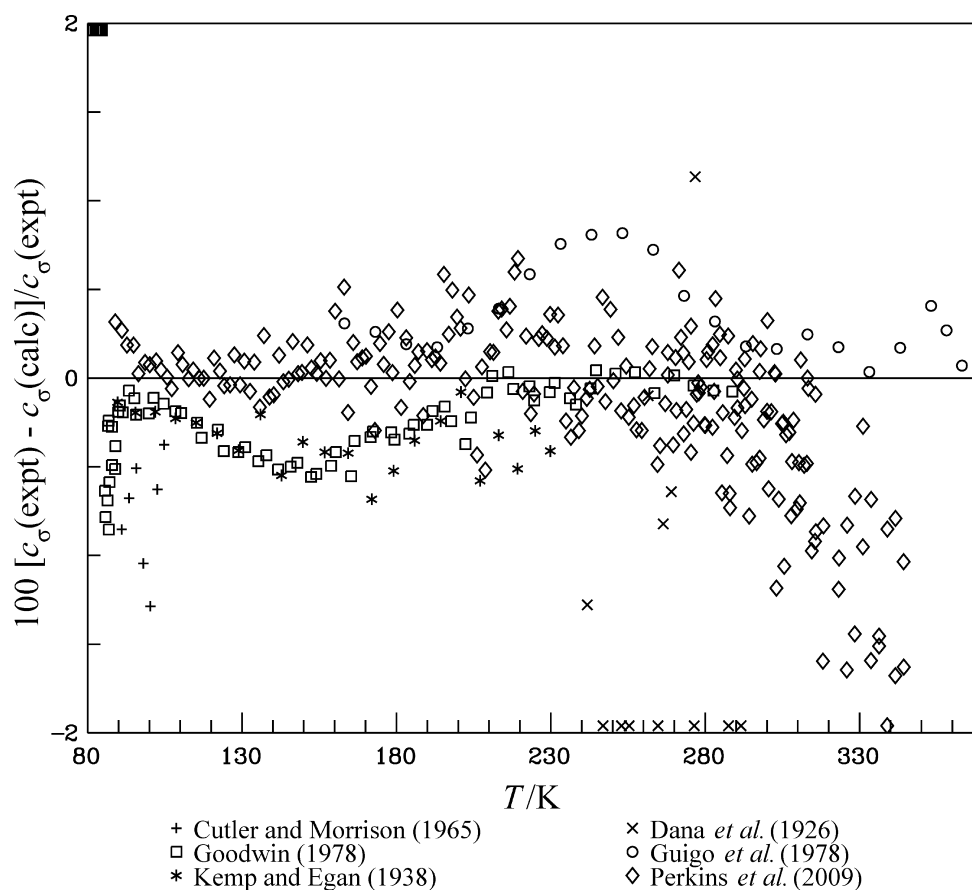


Figure 23. Comparisons of saturation heat capacities c_σ calculated with the equation of state to experimental data as a function of temperature T .

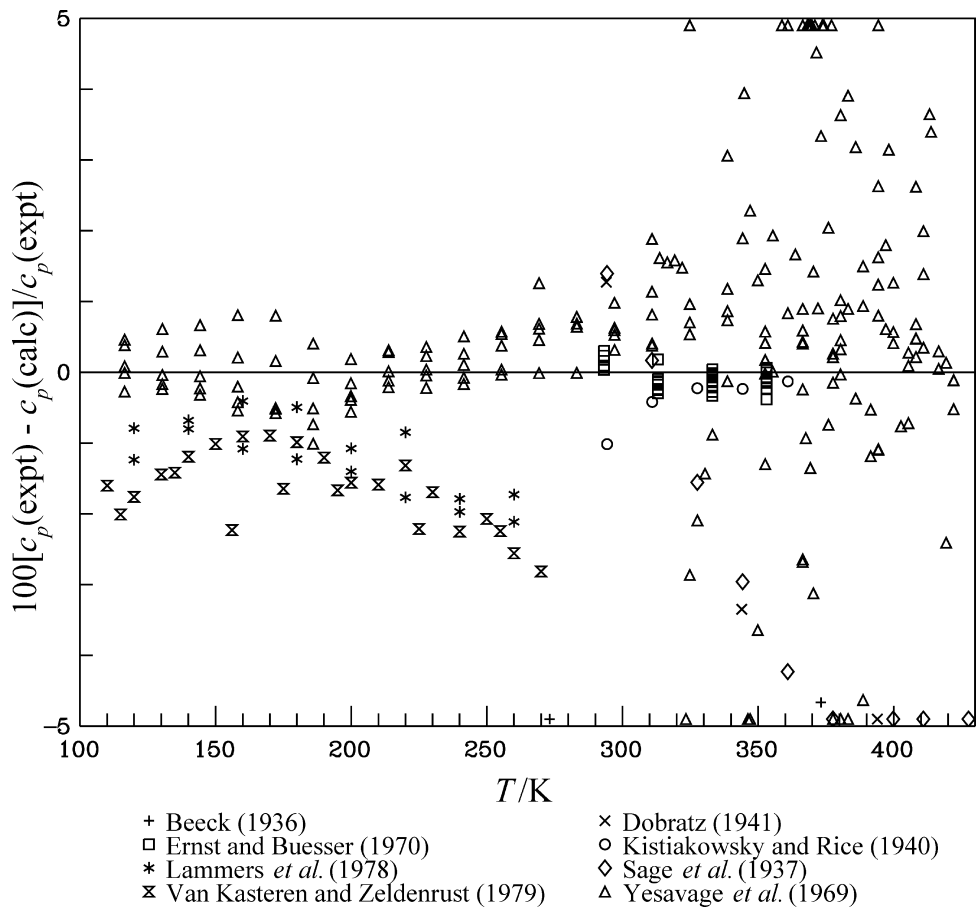


Figure 24. Comparisons of isobaric heat capacities c_p calculated with the equation of state to experimental data as a function of temperature T .

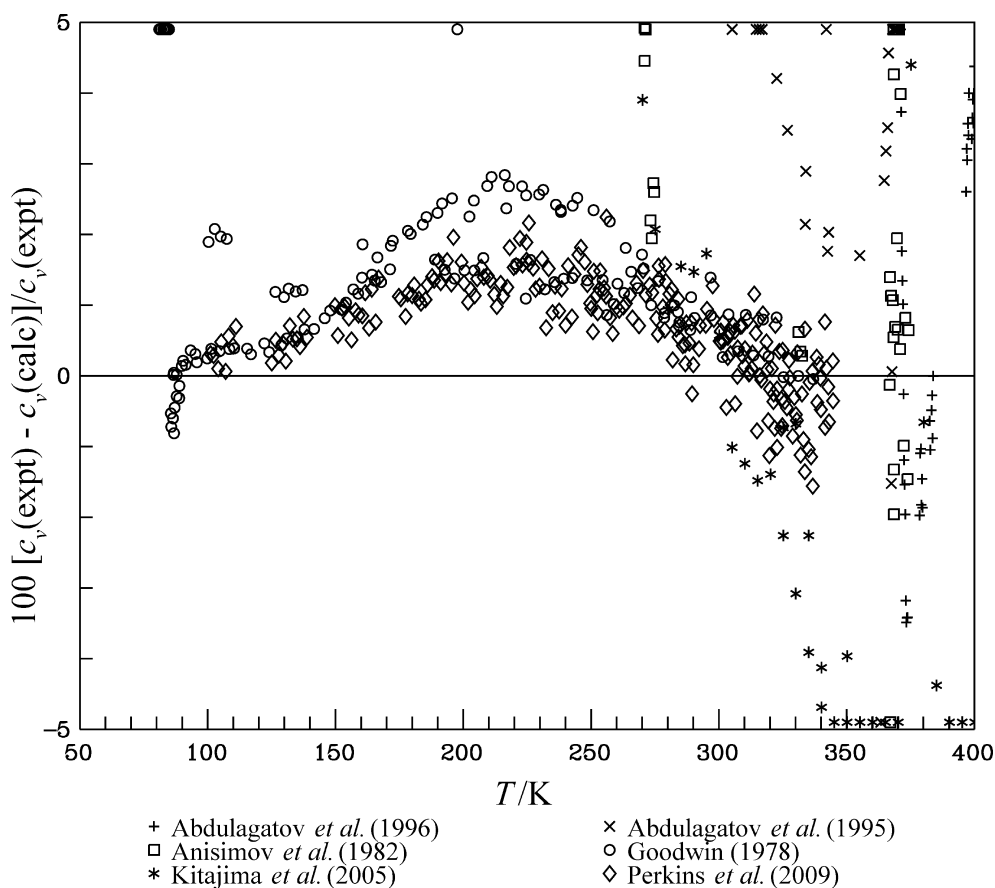


Figure 25. Comparisons of isochoric heat capacities c_v calculated with the equation of state to experimental data as a function of temperature T .

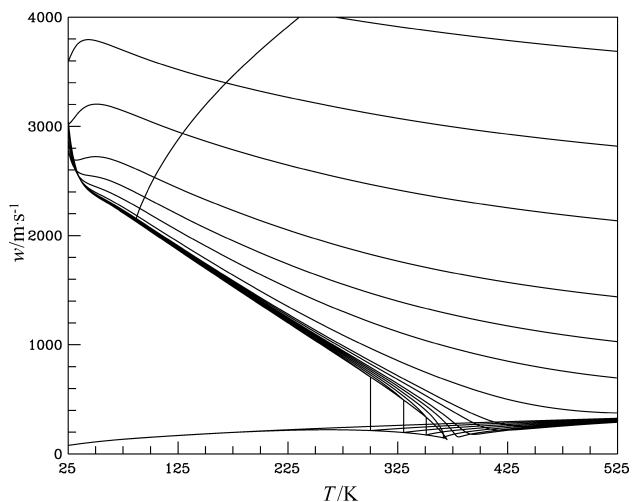


Figure 26. Speed of sound w versus temperature T diagram. Isobars are shown at pressures of (0, 1, 2, 3, 4, 5, 6, 8, 10, 20, 50, 100, 200, 500, 1000, and 2000) MPa. The melting line is shown intersecting the liquid phase isotherms. State points below the melting line are extrapolations of the liquid phase to very low temperatures.

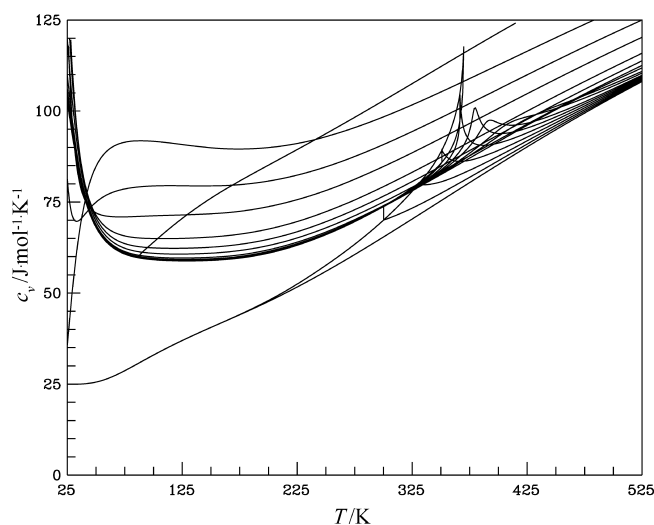


Figure 27. Isochoric heat capacity c_v versus temperature T diagram. Isobars are shown at pressures of (0, 1, 2, 3, 4, 5, 6, 8, 10, 20, 50, 100, 200, 500, 1000, and 2000) MPa. The melting line is shown intersecting the liquid phase isotherms. State points below the melting line are extrapolations of the liquid phase to very low temperatures.

of the equation. Figure 29 shows that the extrapolation is smooth to extremely high temperatures, pressures, and densities. This smooth behavior comes from the term with $t = 1$ and $d = 4$, as explained by Lemmon and Jacobsen.¹⁸⁹

Plots of certain characteristic curves are useful in assessing the behavior of an equation of state in regions away from the available data (Deiters and de Reuck,²¹³ Span and Wagner,¹⁹⁷ Span²¹⁴). The characteristic curves are the Boyle curve, given by the equation

$$\left(\frac{\partial Z}{\partial v}\right)_T = 0 \quad (26)$$

the Joule–Thomson inversion curve

$$\left(\frac{\partial Z}{\partial T}\right)_p = 0 \quad (27)$$

the Joule inversion curve

$$\left(\frac{\partial Z}{\partial T}\right)_v = 0 \quad (28)$$

and the ideal curve

$$\frac{p}{\rho RT} = 1 \quad (29)$$

The temperature at which the Boyle and ideal curves begin (at zero pressure) is also known as the Boyle temperature, or the temperature at which the second virial coefficient is zero. The point at which the Joule inversion curve begins (at zero pressure) corresponds to the temperature at which the second virial coefficient is at a maximum. (Thus, for the Joule inversion curve to extend to zero pressure, the second virial coefficient must pass through a maximum value, a criterion that is not followed by all equations of state.) Although the curves do not provide numerical information, reasonable shapes of the curves, as shown for propane in Figure 30, indicate qualitatively correct extrapolation behavior of the equation of state extending to high pressures and temperatures far in excess of the likely thermal stability of the fluid. The behavior of properties on the ideal curves should always be analyzed during the development of an equation.

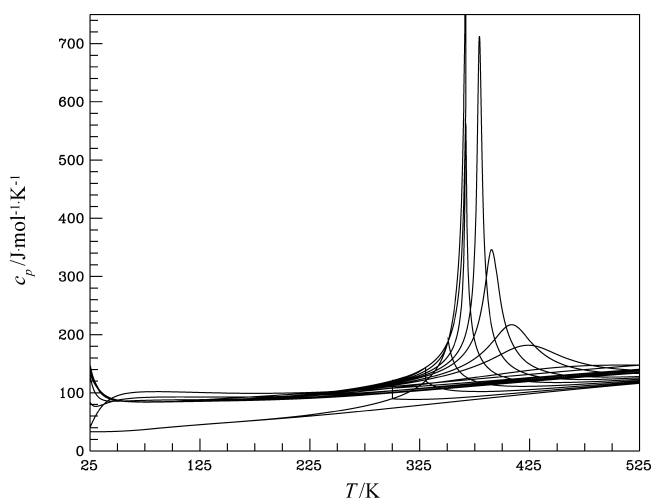


Figure 28. Isobaric heat capacity c_p versus temperature T diagram. Isobars are shown at pressures of (0, 1, 2, 3, 4, 5, 6, 8, 10, 20, 50, 100, 200, 500, 1000, and 2000) MPa. State points below the melting line are extrapolations of the liquid phase to very low temperatures.

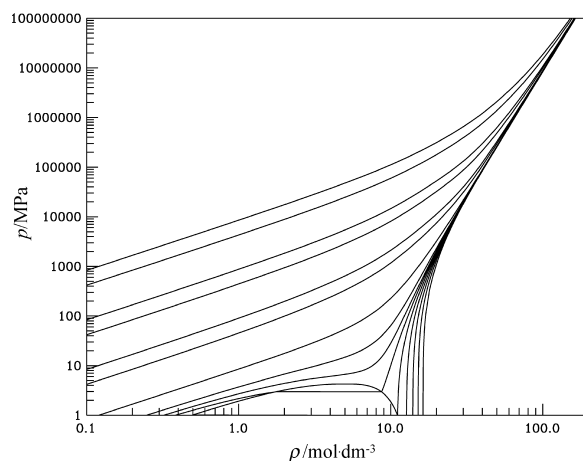


Figure 29. Isothermal behavior of the propane equation of state at extreme conditions of temperature T and pressure p . Isotherms are shown at temperatures of (100, 150, 200, 250, 300, 350, 400, 500, 1000, 5000, 10 000, ..., 1 000 000) K.

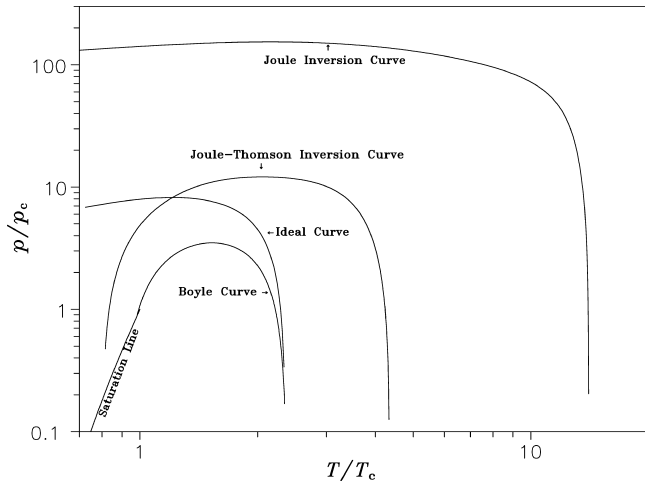


Figure 30. Characteristic (ideal) curves of the equation of state for propane as a function of temperature T and pressure p .

Table 5. Calculated Values of Properties for Algorithm Verification

T K	ρ $\text{mol} \cdot \text{dm}^{-3}$	p MPa	c_v $\text{J} \cdot \text{mol}^{-1} \cdot \text{K}^{-1}$	c_p $\text{J} \cdot \text{mol}^{-1} \cdot \text{K}^{-1}$	w $\text{m} \cdot \text{s}^{-1}$
200.0	14.0	2.3795138	61.078424	93.475362	1381.9552
300.0	12.0	19.053797	73.972542	108.61529	958.40520
300.0	0.4	0.84694991	69.021875	85.753997	221.88959
400.0	5.0	6.6462840	97.017439	271.07044	194.65847
369.9	5.0	4.2519399	117.71621	753625.00	130.89800

Equation of state terms with values of $t < 0$ have a detrimental effect on the shapes of the ideal curves. The effects of all terms should be dampened at high temperatures, but with $t < 0$, the contribution to the equation increases as the temperature rises. Negative temperature exponents should never be allowed in an equation of state of the form presented in this work.

Estimated Uncertainties of Calculated Properties

Below 350 K, the uncertainties ($k = 2$) in the new reference equation of state for propane for density are 0.01 % in the liquid phase and 0.03 % in the vapor phase (including saturated states for both phases). The liquid phase value also applies at temperatures greater than 350 K (to about 500 K) at pressures greater than 10 MPa. In the extended critical region, the uncertainties increase to 0.1 % in density, except very near the critical point, where the uncertainties in density increase rapidly as the critical point is approached. However, in this same region, the uncertainty in pressure calculated from density and temperature is 0.04 %, even at the critical point.

The uncertainties in the speed of sound are 0.01 % in the vapor phase at pressures up to 1 MPa, 0.03 % in the liquid phase between (260 and 420) K, and 0.1 % in the liquid phase at temperatures below 260 K. The uncertainties in vapor pressure are 0.02 % above 180 K and 0.1 % between (120 and 180) K and increase steadily below 120 K. Below 115 K, vapor pressures are less than 1 Pa, and uncertainty values increase to 3 % at the triple point. Uncertainties in heat capacities are 0.5 % in the liquid phase, 0.2 % in the vapor phase, and higher in the supercritical region.

As an aid for computer implementation, calculated values of properties from the equation of state for propane are given in Table 5. The number of digits displayed does not indicate the accuracy in the values but are given for validation of computer code.

Acknowledgment

We thank Mostafa Salehi and Marc Smith for their assistance with data entry and literature searching. We thank Dr. Roland Span

whose insights and collaborations have inspired us in various projects, including this one, over many years.

Appendix A: Thermodynamic Equations

The functional form of the Helmholtz energy equation of state is explicit in the dimensionless Helmholtz energy, α , with independent variables of dimensionless density and temperature

$$\alpha(\delta, \tau) = \alpha^0(\delta, \tau) + \alpha^r(\delta, \tau) \quad (30)$$

where $\delta = \rho/\rho_c$ and $\tau = T/T_c$. The critical parameters are 369.89 K and $5 \text{ mol} \cdot \text{dm}^{-3}$. The ideal gas Helmholtz energy is

$$\alpha^0 = \ln \delta + 3 \ln \tau + a_1 + a_2 \tau + \sum_{i=3}^6 a_i \ln[1 - \exp(-b_i \tau)] \quad (31)$$

where $a_1 = -4.970583$, $a_2 = 4.29352$, $a_3 = 3.043$, $b_3 = 1.062478$, $a_4 = 5.874$, $b_4 = 3.344237$, $a_5 = 9.337$, $b_5 = 5.363757$, $a_6 = 7.922$, and $b_6 = 11.762957$.

The residual fluid Helmholtz energy is

$$\alpha^r(\delta, \tau) = \sum_{k=1}^5 N_k \delta^{d_k} \tau^{t_k} + \sum_{k=6}^{11} N_k \delta^{d_k} \tau^{t_k} \exp(-\delta^{l_k}) + \sum_{k=12}^{18} N_k \delta^{d_k} \tau^{t_k} \exp(-\eta_k(\delta - \varepsilon_k)^2 - \beta_k(\tau - \gamma_k)^2) \quad (32)$$

The coefficients and parameters of this equation are given in Table 4. The functions used for calculating pressure (p), compressibility factor (Z), internal energy (u), enthalpy (h), entropy (s), Gibbs energy (g), isochoric heat capacity (c_v), isobaric heat capacity (c_p), and the speed of sound (w) from eq 30 are given below.

$$p = \rho^2 \left(\frac{\partial \alpha}{\partial \rho} \right)_\tau = \rho RT \left[1 + \delta \left(\frac{\partial \alpha^r}{\partial \delta} \right)_\tau \right] \quad (33)$$

$$Z = \frac{p}{\rho RT} = 1 + \delta \left(\frac{\partial \alpha^r}{\partial \delta} \right)_\tau \quad (34)$$

$$\frac{u}{RT} = \frac{a + Ts}{RT} = \tau \left[\left(\frac{\partial \alpha^0}{\partial \tau} \right)_\delta + \left(\frac{\partial \alpha^r}{\partial \tau} \right)_\delta \right] \quad (35)$$

$$\frac{h}{RT} = \frac{u + pv}{RT} = \tau \left[\left(\frac{\partial \alpha^0}{\partial \tau} \right)_\delta + \left(\frac{\partial \alpha^r}{\partial \tau} \right)_\delta \right] + \delta \left(\frac{\partial \alpha^r}{\partial \delta} \right)_\tau + 1 \quad (36)$$

$$\frac{s}{R} = -\frac{1}{R} \left(\frac{\partial \alpha}{\partial T} \right)_\rho = \tau \left[\left(\frac{\partial \alpha^0}{\partial \tau} \right)_\delta + \left(\frac{\partial \alpha^r}{\partial \tau} \right)_\delta \right] - \alpha^0 - \alpha^r \quad (37)$$

$$\frac{g}{RT} = \frac{h - Ts}{RT} = 1 + \alpha^0 + \alpha^r + \delta \left(\frac{\partial \alpha^r}{\partial \delta} \right)_\tau \quad (38)$$

$$\frac{c_v}{R} = \frac{1}{R} \left(\frac{\partial u}{\partial T} \right)_\rho = -\tau^2 \left[\left(\frac{\partial^2 \alpha^0}{\partial \tau^2} \right)_\delta + \left(\frac{\partial^2 \alpha^r}{\partial \tau^2} \right)_\delta \right] \quad (39)$$

$$\frac{c_p}{R} = \frac{1}{R} \left(\frac{\partial h}{\partial T} \right)_p = \frac{c_v}{R} + \frac{\left[1 + \delta \left(\frac{\partial \alpha^r}{\partial \delta} \right)_\tau - \delta \tau \left(\frac{\partial^2 \alpha^r}{\partial \delta \partial \tau} \right)_\tau \right]^2}{\left[1 + 2\delta \left(\frac{\partial \alpha^r}{\partial \delta} \right)_\tau + \delta^2 \left(\frac{\partial^2 \alpha^r}{\partial \delta^2} \right)_\tau \right]} \quad (40)$$

Table A1. Table of Thermodynamic Properties of Propane at Saturation^a

T	p	ρ	h	s	c_v	c_p	w
°C	MPa	kg·m ⁻³	kJ·kg ⁻¹	kJ·kg ⁻¹ ·K ⁻¹	kJ·kg ⁻¹ ·K ⁻¹	kJ·kg ⁻¹ ·K ⁻¹	m·s ⁻¹
-187.625 ^b	0.17203·10 ⁻⁹	733.13	-196.64	-1.396	1.355	1.916	2136.4
		0.107·10 ⁻⁷	366.26	5.186	0.6907	0.8792	143.3
-185.	0.48526·10 ⁻⁹	730.39	-191.61	-1.338	1.352	1.918	2118.6
		0.292·10 ⁻⁷	368.58	5.017	0.7010	0.8896	145.2
-180.	0.29386·10 ⁻⁸	725.20	-182.01	-1.232	1.346	1.923	2084.6
		0.167·10 ⁻⁶	373.08	4.727	0.7208	0.9093	148.9
-175.	0.14596·10 ⁻⁷	720.05	-172.38	-1.131	1.343	1.928	2050.4
		0.789·10 ⁻⁶	377.67	4.473	0.7404	0.9289	152.4
-170.	0.61256·10 ⁻⁷	714.92	-162.73	-1.035	1.340	1.934	2016.2
		0.315·10 ⁻⁵	382.36	4.249	0.7596	0.9481	155.8
-165.	0.22252·10 ⁻⁶	709.82	-153.04	-0.9437	1.338	1.941	1982.0
		0.0000109	387.15	4.051	0.7784	0.9669	159.2
-160.	0.71368·10 ⁻⁶	704.73	-143.32	-0.8558	1.336	1.947	1947.9
		0.0000335	392.03	3.876	0.7967	0.9852	162.4
-155.	0.20542·10 ⁻⁵	699.67	-133.57	-0.7715	1.335	1.954	1913.9
		0.0000922	397.00	3.719	0.8145	1.003	165.6
-150.	0.53795·10 ⁻⁵	694.61	-123.78	-0.6903	1.334	1.962	1880.0
		0.000232	402.06	3.580	0.8319	1.020	168.8
-145.	0.12965·10 ⁻⁴	689.56	-113.95	-0.6121	1.334	1.969	1846.2
		0.000537	407.21	3.455	0.8489	1.037	171.8
-140.	0.29040·10 ⁻⁴	684.51	-104.09	-0.5366	1.334	1.977	1812.5
		0.00116	412.43	3.343	0.8655	1.054	174.9
-135.	0.60950·10 ⁻⁴	679.46	-94.181	-0.4636	1.335	1.985	1779.0
		0.00234	417.74	3.242	0.8818	1.070	177.8
-130.	0.00012073	674.40	-84.234	-0.3929	1.336	1.994	1745.5
		0.00447	423.12	3.151	0.8979	1.087	180.7
-125.	0.00022708	669.33	-74.243	-0.3243	1.337	2.003	1712.0
		0.00813	428.58	3.070	0.9138	1.103	183.5
-120.	0.00040774	664.26	-64.207	-0.2576	1.339	2.012	1678.6
		0.01413	434.11	2.996	0.9297	1.119	186.3
-115.	0.00070215	659.16	-54.122	-0.1928	1.341	2.022	1645.2
		0.02357	439.71	2.930	0.9455	1.135	189.0
-110.	0.0011644	654.05	-43.988	-0.1298	1.343	2.032	1611.8
		0.03790	445.38	2.870	0.9614	1.151	191.7
-105.	0.0018661	648.91	-33.802	-0.06827	1.346	2.043	1578.4
		0.05897	451.10	2.815	0.9775	1.168	194.2
-100.	0.0028994	643.74	-23.560	-0.00826	1.350	2.054	1544.9
		0.08904	456.88	2.766	0.9937	1.184	196.8
-95.	0.0043795	638.55	-13.260	0.05038	1.355	2.066	1511.5
		0.13085	462.71	2.722	1.010	1.202	199.2
-90.	0.0064475	633.32	-2.8974	0.1077	1.360	2.078	1478.0
		0.18762	468.58	2.682	1.027	1.220	201.5
-85.	0.0092716	628.06	7.5304	0.1639	1.366	2.092	1444.6
		0.26304	474.49	2.646	1.045	1.239	203.8
-80.	0.013049	622.76	18.028	0.2189	1.372	2.106	1411.2
		0.36132	480.44	2.613	1.063	1.258	205.9
-75.	0.018008	617.41	28.600	0.2729	1.380	2.121	1377.8
		0.48715	486.41	2.583	1.081	1.279	208.0
-70.	0.024404	612.02	39.251	0.3259	1.388	2.137	1344.6
		0.64570	492.41	2.557	1.100	1.300	209.9
-65.	0.032527	606.57	49.986	0.3781	1.397	2.154	1311.4
		0.84261	498.42	2.532	1.120	1.323	211.8
-60.	0.042693	601.08	60.811	0.4294	1.406	2.172	1278.4
		1.0840	504.44	2.511	1.140	1.346	213.5
-55.	0.055249	595.52	71.731	0.4799	1.417	2.191	1245.4
		1.3764	510.46	2.491	1.161	1.371	215.0
-50.	0.070569	589.90	82.753	0.5298	1.428	2.212	1212.5
		1.7270	516.48	2.473	1.182	1.397	216.5
-45.	0.089051	584.20	93.881	0.5789	1.439	2.233	1179.7
		2.1430	522.49	2.458	1.204	1.424	217.7
-42.114 ^c	0.101325	580.88	100.36	0.6070	1.446	2.246	1160.8
		2.4161	525.95	2.449	1.217	1.440	218.4
-40.	0.11112	578.43	105.12	0.6275	1.452	2.256	1147.0
		2.6326	528.48	2.443	1.227	1.453	218.9

Table A1. Continued

T	p	ρ	h	s	c_v	c_p	w
°C	MPa	kg·m ⁻³	kJ·kg ⁻¹	kJ·kg ⁻¹ ·K ⁻¹	kJ·kg ⁻¹ ·K ⁻¹	kJ·kg ⁻¹ ·K ⁻¹	m·s ⁻¹
-35.	0.13723	572.58	116.49	0.6755	1.464	2.280	1114.4
		3.2042	534.45	2.431	1.250	1.482	219.8
-30.	0.16783	566.64	127.97	0.7231	1.478	2.305	1081.7
		3.8669	540.38	2.419	1.274	1.513	220.6
-25.	0.20343	560.60	139.60	0.7701	1.492	2.332	1049.1
		4.6302	546.28	2.409	1.298	1.546	221.2
-20.	0.24452	554.45	151.36	0.8168	1.507	2.361	1016.5
		5.5046	552.13	2.400	1.323	1.580	221.6
-15.	0.29162	548.19	163.28	0.8630	1.522	2.391	983.8
		6.5012	557.93	2.392	1.348	1.616	221.9
-10.	0.34528	541.80	175.35	0.9090	1.538	2.423	951.1
		7.6321	563.65	2.385	1.374	1.655	221.9
-5.	0.40604	535.27	187.59	0.9546	1.555	2.457	918.3
		8.9103	569.30	2.378	1.400	1.695	221.7
0.	0.47446	528.59	200.00	1.000	1.572	2.493	885.5
		10.351	574.87	2.372	1.427	1.739	221.3
5.	0.55112	521.75	212.60	1.045	1.590	2.532	852.5
		11.969	580.33	2.367	1.455	1.785	220.7
10.	0.63660	514.73	225.40	1.090	1.608	2.573	819.4
		13.783	585.67	2.363	1.484	1.835	219.8
15.	0.73151	507.50	238.40	1.135	1.627	2.618	786.2
		15.813	590.89	2.358	1.514	1.890	218.6
20.	0.83646	500.06	251.64	1.180	1.647	2.666	752.9
		18.082	595.95	2.354	1.544	1.949	217.2
25.	0.95207	492.36	265.11	1.225	1.667	2.719	719.3
		20.618	600.84	2.351	1.576	2.015	215.5
30.	1.0790	484.39	278.83	1.269	1.688	2.777	685.5
		23.451	605.54	2.347	1.609	2.088	213.5
35.	1.2179	476.10	292.84	1.314	1.710	2.841	651.4
		26.618	610.01	2.344	1.643	2.170	211.2
40.	1.3694	467.46	307.15	1.359	1.732	2.913	617.0
		30.165	614.21	2.340	1.678	2.263	208.6
45.	1.5343	458.40	321.79	1.405	1.756	2.995	582.1
		34.146	618.12	2.336	1.715	2.371	205.6
50.	1.7133	448.87	336.80	1.450	1.780	3.089	546.8
		38.630	621.66	2.332	1.753	2.499	202.2
55.	1.9072	438.76	352.23	1.496	1.805	3.201	510.9
		43.706	624.77	2.327	1.794	2.652	198.3
60.	2.1168	427.97	368.14	1.543	1.832	3.337	474.2
		49.493	627.36	2.321	1.836	2.841	194.1
65.	2.3430	416.34	384.60	1.590	1.861	3.509	436.6
		56.152	629.29	2.314	1.880	3.086	189.3
70.	2.5868	403.62	401.75	1.639	1.892	3.735	397.9
		63.916	630.37	2.305	1.930	3.421	184.0
75.	2.8493	389.47	419.76	1.689	1.927	4.053	357.5
		73.140	630.33	2.294	1.987	3.914	178.2
80.	3.1319	373.29	438.93	1.742	1.969	4.545	314.9
		84.406	628.73	2.279	2.057	4.707	171.6
85.	3.4361	353.96	459.81	1.798	2.023	5.433	269.1
		98.818	624.75	2.259	2.144	6.182	164.1
90.	3.7641	328.83	483.71	1.862	2.107	7.623	218.3
		119.00	616.47	2.227	2.260	9.888	155.5
95.	4.1195	286.51	516.33	1.948	2.302	23.59	158.1
		156.31	595.81	2.164	2.467	36.07	144.1
96.740 ^d	4.2512	220.48	555.24	2.052			

^a The first line at each temperature gives saturated liquid properties, and the second line gives saturated vapor properties. ^b Triple point. ^c Normal boiling point. ^d Critical point.

$$\begin{aligned} \frac{w^2 M}{RT} &= \frac{M}{RT} \left(\frac{\partial p}{\partial \rho} \right)_s \\ &= 1 + 2\delta \left(\frac{\partial \alpha^r}{\partial \delta} \right)_\tau + \delta^2 \left(\frac{\partial^2 \alpha^r}{\partial \delta^2} \right)_\tau - \frac{\left[1 + \delta \left(\frac{\partial \alpha^r}{\partial \delta} \right)_\tau - \delta \tau \left(\frac{\partial^2 \alpha^r}{\partial \delta \partial \tau} \right) \right]^2}{\tau^2 \left[\left(\frac{\partial^2 \alpha^0}{\partial \tau^2} \right)_\delta + \left(\frac{\partial^2 \alpha^r}{\partial \tau^2} \right)_\delta \right]} \end{aligned} \quad (41)$$

The fugacity coefficient and second and third virial coefficients are given in the following equations.

$$\phi = \exp[Z - 1 - \ln(Z) + \alpha^r] \quad (42)$$

$$B(T) = \lim_{\delta \rightarrow 0} \left[\frac{1}{\rho_c} \left(\frac{\partial \alpha^r}{\partial \delta} \right)_\tau \right] \quad (43)$$

$$C(T) = \lim_{\delta \rightarrow 0} \left[\frac{1}{\rho_c^2} \left(\frac{\partial^2 \alpha^r}{\partial \delta^2} \right)_\tau \right] \quad (44)$$

Other derived properties, given below, include the first derivative of pressure with respect to density at constant temperature $(\partial p / \partial \rho)_T$, the second derivative of pressure with respect to density at constant temperature $(\partial^2 p / \partial \rho^2)_T$, and the first derivative of pressure with respect to temperature at constant density $(\partial p / \partial T)_\rho$.

$$\left(\frac{\partial p}{\partial \rho} \right)_T = RT \left[1 + 2\delta \left(\frac{\partial \alpha^r}{\partial \delta} \right)_\tau + \delta^2 \left(\frac{\partial^2 \alpha^r}{\partial \delta^2} \right)_\tau \right] \quad (45)$$

$$\left(\frac{\partial^2 p}{\partial \rho^2} \right)_T = \frac{RT}{\rho} \left[2\delta \left(\frac{\partial \alpha^r}{\partial \delta} \right)_\tau + 4\delta^2 \left(\frac{\partial^2 \alpha^r}{\partial \delta^2} \right)_\tau + \delta^3 \left(\frac{\partial^3 \alpha^r}{\partial \delta^3} \right)_\tau \right] \quad (46)$$

$$\left(\frac{\partial p}{\partial T} \right)_\rho = R\rho \left[1 + \delta \left(\frac{\partial \alpha^r}{\partial \delta} \right)_\tau - \delta \tau \left(\frac{\partial^2 \alpha^r}{\partial \delta \partial \tau} \right) \right] \quad (47)$$

Equations for additional thermodynamic properties such as the isothermal compressibility and the Joule–Thomson coefficient are given in Lemmon et al.²¹⁵

The derivatives of the ideal gas Helmholtz energy required by the equations for the thermodynamic properties are

$$\tau \frac{\partial \alpha^0}{\partial \tau} = 3 + a_2 \tau + \tau \sum_{k=3}^6 a_k b_k \left[\frac{1}{\exp(b_k \tau) - 1} \right] \quad (48)$$

and

$$\tau^2 \frac{\partial^2 \alpha^0}{\partial \tau^2} = -3 - \tau^2 \sum_{k=3}^6 a_k b_k^2 \frac{\exp(b_k \tau)}{[\exp(b_k \tau) - 1]^2} \quad (49)$$

The derivatives of the residual Helmholtz energy are given in the following equations.

$$\begin{aligned} \delta \frac{\partial \alpha^r}{\partial \delta} &= \sum_{k=1}^5 N_k \delta^{d_k} \tau^{l_k} d_k + \sum_{k=6}^{11} N_k \delta^{d_k} \tau^{l_k} \exp(-\delta^{l_k}) \times \\ &[d_k - l_k \delta^{l_k}] + \sum_{k=12}^{18} N_k \delta^{d_k} \tau^{l_k} \exp(-\eta_k (\delta - \varepsilon_k)^2 - \beta_k (\tau - \gamma_k)^2) \cdot \\ &[d_k - 2\eta_k \delta (\delta - \varepsilon_k)] \end{aligned} \quad (50)$$

$$\begin{aligned} \delta^2 \frac{\partial^2 \alpha^r}{\partial \delta^2} &= \sum_{k=1}^5 N_k \delta^{d_k} \tau^{l_k} [d_k (d_k - 1)] + \sum_{k=6}^{11} N_k \delta^{d_k} \tau^{l_k} \times \\ &\exp(-\delta^{l_k}) [(d_k - l_k \delta^{l_k}) (d_k - 1 - l_k \delta^{l_k}) - l_k^2 \delta^{l_k}] + \\ &\sum_{k=12}^{18} N_k \delta^{d_k} \tau^{l_k} \exp(-\eta_k (\delta - \varepsilon_k)^2 - \beta_k (\tau - \gamma_k)^2) \cdot \\ &\{[d_k - 2\eta_k \delta (\delta - \varepsilon_k)]^2 - d_k - 2\eta_k \delta^2\} \end{aligned} \quad (51)$$

$$\begin{aligned} \delta^3 \frac{\partial^3 \alpha^r}{\partial \delta^3} &= \sum_{k=1}^5 N_k \delta^{d_k} \tau^{l_k} [d_k (d_k - 1) (d_k - 2)] + \\ &\sum_{k=6}^{11} N_k \delta^{d_k} \tau^{l_k} \exp(-\delta^{l_k}) \{d_k (d_k - 1) (d_k - 2) + \\ &l_k \delta^{l_k} [-2 + 6d_k - 3d_k^2 - 3d_k l_k + 3l_k - l_k^2] + \\ &3l_k^2 \delta^{2l_k} [d_k - 1 + l_k] - l_k^3 \delta^{3l_k}\} + \\ &\sum_{k=12}^{18} N_k \delta^{d_k} \tau^{l_k} \exp(-\eta_k (\delta - \varepsilon_k)^2 - \beta_k (\tau - \gamma_k)^2) \cdot \\ &\{[d_k - 2\eta_k \delta (\delta - \varepsilon_k)]^3 - 3d_k^2 + 2d_k - \\ &6d_k \eta_k \delta^2 + 6\eta_k \delta (\delta - \varepsilon_k) (d_k + 2\eta_k \delta^2)\} \end{aligned} \quad (52)$$

$$\begin{aligned} \tau \frac{\partial \alpha^r}{\partial \tau} &= \sum_{k=1}^5 N_k \delta^{d_k} \tau^{l_k} l_k + \sum_{k=6}^{11} N_k \delta^{d_k} \tau^{l_k} \exp(-\delta^{l_k}) l_k + \\ &\sum_{k=12}^{18} N_k \delta^{d_k} \tau^{l_k} \exp(-\eta_k (\delta - \varepsilon_k)^2 - \beta_k (\tau - \gamma_k)^2) \times \\ &[l_k - 2\beta_k \tau (\tau - \gamma_k)] \end{aligned} \quad (53)$$

$$\begin{aligned} \tau^2 \frac{\partial^2 \alpha^r}{\partial \tau^2} &= \sum_{k=1}^5 N_k \delta^{d_k} \tau^{l_k} [l_k (l_k - 1)] + \sum_{k=6}^{11} N_k \delta^{d_k} \tau^{l_k} \exp(-\delta^{l_k}) \\ &[l_k (l_k - 1)] + \sum_{k=12}^{18} N_k \delta^{d_k} \tau^{l_k} \exp(-\eta_k (\delta - \varepsilon_k)^2 - \beta_k (\tau - \gamma_k)^2) \cdot \\ &\{[l_k - 2\beta_k \tau (\tau - \gamma_k)]^2 - l_k - 2\beta_k \tau^2\} \end{aligned} \quad (54)$$

$$\begin{aligned} \tau \delta \frac{\partial^2 \alpha^r}{\partial \tau \partial \delta} &= \sum_{k=1}^5 N_k \delta^{d_k} \tau^{l_k} [d_k l_k] + \sum_{k=6}^{11} N_k \delta^{d_k} \tau^{l_k} \exp(-\delta^{l_k}) \times \\ &[l_k (d_k - l_k \delta^{l_k})] + \sum_{k=12}^{18} N_k \delta^{d_k} \tau^{l_k} \exp(-\eta_k (\delta - \varepsilon_k)^2 - \\ &\beta_k (\tau - \gamma_k)^2) \cdot [d_k - 2\eta_k \delta (\delta - \varepsilon_k)] [l_k - 2\beta_k \tau (\tau - \gamma_k)] \end{aligned} \quad (55)$$

$$\begin{aligned} \delta \tau^2 \frac{\partial^3 \alpha^r}{\partial \delta \partial \tau^2} &= \sum_{k=1}^5 N_k \delta^{d_k} \tau^{l_k} [d_k l_k (l_k - 1)] + \sum_{k=6}^{11} N_k \delta^{d_k} \tau^{l_k} \times \\ &\exp(-\delta^{l_k}) [l_k (l_k - 1) (d_k - l_k \delta^{l_k})] + \\ &\sum_{k=12}^{18} N_k \delta^{d_k} \tau^{l_k} \exp(-\eta_k (\delta - \varepsilon_k)^2 - \\ &\beta_k (\tau - \gamma_k)^2) \cdot [d_k - 2\eta_k \delta (\delta - \varepsilon_k)] \{[l_k - \\ &2\beta_k \tau (\tau - \gamma_k)]^2 - l_k - 2\beta_k \tau^2\} \end{aligned} \quad (56)$$

Literature Cited

- (1) Aalto, M.; Liukkonen, S. *J. Chem. Eng. Data* **1996**, *41*, 79–83.
- (2) Abdulagatov, I. M.; Kiselev, S. B.; Levina, L. N.; Zakaryayev, Z. R.; Mamchenkova, O. N. *Int. J. Thermophys.* **1996**, *17*, 423–440.
- (3) Abdulagatov, I. M.; Levina, L. N.; Zakaryayev, Z. R.; Mamchenkova, O. N. *J. Chem. Thermodyn.* **1995**, *27*, 1385–1406.
- (4) Abdulagatov, I. M.; Levina, L. N.; Zakaryayev, Z. R.; Mamchenkova, O. N. *Fluid Phase Equilib.* **1997**, *127*, 205–236.
- (5) Ambrose, D.; Tsonopoulos, C. *J. Chem. Eng. Data* **1995**, *40*, 531–546.
- (6) Anisimov, M. A.; Beketov, V. G.; Voronov, V. P.; Nagaev, V. B.; Smirnov, V. A. *Thermophys. Prop. Subst.* **1982**, *16*, 48–59.
- (7) Babb, S. E., Jr.; Robertson, S. L. *J. Chem. Phys.* **1970**, *53*, 1097.
- (8) Barber, J. R. Phase relationships of binary hydrocarbon systems propane-n-butane. Masters Thesis, Ohio State University, 1964.
- (9) Barber, J. R.; Kay, W. B.; Teja, A. S. *AIChE J.* **1982**, *28*, 134–138.
- (10) Barber, J. R.; Kay, W. B.; Teja, A. S. *AIChE J.* **1982**, *28*, 142–147.
- (11) Barkan, E. S. *Russ. J. Phys. Chem.* **1983**, *57*, 1351–1355.
- (12) Beattie, J. A.; Poffenberger, N.; Hadlock, C. J. *J. Chem. Phys.* **1935**, *3*, 96–97.
- (13) Beeck, O. *J. Chem. Phys.* **1936**, *4*, 680–689.
- (14) Bobbo, S.; Fedele, L.; Camporese, R.; Stryjek, R. *Fluid Phase Equilib.* **2002**, *199*, 175–183.

- (15) Brunner, E. J. *Chem. Thermodyn.* **1985**, *17*, 871–885.
- (16) Brunner, E. J. *Chem. Thermodyn.* **1988**, *20*, 273–297.
- (17) Burgoyne, J. H. *Proc. R. Soc. London* **1940**, A176, 280–294.
- (18) Burrell, G. A.; Robertson, I. W. *Vapor pressures of various compounds at low temperatures*. U.S. Bur. Mines Tech. Pap., Number 142, **1916**.
- (19) Calado, J. C. G.; Filipe, E. J. M.; Lopes, J. N. C. *Fluid Phase Equilib.* **1997**, *135*, 249–257.
- (20) Carney, B. R. *Pet. Ref.* **1942**, *21*, 84–92.
- (21) Carruth, G. F.; Kobayashi, R. J. *Chem. Eng. Data* **1973**, *18*, 115–126.
- (22) Chao, J.; Wilhoit, R. C.; Zwolinski, B. J. *J. Phys. Chem. Ref. Data* **1973**, *2*, 427–432.
- (23) Cherney, B. J.; Marchman, H.; York, R. *Ind. Eng. Chem.* **1949**, *41*, 2653–2658.
- (24) Chun, S. W. The phase behavior of binary systems in the critical region: Effect of molecular structure (The propane-isomeric hexane system). Ph.D. Dissertation, Ohio State University, 1964.
- (25) Chun, S. W.; Kay, W. B.; Teja, A. S. *Ind. Eng. Chem. Fundam.* **1981**, *20*, 278–280.
- (26) Clark, F. G. Molecular thermodynamics and phase equilibria in the propane-methyl chloride system. Ph.D. Dissertation, University of Illinois, 1973.
- (27) Claus, P.; Schilling, G.; Kleinrahn, R.; Wagner, W. *Internal Report*, Ruhr-Universität Bochum, **2002**. Data were reported by Glos et al.⁴⁸
- (28) Clegg, H. P.; Rowlinson, J. S. *Trans. Faraday Soc.* **1955**, *51*, 1333–1340.
- (29) Coquelet, C.; Chareton, A.; Valtz, A.; Baba-Ahmed, A.; Richon, D. *J. Chem. Eng. Data* **2003**, *48*, 317–323.
- (30) Cutler, A. J. B.; Morrison, J. A. *Trans. Faraday Soc.* **1965**, *61*, 429–442.
- (31) Dailey, B. P.; Felsing, W. A. *J. Am. Chem. Soc.* **1943**, *65*, 42–44.
- (32) Dana, L. I.; Jenkins, A. C.; Burdick, J. N.; Timm, R. C. *Refrig. Eng.* **1926**, *12*, 387–405.
- (33) Dawson, P. P., Jr.; McKetta, J. J. *Pet. Ref.* **1960**, *39*, 151–154.
- (34) Defibaugh, D. R.; Moldover, M. R. *J. Chem. Eng. Data* **1997**, *42*, 160–168.
- (35) Delaplace, R. *Compt. Rend.* **1937**, *204*, 493–496.
- (36) Deschner, W. W.; Brown, G. G. *Ind. Eng. Chem.* **1940**, *32*, 836–840.
- (37) Dittmar, P.; Schultz, F.; Strese, G. *Chem. Ing. Tech.* **1962**, *34*, 437–441.
- (38) Djordjević, L.; Budenholzer, R. A. *J. Chem. Eng. Data* **1970**, *15*, 10–12.
- (39) Dobratz, C. J. *Ind. Eng. Chem.* **1941**, *33*, 759–762.
- (40) Echols, L. S., Jr.; Gelus, E. *Anal. Chem.* **1947**, *19*, 668–675.
- (41) Ely, J. F.; Kobayashi, R. J. *Chem. Eng. Data* **1978**, *23*, 221–223.
- (42) Ernst, G.; Büsler, J. J. *Chem. Thermodyn.* **1970**, *2*, 787–791.
- (43) Esper, G.; Lemming, W.; Beckermann, W.; Kohler, F. *Fluid Phase Equilib.* **1995**, *105*, 173–192.
- (44) Eubank, P. T.; Das, T. R.; Reed, C. O., Jr. *Adv. Cryog. Eng.* **1973**, *18*, 220–233.
- (45) Francis, A. W.; Robbins, G. W. *J. Am. Chem. Soc.* **1933**, *55*, 4339–4342.
- (46) Galicia-Luna, L. A.; Richon, D.; Renon, H. *J. Chem. Eng. Data* **1994**, *39*, 424–431.
- (47) Giles, N. F.; Wilson, G. M. *J. Chem. Eng. Data* **2000**, *45*, 146–153.
- (48) Glos, S.; Kleinrahn, R.; Wagner, W. *J. Chem. Thermodyn.* **2004**, *36*, 1037–1059.
- (49) Glowka, S. *Bull. Acad. Pol. Sci., Ser. Sci. Chim.* **1972**, *20*, 163–167.
- (50) Golovskoi, E. A.; Zagoruchenko, V. A.; Tsymarny, V. A. *Measurements of propane density at temperatures 88.24–272.99 K and pressures up to 609.97 bar*. Deposited at the Institute VNIIEGasprom, No. 45, 1978. Data are given in: Sychev, V. V.; Vasserman, A. A.; Kozlov, A. D.; Tsymarny, V. A. *Thermodynamic Properties of Propane*; Hemisphere Publishing Corporation: New York, 1991.
- (51) Gomez-Nieto, M.; Thodos, G. *Ind. Eng. Chem. Fundam.* **1977**, *16*, 254–259.
- (52) Goodwin, A. R. H.; Lemmon, E. W. *unpublished data*, University of Idaho: Moscow, 1995.
- (53) Goodwin, R. D. *J. Res. Natl. Bur. Stand.* **1978**, *83*, 449–458.
- (54) Guigo, E. I.; Ershova, N. S.; Margolin, M. F. *Kholod. Tekhnika* **1978**, *11*, 29–30.
- (55) Gunn, R. D. The volumetric properties of nonpolar gaseous mixtures. M.S. Thesis, Univ. of California, Berkeley, CA, 1958.
- (56) Hahn, R.; Schäfer, K.; Schramm, B. *Ber. Bunsenges. Phys. Chem.* **1974**, *78*, 287–289.
- (57) Hainlen, A. *Justus Liebig's Ann. Chem.* **1894**, *282*, 229–245.
- (58) Hanson, G. H.; Hogan, R. J.; Nelson, W. T.; Cines, M. R. *Ind. Eng. Chem.* **1952**, *44*, 604–609.
- (59) Harteck, P.; Edse, R. Z. *Phys. Chem.* **1938**, A182, 220–224.
- (60) Haynes, W. M. *J. Chem. Thermodyn.* **1983**, *15*, 419–424.
- (61) Haynes, W. M.; Hiza, M. J. *J. Chem. Thermodyn.* **1977**, *9*, 179–187.
- (62) He, M. G.; Liu, Z. G.; Yin, J. M. *Int. J. Thermophys.* **2002**, *23*, 1599–1615.
- (63) Helgeson, N. L.; Sage, B. H. *J. Chem. Eng. Data* **1967**, *12*, 47–49.
- (64) Higashi, Y. *Fluid Phase Equilib.* **2004**, *219*, 99–103.
- (65) Higashi, Y.; Funakura, M.; Yoshida, Y. *Proc. International Conference: "CFCs, The Day After"*, Padova, Italy, 1994; pp 493–500.
- (66) Hipkin, H. *AIChE J.* **1966**, *12*, 484–487.
- (67) Hirata, M.; Suda, S.; Hakuta, T.; Nagahama, K. *Mem. Fac. Technol., Tokyo Metrop. Univ.* **1969**, *19*, 103–122.
- (68) Hirschfelder, J. O.; McClure, F. T.; Weeks, I. F. *J. Chem. Phys.* **1942**, *10*, 201–211.
- (69) Ho, Q. N.; Yoo, K. S.; Lee, B. G.; Lim, J. S. *Fluid Phase Equilib.* **2006**, *245*, 63–70.
- (70) Holcomb, C. D.; Magee, J. W.; Haynes, W. M. *Density measurements on natural gas liquids. Research Report RR-147*, Gas Processors Association, **1995**.
- (71) Holcomb, C. D.; Outcalt, S. L. *Fluid Phase Equilib.* **1998**, *150*–*151*, 815–827.
- (72) Honda, Y.; Sato, T.; Uematsu, M. *J. Chem. Thermodyn.* **2008**, *40*, 208–211.
- (73) Horstmann, S.; Fischer, K.; Gmehling, J. *Chem. Eng. Sci.* **2001**, *56*, 6905–6913.
- (74) Huang, E. T. S.; Swift, G. W.; Kurata, F. *AIChE J.* **1966**, *12*, 932–936.
- (75) Huff, J. A.; Reed, T. M., III. *J. Chem. Eng. Data* **1963**, *8*, 306–311.
- (76) Hurly, J. J.; Gillis, K. A.; Mehl, J. B.; Moldover, M. R. *Int. J. Thermophys.* **2003**, *24*, 1441–1474.
- (77) Im, J.; Lee, G.; Shin, M. S.; Lee, J.; Kim, H. *Fluid Phase Equilib.* **2006**, *248*, 19–23.
- (78) Jensen, R. H.; Kurata, F. *J. Petrol. Technol.* **1969**, *21*, 683–691.
- (79) Jepson, W. B.; Richardson, M. J.; Rowlinson, J. S. *Trans. Faraday Soc.* **1957**, *53*, 1586–1591.
- (80) Jou, F.-Y.; Carroll, J. J.; Mather, A. E. *Fluid Phase Equilib.* **1995**, *109*, 235–244.
- (81) Kahre, L. C. *J. Chem. Eng. Data* **1973**, *18*, 267–270.
- (82) Kaminishi, G.-I.; Yokoyama, C.; Takahashi, S. *Sekiyu Gakkaishi* **1988**, *31*, 433–438.
- (83) Kay, W. B. *J. Chem. Eng. Data* **1970**, *15*, 46–52.
- (84) Kay, W. B. *J. Chem. Eng. Data* **1971**, *16*, 137–140.
- (85) Kay, W. B. *J. Phys. Chem.* **1964**, *68*, 827–831.
- (86) Kay, W. B.; Ramesek, G. M. *Ind. Eng. Chem.* **1953**, *45*, 221–226.
- (87) Kayukawa, Y.; Hasumoto, M.; Kano, Y.; Watanabe, K. *J. Chem. Eng. Data* **2005**, *50*, 556–564.
- (88) Kayukawa, Y.; Watanabe, K. *J. Chem. Eng. Data* **2001**, *46*, 1025–1030.
- (89) Kemp, J. D.; Egan, C. J. *J. Am. Chem. Soc.* **1938**, *60*, 1521–1525.
- (90) Kim, J. H.; Kim, M. S. *Fluid Phase Equilib.* **2005**, *238*, 13–19.
- (91) Kim, J. H.; Kim, M. S.; Kim, Y. *Fluid Phase Equilib.* **2003**, *211*, 273–287.
- (92) Kistiakowsky, G. B.; Lacher, J. R.; Ransom, W. W. *J. Chem. Phys.* **1940**, *8*, 970–977.
- (93) Kistiakowsky, G. B.; Rice, W. W. *J. Chem. Phys.* **1940**, *8*, 610–618.
- (94) Kitajima, H.; Kagawa, N.; Tsuruno, S.; Watanabe, K. *Int. J. Thermophys.* **2005**, *26*, 1733–1742.
- (95) Kleiber, M. *Fluid Phase Equilib.* **1994**, *92*, 149–194.
- (96) Klosek, J.; McKinley, C. *Proc. First International Conference on LNG*, Chicago, 1968; Vol. 5.
- (97) Kratzke, H. Experimental determination of the thermal state quantities of liquid propane, n-butane, n-pentane and acetonitrile at pressures up to 60 MPa. Ph.D. Dissertation, Ruh-Universität, Bochum, 1983.
- (98) Kratzke, H. *J. Chem. Thermodyn.* **1980**, *12*, 305–309.
- (99) Kratzke, H.; Müller, S. *J. Chem. Thermodyn.* **1984**, *16*, 1157–1174.
- (100) Kreglewski, A.; Kay, W. B. *J. Phys. Chem.* **1969**, *73*, 3359–3366.
- (101) Kretschmer, C. B.; Wiebe, R. J. *J. Am. Chem. Soc.* **1951**, *73*, 3778–3781.
- (102) Kuenen, J. P. *Philos. Mag.* **1903**, *6*, 637–653.
- (103) Lacam, A. *J. Rech. CNRS* **1956**, *34*, 25–56.
- (104) Lammers, J. N. J. H.; van Kasteren, P. H. G.; Kroon, G. F.; Zeldenrust, H. *Proc. Fifty-Seventh Ann. Conv. Gas Proc. Assoc.* **1978**, *57*, 18–24.
- (105) Laurance, D. R.; Swift, G. W. *J. Chem. Eng. Data* **1972**, *17*, 333–337.
- (106) Lebeau, P. *Bull. Soc. Chim. Fr.* **1905**, *33*, 1454–1456.
- (107) Lee, B. G.; Yang, W.-J.; Kim, J.-D.; Lim, J. S. *J. Chem. Eng. Data* **2003**, *48*, 841–846.
- (108) Legatski, T. W.; Nelson, W. R.; Dean, M. R.; Fruit, L. R. *Ind. Eng. Chem.* **1942**, *34*, 1240–1243.
- (109) Lichtenhaler, R. N.; Schäfer, K. *Ber. Bunsenges. Phys. Chem.* **1969**, *73*, 42–48.
- (110) Lim, J. S.; Ho, Q. N.; Park, J.-Y.; Lee, B. G. *J. Chem. Eng. Data* **2004**, *49*, 192–198.

- (111) Lim, J. S.; Park, J. Y.; Lee, K.-S.; Kim, J.-D.; Lee, B. G. *J. Chem. Eng. Data* **2004**, *49*, 750–755.
- (112) Lim, J. S.; Park, J.-Y.; Kang, J. W.; Lee, B.-G. *Fluid Phase Equilib.* **2006**, *243*, 57–63.
- (113) Luo, C. C.; Miller, R. C. *Cryogenics* **1981**, *21*, 85–93.
- (114) Maass, O.; Wright, C. H. *J. Am. Chem. Soc.* **1921**, *43*, 1098–1111.
- (115) Manley, D. B.; Swift, G. W. *J. Chem. Eng. Data* **1971**, *16*, 301–307.
- (116) Matschke, D. E.; Thodos, G. *J. Chem. Eng. Data* **1962**, *7*, 232–234.
- (117) Matteson, R. Physical constants of hydrocarbons boiling below 350 °F. *ASTM, Special Tech. Publication No. 109*, **1950**.
- (118) McClune, C. R. *Cryogenics* **1976**, *16*, 289–295.
- (119) McGlashan, M. L.; Potter, D. J. B. *Proc. R. Soc. London, Ser. A* **1962**, *267*, 478–500.
- (120) McLinden, M. O. *J. Chem. Eng. Data* **2009**, in press.
- (121) Meier, K. *J. Chem. Eng. Data*, to be submitted.
- (122) Mikovsky, J.; Wichterle, I. *Collect. Czech. Chem. Commun.* **1975**, *40*, 365–370.
- (123) Miranda, R. D.; Robinson, D. B.; Kalra, H. *J. Chem. Eng. Data* **1976**, *21*, 62–65.
- (124) Miyamoto, H.; Shigetoyo, K.; Uematsu, M. *J. Chem. Thermodyn.* **2007**, *39*, 1423–1431.
- (125) Miyamoto, H.; Uematsu, M. *Int. J. Thermophys.* **2006**, *27*, 1052–1060.
- (126) Miyamoto, H.; Uematsu, M. *J. Chem. Thermodyn.* **2007**, *39*, 225–229.
- (127) Mousa, A. H. N. *J. Chem. Thermodyn.* **1977**, *9*, 1063–1065.
- (128) Mousa, A. H. N.; Kay, W. B.; Kreglewski, A. *J. Chem. Thermodyn.* **1972**, *4*, 301–311.
- (129) Niepmann, R. *J. Chem. Thermodyn.* **1984**, *16*, 851–860.
- (130) Niesen, V. G.; Rainwater, J. C. *J. Chem. Thermodyn.* **1990**, *22*, 777–795.
- (131) Noda, K.; Inoue, K.; Asai, K.; Ishida, K. *J. Chem. Eng. Data* **1993**, *38*, 9–11.
- (132) Olszewski, K. *Philos. Mag.* **1895**, *39*, 188–213.
- (133) Opfell, J. B.; Sage, B. H.; Pitzer, K. S. *Ind. Eng. Chem.* **1956**, *48*, 2069–2076.
- (134) Orrit, J. E.; Laupretre, J. M. *Adv. Cryog. Eng.* **1978**, *23*, 573–579.
- (135) Outcalt, S. L.; Lee, B.-C. *J. Res. Natl. Inst. Stand. Technol.* **2004**, *109*, 525–531.
- (136) Park, Y. M.; Jung, M. Y. *J. Chem. Eng. Data* **2002**, *47*, 818–822.
- (137) Park, Y.; Kang, J.; Choi, J.; Yoo, J.; Kim, H. *J. Chem. Eng. Data* **2007**, *52*, 1203–1208.
- (138) Patel, M. R.; Joffrion, L. L.; Eubank, P. T. *AIChE J.* **1988**, *34*, 1229–1232.
- (139) Perkins, R. A.; Sanchez Ochoa, J. C.; Magee, J. W. *J. Chem. Eng. Data* **2009**, in press.
- (140) Pompe, A.; Spurling, T. H. Virial coefficients for gaseous hydrocarbons. *Div. Appl. Org. Chem. (Aust. C.S.I.R.O.), Tech. Pap. 1*, **1974**.
- (141) Prasad, D.; H., L. *AIChE J.* **1982**, *28*, 695–696.
- (142) Ramjugernath, D.; Valtz, A.; Coquelet, C.; Richon, D. *J. Chem. Eng. Data* **2009**, *54*, 1292–1296.
- (143) Rao, M. G. S. *Indian J. Pure Appl. Phys.* **1971**, *9*, 169–170.
- (144) Reamer, H. H.; Sage, B. H.; Lacey, W. N. *Ind. Eng. Chem.* **1949**, *41*, 482–484.
- (145) Reamer, H. H.; Sage, B. H.; Lacey, W. N. *Ind. Eng. Chem.* **1951**, *43*, 2515–2520.
- (146) Richter, M.; Kleinrahm, R.; Glos, S.; Span, R.; Schley, P.; Uhrig, M. *Int. J. Thermophys.* **2009**, submitted.
- (147) Rodosevich, J. B.; Miller, R. C. *AIChE J.* **1973**, *19*, 729–735.
- (148) Roof, J. G. *J. Chem. Eng. Data* **1970**, *15*, 301–303.
- (149) Sage, B. H.; Evans, H. D.; Lacey, W. N. *Ind. Eng. Chem.* **1939**, *31*, 763–767.
- (150) Sage, B. H.; Lacey, W. N. *Ind. Eng. Chem.* **1940**, *32*, 992–996.
- (151) Sage, B. H.; Schaafsma, J. G.; Lacey, W. N. *Ind. Eng. Chem.* **1934**, *26*, 1218–1224.
- (152) Sage, B. H.; Webster, D. C.; Lacey, W. N. *Ind. Eng. Chem.* **1937**, *29*, 1309–1314.
- (153) Schäfer, K.; Schramm, B.; Urieta Navarro, J. S. *Z. Phys. Chem.* **1974**, *93*, 203–216.
- (154) Scheeline, H. W.; Gilliland, E. R. *Ind. Eng. Chem.* **1939**, *31*, 1050–1057.
- (155) Schindler, D. L.; Swift, G. W.; Kurata, F. *Hydro. Process. Pet. Ref.* **1966**, *45*, 205–210.
- (156) Scott, D. W. *J. Chem. Phys.* **1974**, *60*, 3144–3165.
- (157) Seeman, F.-W.; Urban, M. *Erdoel Kohle, Erdgas, Petrochem.* **1963**, *16*, 117–119.
- (158) Seibt, D. Schwingdrahtviskosimeter mit integriertem Ein-Senkkörper-Dichtemessverfahren für Untersuchungen an Gasen in größeren Temperatur- und Druckbereichen. Ph.D. Dissertation, University of Rostock. Also published as: *Fortschr.-Ber. VDI, Reihe 6: Energietechnik, Nr. 571*, VDI-Verlag: Düsseldorf, 2008.
- (159) Seong, G.; Yoo, K.-P.; Lim, J. S. *J. Chem. Eng. Data* **2008**, *53*, 2783–2786.
- (160) Skripka, V. G.; Nikitina, I. E.; Zhdanovich, L. A.; Sirotnin, A. G.; Benyaminovich, O. A. *Gazov. Promst.* **1970**, *15*, 35–36.
- (161) Sliwinski, P. *Z. Phys. Chem. (Wiesbaden)* **1969**, *68*, 91–98.
- (162) Sliwinski, P. *Z. Phys. Chem. Neue Folge* **1969**, *63*, 263–279.
- (163) Starling, K. E.; Kumar, K. H.; Reintsema, S. R.; Savidge, J. L.; Eckhardt, B.; Gopalkrishnan, R.; McFall, R. M. University of Oklahoma, 1984.
- (164) Straty, G. C.; Palavra, A. M. F. *J. Res. Natl. Bur. Stand.* **1984**, *89*, 375–383.
- (165) Strein, V. K.; Lichtenthaler, R. N.; Schramm, B.; Schäfer, K. *Ber. Bunsenges. Phys. Chem.* **1971**, *75*, 1308–1313.
- (166) Teichmann, J. Pressure-volume-temperature measurement with liquid propane and benzene. Dissertation, Ruhr-Universität, Bochum, 1978.
- (167) Terres, E.; Jahn, W.; Reissmann, H. *Brennst.-Chem.* **1957**, *38*, 129–160.
- (168) Thomas, R. H. P.; Harrison, R. H. *J. Chem. Eng. Data* **1982**, *27*, 1–11.
- (169) Tickner, A. W.; Lossing, F. P. *J. Phys. Colloid Chem.* **1951**, *55*, 733–740.
- (170) Tomlinson, J. R. Liquid densities of ethane, propane, and ethane-propane mixtures. *Nat. Gas Process. Assoc., Tech. Publ. TP-1*, **1971**.
- (171) Trusler, J. P. M.; Wakeham, W. A.; Zarari, M. P. *Int. J. Thermophys.* **1996**, *17*, 35–42.
- (172) Trusler, J. P. M.; Zarari, M. P. *J. Chem. Thermodyn.* **1996**, *28*, 329–335.
- (173) Uchytel, P.; Wichterle, I. *Fluid Phase Equilib.* **1983**, *15*, 209–217.
- (174) van der Vet, A. P. *Congr. Mond. Pet. (Paris)* **1937**, *2*, 515–521.
- (175) Van Kasteren, P. H. G.; Zeldenrust, H. *Ind. Eng. Chem. Fundam.* **1979**, *18*, 339–345.
- (176) Warowny, W.; Wielopolski, O.; Stecki, J. *Physica A* **1978**, *91*, 73–87.
- (177) Wichterle, I.; Kobayashi, R. *J. Chem. Eng. Data* **1972**, *17*, 4–9.
- (178) Yasumoto, M.; Uchida, Y.; Ochi, K.; Furuya, T.; Otake, K. *J. Chem. Eng. Data* **2005**, *50*, 596–602.
- (179) Yesavage, V. F. The measurement and prediction of the enthalpy of fluid mixtures under pressure. Ph.D. Dissertation, University of Michigan, 1968.
- (180) Yesavage, V. F.; Katz, D. L.; Powers, J. E. *J. Chem. Eng. Data* **1969**, *14*, 137–149.
- (181) Yesavage, V. F.; Katz, D. L.; Powers, J. E. *J. Chem. Eng. Data* **1969**, *14*, 197–204.
- (182) Young, S. *Proc. R. Irish Acad.* **1928**, *38B*, 65–92.
- (183) Younglove, B. A. *J. Res. Natl. Bur. Stand.* **1981**, *86*, 165–170.
- (184) Yucelen, B.; Kidnay, A. J. *J. Chem. Eng. Data* **1999**, *44*, 926–931.
- (185) Zanolini, D. A. Measurements of vapor pressures of volatile hydrocarbons. Masters Thesis, Pennsylvania State University, 1964.
- (186) Zhang, Y.; Gong, M.; Zhu, H.; Liu, J.; Wu, J. *J. Eng. Thermophys.* **2007**, *28*, 27–29.
- (187) Bücker, D.; Wagner, W. *J. Phys. Chem. Ref. Data* **2006**, *35*, 205–266.
- (188) Bücker, D.; Wagner, W. *J. Phys. Chem. Ref. Data* **2006**, *35*, 929–1019.
- (189) Lemmon, E. W.; Jacobsen, R. T. *J. Phys. Chem. Ref. Data* **2005**, *34*, 69–108.
- (190) Span, R.; Wagner, W. *J. Phys. Chem. Ref. Data* **1996**, *25*, 1509–1596.
- (191) Schmidt, R.; Wagner, W. *Fluid Phase Equilib.* **1985**, *19*, 175–200.
- (192) Lemmon, E. W.; Span, R. *J. Chem. Eng. Data* **2006**, *51*, 785–850.
- (193) Pavese, F.; Besley, L. M. *J. Chem. Thermodyn.* **1981**, *13*, 1095–1104.
- (194) Frenkel, M.; Chirico, R. D.; Diky, V.; Muzny, C. D.; Kazakov, A. F.; Lemmon, E. W. *NIST Standard Reference Database 103b: ThermoData Engine (TDE)*, Version 3.0; National Institute of Standards and Technology, Standard Reference Data Program: Gaithersburg, 2008.
- (195) Wagner, W. *Fortschr.-Ber. VDI*, VDI-Verlag: Düsseldorf, 1974, *3*.
- (196) Lemmon, E. W.; Goodwin, A. R. H. *J. Phys. Chem. Ref. Data* **2000**, *29*, 1–39.
- (197) Span, R.; Wagner, W. *Int. J. Thermophys.* **1997**, *18*, 1415–1443.
- (198) Setzmann, U.; Wagner, W. *J. Phys. Chem. Ref. Data* **1991**, *20*, 1061–1155.
- (199) Wagner, W.; Pruss, A. *J. Phys. Chem. Ref. Data* **2002**, *31*, 387–535.
- (200) Tillner-Roth, R. *Fundamental equations of state*; Shaker Verlag: Aachen, Germany, 1998.
- (201) Lemmon, E. W.; Huber, M. L.; McLinden, M. O. *NIST Standard Reference Database 23: Reference Fluid Thermodynamic and Transport Properties-REFPROP*, Version 8.0, National Institute of Standards and Technology, Standard Reference Data Program: Gaithersburg, 2007.
- (202) Lemmon, E. W.; Overhoff, U.; Wagner, W. A reference equation of state for propylene. *J. Phys. Chem. Ref. Data*, to be published.
- (203) Span, R.; Wagner, W. *Int. J. Thermophys.* **2003**, *24*, 1–39.
- (204) Kunz, O.; Klimeck, R.; Wagner, W.; Jaeschke, M. *The GERG-2004 wide-range equation of state for natural gases and other mixtures. GERG TM15*, Fortschritt-Berichte VDI, Number 557, 2007; Vol. 6.
- (205) Miyamoto, H.; Watanabe, K. *Int. J. Thermophys.* **2000**, *21*, 1045–1072.
- (206) Younglove, B. A.; Ely, J. F. *J. Phys. Chem. Ref. Data* **1987**, *16*, 577–798.
- (207) Sychev, V. V.; Vasserman, A. A.; Kozlov, A. D.; Tsymarny, V. A. *Thermodynamic properties of propane*, 1991.

- (208) Goodwin, R. D.; Haynes, W. M. *Thermophysical properties of propane from 85 to 700 K at pressures to 70 MPa*. Natl. Bur. Stand., Monogr. 170, 1982.
- (209) Bühner, K.; Maurer, G.; Bender, E. *Cryogenics* **1981**, 21, 157–164.
- (210) Teja, A. S.; Singh, A. *Cryogenics* **1977**, 17, 591–596.
- (211) Preston-Thomas, H. *Metrologia* **1990**, 27, 3–10.
- (212) Mohr, P. J.; Taylor, B. N.; Newell, D. B. *J. Phys. Chem. Ref. Data* **2008**, 37, 1187–1284.
- (213) Deiters, U. K.; de Reuck, K. M. *Pure Appl. Chem.* **1997**, 69, 1237–1249.
- (214) Span, R. *Multiparameter equations of state - An accurate source of thermodynamic property data*; Springer: Berlin, Heidelberg, NY, 2000.
- (215) Lemmon, E. W.; Jacobsen, R. T.; Penoncello, S. G.; Friend, D. G. *J. Phys. Chem. Ref. Data* **2000**, 29, 331–385.

Received for review February 25, 2009. Accepted September 28, 2009.

JE900217V